2005

Computational models of the thalamocortical circuit: sleep oscillations and receptive fields.

Yousif, Nada

COMPUTATIONAL MODELS OF THE THALAMOCORTICAL CIRCUIT: SLEEP OSCILLATIONS AND RECEPTIVE FIELDS

N. YOUSIF

Ph.D.

2005

Copyright Statement

Computational models of the thalamocortical circuit: sleep oscillations and receptive fields.

Nada Yousif

Centre for Theoretical and Computational Neuroscience
Faculty of Science

University of Plymouth

A thesis submitted for the degree of

Ph.D.

August 2005

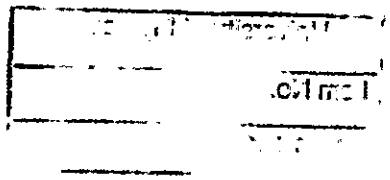

Abstract

Computational models of the thalamocortical circuit: sleep oscillations and receptive fields.

Nada Yousif

The thalamus is a subcortical structure, which consists of a collection of functionally and morphologically defined nuclei. A subset of these, the sensory nuclei, receive information from the periphery and relay it to the related primary cortical area. Hence the thalamus was traditionally assumed to passively relay afferent information. However, the fact that thalamic relay cells receive a large proportion of their synaptic inputs from the cortical cells to which they project, has led to the consensus that there is a more significant thalamic contribution to sensory processing. This thesis investigates the role of the thalamocortical feedback loop using population-level computational models. In particular two states of thalamocortical activity are investigated: early sleep, and active visual processing. During early sleep, the network displays 7-14Hz spindle oscillations. These oscillations have been previously modelled using conductance-based paradigms, but here the activity is investigated through the nonlinear dynamics of the circuitry. It is shown that the circuit has an intrinsic resonant frequency in the spindles range. During visual processing, the role of the lateral geniculate nucleus (the primary visual thalamic nucleus) was previously overlooked, as thalamic receptive fields are spatially identical to those in the retina. Temporally however, thalamic and retinal responses differ in magnitude, and the second model in this thesis shows how cortical feedback can have a role in augmenting thalamic temporal responses. This model was reduced in order to find the minimal thalamic circuitry that can produce such responses, and this final model can also exhibit steady state oscillatory behaviour. The transition from transient visual activity to sustained oscillatory activity in this model, required a switch in the relative cortical feedback weights to the thalamocortical and the reticular populations. Together, these results indicate that the contribution of the thalamus to neural activity can no longer be ignored.

Contents

List of Figures

List of Tables

Acknowledgements

I would like to take this opportunity to thank a number of people, whose support was crucial for me to be able to complete this work.

Primarily I would like to acknowledge my supervisor Mike Denham, for first giving me the chance to pursue this interesting line of research, and subsequently for his wise and patient guidance over the past three years. I also owe thanks to my second supervisor Roman Borisyuk, always generous with his time, his aid and advice was a treat. I also thank Thomas Wennekers for taking the time to read this thesis, and whose helpful comments were welcome. More globally, I am grateful for the support of the entire department, all of whom are great colleagues, many of whom are friends. You have been a wonderful source of coffee-fuelled discussions over the past years.

To my parents, my mum Anwar and my dad Athir, I owe a debt of gratitude for their unfaltering confidence and invaluable parental pride and reassurance. I also thank my sisters Saba and Rana, for their insane enthusiasm, and without whom I would not be the person I am today.

Finally to all of those people who I am lucky enough to call a friend, and who must forgive me for not naming them all individually. From London: Clare, Cath, and Nic. In Plymouth: Linda for the tour on my first day, Pauline and Martin for coffee times and advice, and Andy for reading the thesis. In particular I thank Benoit, a most agreeable distraction, who always recommends calm and optimism as options in the most turbulent of times.

Author's Declaration

At no time during the registration for the degree of Doctor of Philosophy has the author been registered for any other University award. This study was financed with the aid of a studentship from the University of Plymouth. A programme of advanced study was undertaken, which included attendance of relevant scientific seminars and conferences, at which work was often presented; several papers prepared for publication.

Publications:

N.A.B. Yousif, W. Wang, H.E. Jones, M.J. Denham, A.M.Sillito. Spatiotemporal thalamic responses arising from the dynamics of functionally aligned corticothalamic feedback. SfN abstracts 2005.

N. A. B. Yousif, M. Denham. The Role of Cortical Feedback in the Generation of the Temporal Receptive Field Responses of Lateral Geniculate Nucleus Neurons: a Computational Modelling Study. (Submitted).

Yousif N., Denham M. A population-based model of the nonlinear dynamics of the thalamocortical feedback network displays intrinsic oscillations in the spindling (7-14 Hz) range. (Submitted).

W. Wang, N.A.B. Yousif, H.E. Jones, I.M. Andolina, T.E.Salt, A.M.Sillito, M.J. Denham. Functional significance of alignment of feedback effects from visual cortex to thalamus. BNA abstracts 2005.

N. A. B. Yousif, M. Denham. Spatiotemporal dynamics of information flow in a

model of the visual thalamocortical system. Perception: ECVP 2004 abstracts.

Yousif N., Borisyuk R. & Denham M. Spindle oscillations in a Wilson-Cowan type computational model of a thalamocortical network. FENS Forum Abstracts, vol. 2, 2004.

Nada A. B. Yousif and Mike Denham. Action potential backpropagation in a model thalamocortical relay cell. Neurocomputing. Vol. 58-60, 2004.

Nada A. B. Yousif and Mike Denham. Action potential backpropagation in a model thalamocortical relay cell. CNS 2003 proceedings.

Presentation and Conferences Attended:

September 2004: British Neuroscience Association postgraduate symposium.

August 2004: European Congress on Visual Perception (ECVP).

July 2004: Forum for European Neuroscience (FENS).

September 2003: MBA microelectrodes course.

August 2003: Edinburgh summer school in neuroinformatics simulation tools.

July 2003: Computational Neuroscience (CNS) meeting.

August 2002: EU Advanced Course in Computational Neuroscience.

Word count of main body of thesis:

47,904

Signed 

Date March 2006

Glossary

LGN	Lateral Geniculate Nucleus	**TRN**	Thalamic Reticular Nucleus
V1	Primary visual cortex	**TC**	Thalamocortical cells
RE	Thalamic reticular cell	**PY**	Cortical Pyramidal cells
TIN	Thalamic Inhibitory Interneurons	**IN6**	Cortical Interneurons
MGB	Medial Geniculate Body	**VPN**	Ventral Posterior Nucleus
VPM	Ventral Posterior Medial Nucleus	**RL**	Round large (synapse)
RS	Round Small (synapse)	**IPSP**	Inhibitory Postsynaptic Potential
EPSP	Excitatory Postsynaptic Potential	**ACh**	Acetylcholine
NE	Noradrenaline	**RF**	Receptive field
STRF	Spatiotemporal Receptive Field	**SI**	Somatosensory (cortex)
MT	Mediotemporal (cortex)	**PFC**	Prefrontal Cortex
PGN	Perigeniculate nucleus	**AHP**	Afterhyperpolarisation Potential
ODE	Ordinary Differential Equation	**SNIC**	Saddle-Node on Invariant Curve
B-T	Bogdanov-Takens (bifurcation)	**fMRI**	Functional Magnetic Resonance Imaging

Chapter 1

Introduction

This thesis describes three population-level computational models of the thalamocortical network. The first is an extremely simplified circuit, which is used to investigate the existence of spindle oscillations as a result of the intrinsic network dynamics. The second is a more detailed model, which explores the effect of cortical feedback on temporal thalamic response properties. The third produces both spindle oscillations and temporal thalamic receptive fields, and examines the transition between these states. This chapter outlines the specific motivations for carrying out this research.

1.1 The thalamus

The thalamus is a subcortical structure found at the centre of the brain as shown in figure 1.1. It is a structure that is comprised of a collection of functionally and morphologically defined nuclei, and figure 1.2 shows a schematic diagram depicting the division of the thalamus into these constituent nuclei. Those labelled are the three primary sensory nuclei, and the thalamic reticular nucleus. The thalamus is a structure that is conserved across species, and its relative size has grown proportionately to the

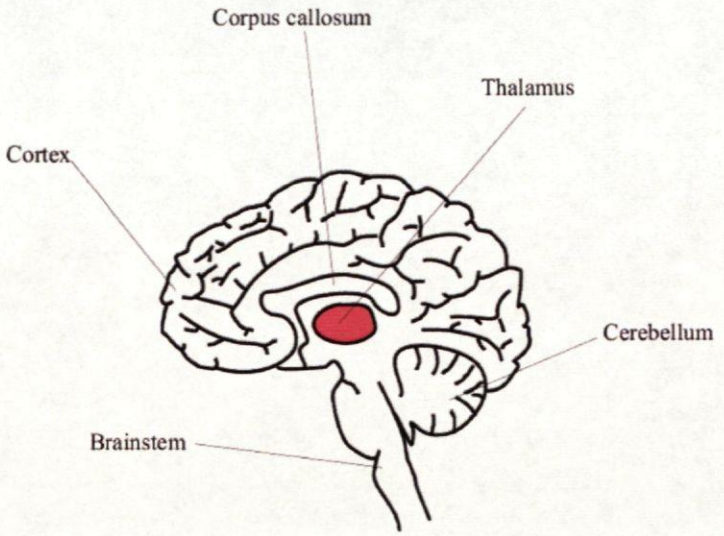

Figure 1.1: The location of the thalamus is shown relative to the cortex, the cerebellum, the brainstem, and the corpus callosum. The central position of the thalamus between the cortex and subcortical structures is clear.

cortex through evolution. The central location that the thalamus occupies within the brain reflects the central position that it also holds along many pathways of information transfer between various brain regions. Thalamic nuclei can be divided into two classes based on connectivity and consequently functionality (Sherman & Gullery, 2001): the first-order and the higher-order nuclei.

1.1.1 Thalamic nuclei

First-order nuclei receive information from subcortical areas and relay this information to the relevant cortical area. In this thesis, the term first-order specifically refers to the primary sensory nuclei of the thalamus. These sensory nuclei receive signals from peripheral sensors in the eyes, ears, and skin, and relay this information to the relevant sensory cortical area. The connectivity of the thalamus preserves the topographic arrangement that is crucial to early sensory areas, such as retinotopy in the visual sys-

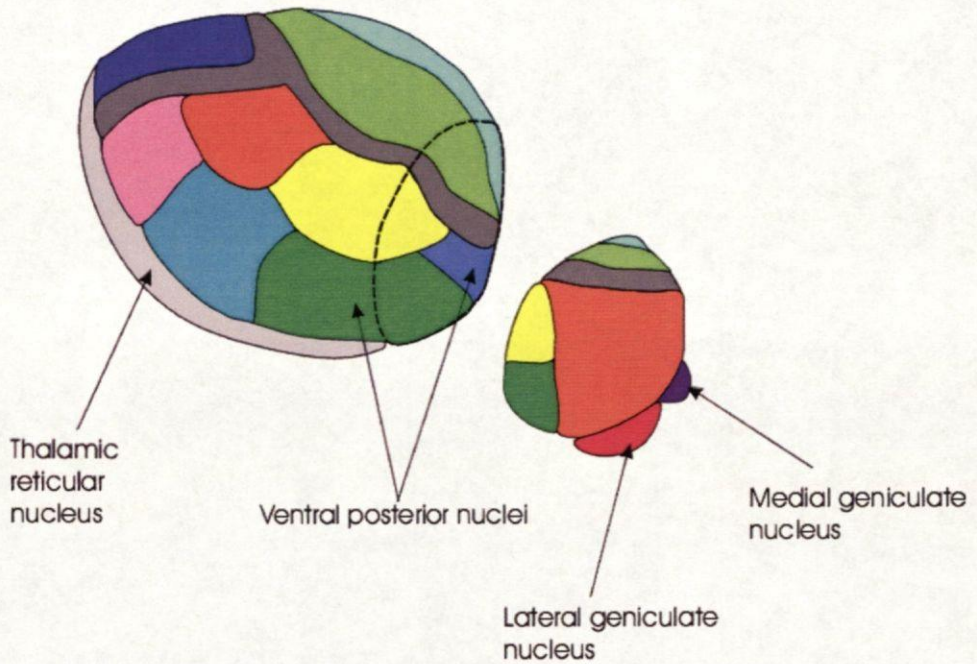

Figure 1.2: The division of the thalamus into its constituent nuclei is schematised in this figure. The classification of thalamic nuclei is based on function and morphology. Within the main thalamic mass, nuclei are not separate structures, but the lateral and medial geniculate nuclei are conspicuous due to their disconnected locations. Only the primary sensory nuclei and the thalamic reticular nucleus are labelled. Adapted from Kandel *et al.* (2000).

tem, tonotopy in the auditory system, and somatotopy in the somatosensory system. Note that motor nuclei can also be described as first order, as in previous literature (Sherman & Gullery, 2001), as these nuclei also receive subcortical information which is relayed to cortex. Much less is known about the higher-order nuclei of the thalamus, which similarly to the first-order nuclei essentially receive and relay information. However, higher-order nuclei both receive information from, and transmit information to, cortical areas. Therefore, these nuclei mediate various forms of cortico-cortical communication. Table 1.1 shows the afferent and efferent connections of mammalian thalamic nuclei, and demonstrates that the sensory nuclei can be clearly identified.

The present thesis investigates the role of the first-order, rather than higher-order, thalamic nuclei. The main reason for this is that these nuclei have been studied in more depth than their higher-order counterparts, which is likely to be because sensory pathways are simpler to observe and manipulate experimentally. By initially exploring first-order nuclei, it is intended that the results and hypotheses of such studies can be extrapolated to all thalamic nuclei. Similarly, by focussing the current study onto one sensory modality (vision), the obtained results can be used to understand the processing that occurs in other sensory modalities. The latter objective is especially feasible as the architecture of the thalamocortical network is extremely similar for the three primary sensory nuclei: the lateral geniculate nucleus (LGN) in the visual system, the medial geniculate nucleus (MGN) in the auditory system, and the ventral posterior nuclei (VPN) in the somatosensory system. This feature is demonstrated in figure 1.3, which depicts the pathways to the cortex through the three sensory nuclei. However the specific contribution of these thalamic nuclei, particularly in terms of sensory processing, remain largely unknown.

The prominent position that these nuclei occupy along the sensory pathways hints

Afferent	Nucleus	Efferent
Mamilliary bodies of the Hypothalamus	Anterior nucleus	Cingulate gyrus
Hypothalamus and prefrontal cortex (PFC)	Dorsomedial nucleus	PFC
Cingulate gyrus	Lateral dorsal nucleus	Cingulate gyrus
Visual cortex	Lateral posterior nucleus	Parietal association areas
Visual cortex	Pulvinar	Visual cortex and adjacent areas of temporal and parietal cortex
Basal ganglia	Ventral anterior nucleus	Premotor cortex
Cerebellar nuclei	Ventral lateral nucleus	Motor cortex
Sensory input from face, and the oral and nasal cavities	Ventral posterior medial nucleus	Primary somatosensory cortex
Sensory input from trunk and extremities	Ventral posterior lateral nucleus	Primary somatosensory cortex
Cochlea	MGN	Primary auditory cortex
Retina	LGN	Primary visual cortex
Basal ganglia, midbrain, frontal cortex and PFC	Intralaminar nuclei	Basal ganglia and association areas of cerebral cortex

Table 1.1: This table shows the main mammalian thalamic nuclei, along with their afferents and efferents (Jones, 1985). The three primary sensory nuclei can be swiftly recognised due to their peripheral inputs and primary cortical targets.

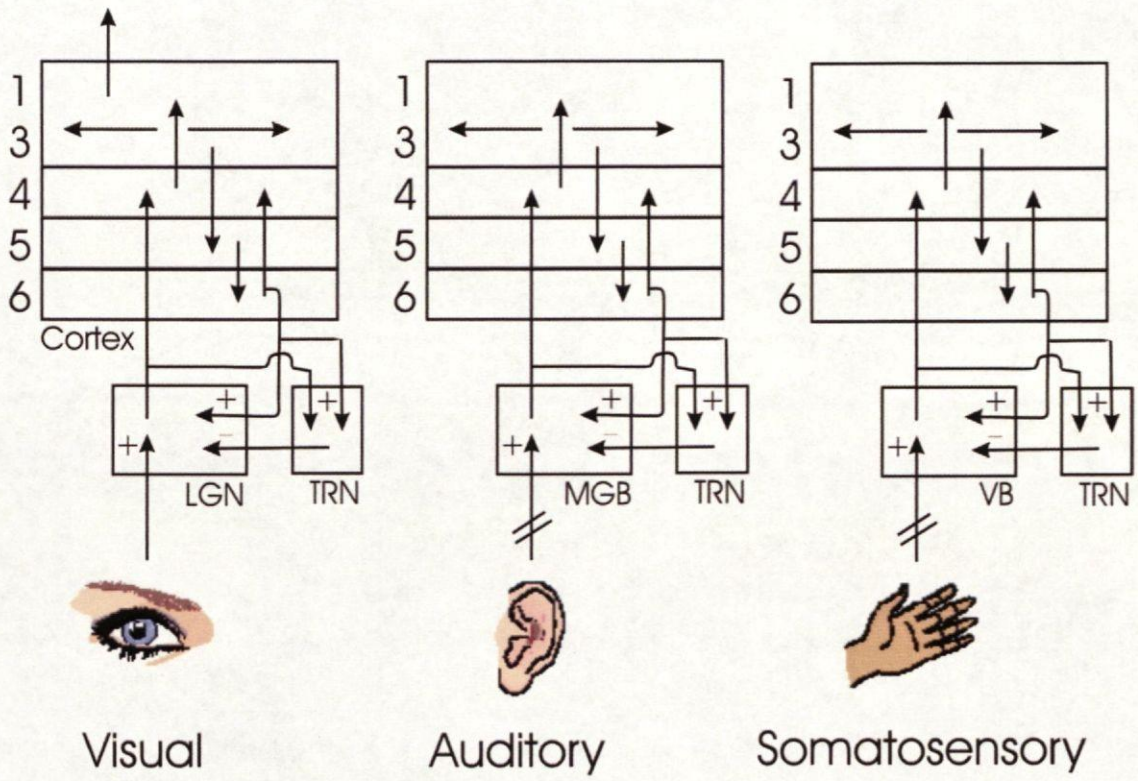

Figure 1.3: The three primary sensory nuclei of the thalamus, and their reciprocal connections with the primary cortical area and reticular nucleus are schematised in this figure, which is redrawn from Alitto & Usrey (2003). The similarity of these pathways across the three nuclei is clearly observed.

that they possess a key role. This is particularly true for the LGN, due to the direct and seemingly hierarchical structure of the visual system. The peripheral sensors of the retina with their simple centre/surround receptive fields project to the LGN, which in turn projects to the primary visual cortex. Here the receptive fields, and consequently the visual processing, clearly become more complex. The fact that the LGN lies in the centre of this otherwise direct pathway, suggests that it performs an active role rather than passively relaying visual information from the retina to the cortex. However, in the auditory system there is a great deal of processing that occurs between the periphery (essentially the cochlea) and the MGN. This pre-thalamic processing complicates the circuitry of the auditory pathway. Similarly, in the somatosensory system signals are relayed via a number of pre-thalamic nuclei, and these may each contribute something new to the processing of the afferent information.

In addition to this seemingly straightforward relay of sensory information, the thalamus is implicated in more complex activity. Recently there has been an upsurge in studies which investigate the thalamic involvement in eye movements. When an animal's eyes move, the image of the world moves on the retina, and yet the animal's visual perception of the world remains static. In order to account for this discrepancy, there must be some mechanism which suppresses visual perception during the movement of the eyes. Such a mechanism is commonly referred to as saccadic suppression. A recent study by Sylvester *et al.* (2005) investigated the geniculate involvement in saccadic suppression by measuring responses in the human LGN and V1 with fMRI during visually guided saccades, and also during saccades in darkness. In darkness, saccades lead to signal increases in both the LGN and V1, but while visual stimuli were present, the authors observed a saccadic suppression of visual responses. These results suggest that visual responses as early as at the LGN may be affected by or even

involved in saccadic suppression.

There have also been studies which have looked at the properties of saccades in patients with various types of thalamic lesions, two such examples Gaymard *et al.* (1994), and Bellebaum *et al.* (2005). The earlier of these studies compared the ability of patients with lesions in intralaminar nuclei to perform memory-guided saccades and visually-guided saccades. During the latter task, the eyes were initially displaced, and therefore extra-retinal information is needed to accurately make the saccade. Such information is termed corollary discharge in the literature. The authors found that lesions in intralaminar nuclei affected the accuracy of visually guided saccades, but not memory guided saccades. These results indicate that patients had an impaired ability to determine eye position. The more recent study by Bellebaum *et al.* used a double-step saccadic task, where subjects had to fixate two sequentially flashed targets by two successive saccades after the disappearance of the stimuli. The second saccade is made from a different spatial location from which the target was seen, therefore once again non-retinal information about eye position must be used to guide the saccade. The authors of this study found that patients with lesions in the ventrolateral and mediodorsal nuclei made smaller saccades than normal subjects. Similarly, lesions of the mediodorsal nucleus in monkeys, using focal injection of muscimol (a $GABA_A$ agonist) caused the animals to misjudge the saccade amplitude and variability (Sommer & Wurtz, 2004).

A well studied feature of thalamic cells is their ability to fire in two different modes depending upon the membrane potential. The first of these two modes is tonic (or single spike) firing, and the other is burst firing. During the latter, action potentials are fired in high frequency (>200Hz) groups, due to the activation of a low threshold calcium current (Jahnsen & Llinas, 1984a,b). Another recent study finds a higher correlation

between thalamic burst firing and a preceding eye movement, specifically a microsaccade, which is an involuntary eye movement performed during fixation (Martinez-Conde *et al.*, 2002). As microsaccadic activity is related to maintaining visual perception, the authors suggest that these results indicate that thalamic bursts are more reliable than single spikes for coding visibility. A subsequent theoretical study has postulated that such changes in neuronal activity in the thalamus during eye movements are implicated in the normal development of visual pathways (Rucci & Casile, 2004).

Taken together these studies show mounting evidence for a thalamic influence on visual perception during eye movements, and the processing of information regarding eye position. The involvement of thalamic nuclei in eye movements does not constitute a major part of the work in this thesis, however chapters 4 and 6 refer back to these ideas when considering the role of the thalamus and the thalamocortical network in active vision.

1.2 The thalamocortical feedback circuit

The thalamus' specific contribution to neuronal information processing remains elusive, and its role is often relegated to one of a simple relay. In recent years however, an intriguing fact regarding thalamocortical circuitry has altered this dismissive view. The excitatory thalamocortical cells of the thalamus (also called relay cells or TC cells) were found to receive a large proportion of their synaptic inputs from cortical projections, and specifically from the same regions of cortex which they themselves innervate. The anatomical connections between the mammalian LGN and primary visual cortex were described in a recent review by Thomson & Bannister (2003). The results, from a number of different anatomical studies performed both in primate and

To LGN from	From LGN to	To TRN from	From TRN to
Layer 6B	Layer 6A	Layer 6B	Superior colliculus
Layer 5A	Layer 4Cβ	Layer 4Cα	Other cortical areas
Layer 5B	Layer 4Cα	Layer 4A	
TRN	Layer 4A	Layer 3B	
	Layer 3B		

Table 1.2: Summary of the results presented in a review by Thomson & Bannister (2003), which looked at the circuitry between the LGN, TRN, and layers of the primary visual cortex (V1).

cat, show that although layer 4 is the main target of thalamocortical axons, there also exists a feedback loop between the TC cells of the LGN and the corticothalamic cells in layer 6. Layer 6 also innervates the thalamic reticular nucleus (TRN), which is an inhibitory thalamic nucleus that surrounds much of, and has reciprocal connectivity with, the dorsal thalamus (this nucleus is shown in figure 1.2). These results are summarised both in table 1.2 and figure 1.4.

The feedback loop between the LGN and layer 6 of V1 is the main focus of this thesis. The TC relay cells of the LGN send a projection to cortical cells in layer 4, which is considered to be the main thalamo-recipient layer of the neocortex. The thalamic input is then processed by the cortical micro-circuitry, which is not considered in the current work. The role of this thalamic input to layer 4 is clear; it is the main feed-forward route for sensory information into the cortex. The role of the input to, and subsequent feedback from layer 6 does not have such an obvious function, and is therefore of more interest.

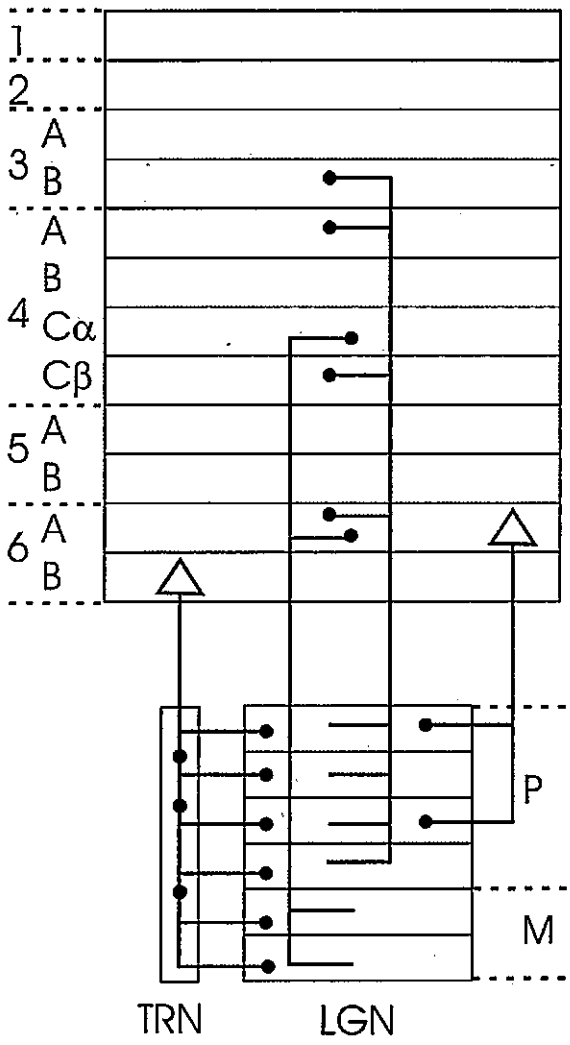

Figure 1.4: Summary diagram redrawn from Thomson & Bannister (2003), which shows the connections between the LGN, the TRN, and the various layers of primary visual cortex.

1.2.1 Synaptic dominance of the feedback projection

The lack of understanding about the nature of this monosynaptic feedback circuit, is confounded by the fact that the feedback projections constitute a significant portion of the synaptic input of thalamocortical cells. Two main studies that have measured the relative numbers of three types of synapses made onto TC cells, and inhibitory interneurons (INs) of the cat LGN are discussed here (Montero, 1991; van Horn *et al.*, 2000). Both studies were performed in slices of cat LGN, using GABA immunostaining techniques. Each of the three types, round large (RL), round small (RS), and F-type synapses, were attributed to originating from retinal, cortical, and GABAergic sources respectively, and this classification is based on earlier tracing studies (for example see Szentagothai *et al.* (1966)). In particular, the aim of the study by van Horn *et al.* was to correct such synaptic measures by accounting for the relative sizes of the synapses, a factor that was not considered in previous studies. The results of these studies are presented in table 1.3, and clearly show that TC cells have between five and nine times more cortical synaptic inputs than retinal inputs. This seems counterintuitive if the role of geniculate TC cells is simply to receive visual information and relay it to the cortex. The thalamic INs however, have similar percentages of cortical inputs and retinal inputs, which suggests that interneurons provide feed-forward inhibition onto TC cells.

A similar study was performed by Liu & Jones (1999) in slices of rat reticular nucleus by staining and imaging individual cells, and the distribution of synapses was found to be as shown in table 1.4. Three locations throughout the neuronal structure (soma, proximal dendrites, and distal dendrites) were examined, and corticothalamic terminals were consistently found to be the most numerous. Compared with the inhibitory

Study	Montero (1991)	van Horn *et al.* (2000)
Animal	Cat	Cat
Nucleus	LGN	LGN
TC inhibitory	24%	30.9%
TC cortical	58%	62%
TC retinal	12%	7.1%
IN GABAergic	26%	24.4%
IN cortical	37%	26.9%
IN retinal	25%	48.7%

Table 1.3: Results from two studies (Montero, 1991; van Horn *et al.*, 2000) which measured the relative numbers of synapses made onto LGN cells in the cat. Both excitatory relay cells (TC) and inhibitory interneurons (IN) were investigated. Synapses that are cortical in origin are the most numerous type in TC cells. In interneurons, retinal inputs constitute a much higher relative percentage than in TC cells. Note that the remaining percentage of synapses in the Montero study were undetermined, or assigned to axonal collaterals of relay cells.

Input type	Somata	Proximal Dendrites	Distal Dendrites
Thalamocortical inputs	8-16%	25-30%	20%
Corticothalamic inputs	65%	50-55%	65-70%
GABAergic inputs	20-25%	15-25%	10-15%

Table 1.4: The relative numbers of synapses made onto cells in the rat thalamic reticular nucleus, from three sources, in three locations throughout the cell (Liu & Jones, 1999). Synapses that are cortical in origin, are relatively more numerous in each location of the cell.

interneurons of the LGN, corticothalamic feedback is numerically larger than all other inputs to the reticular (RE) cells. Therefore, it seems likely that these cells mediate feedback inhibition onto TC cells. This study highlights an important issue that was not raised when discussing the synaptic studies of the LGN, that is the morphology of the cells. The location of corticothalamic terminals in TC cells is known to be different to that in RE cells, such that corticothalamic terminals are often confined to the distal portions of the dentritic arbor in TC cells (Yousif & Denham, 2004). This ought to be taken into account in order to obtain an accurate estimate of the synaptic distribution. In his study, Montero does refer to the locations of the synapses within the cells, but the study by van Horn *et al.* does not seem to account for this factor.

In addition to the location of synapses, there are other limitations that must be recognised when looking at studies that measure synaptic densities. One of these was highlighted in a study by Erisir *et al.* (1997), which found that the synaptic terminals that were described as cortical in origin (RS terminals), also subserve brainstem connections. Furthermore, they show that cortical and brainstem inputs in the cat LGN each account for 50% of the RS terminals. Therefore, when considering the results of

these studies all possible sources for a given synapse type must be considered.

Additionally, the efficacy of synaptic transmission for each type of connection must also be kept in mind. Although the retinal input to TC cells is synaptically less numerous than those of any other origin, it may be that the efficacy of this connection far outweighs that of cortical inputs. However, there have been no studies that directly compare the relative efficacy of these two connections. In a study by Turner & Salt (1998), retinogeniculate and corticothalamic inputs were examined in slices of the rat LGN by comparing the excitatory postsynaptic potentials (EPSPs) elicited by each type of input. The main findings were that retinogeniculate EPSPs have a large amplitude, are fast-rising and exhibited paired-pulse depression. While corticothalamic EPSPs have smaller amplitudes, are slower-rising, and exhibited paired-pulse facilitation. From these results assumptions could be made about the relative strength of these connections, however these would be fairly speculative. A later study by Li *et al.* (2003) compared the structure of cortical and retinal synapses in the LGN and the lateral posterior nucleus (LPN), which is a higher-order visual thalamic nucleus. Once more, the authors draw no conclusions about the effect of these structural properties on the relative efficacy of retinal and cortical connections in the LGN.

Recent studies, have compared the efficacy of afferent thalamic projections and intra-cortical connections onto cortical cells (Amitai, 2001; Beierlein & Connors, 2002), via comparisons of evoked EPSP properties in both cat and rat preparations, and found that thalamocortical innervation is stronger than intra-cortical innervation. The thalamocortical projection is feed-forward, and we could assume that the intra-cortical projection serves as a feedback projection. By inference, we could conclude that the efficacy of feed-forward projections is always more than that of feedback connections, however this is extremely tentative. The results of a similar study performed in slices

of mouse thalamus and cortex, measured EPSPs and used a poisson model of synaptic release to estimate quantal conductance size. This study indicated that the efficacy of the corticoreticular synapse is higher than that of the corticothalamic synapse (Golshani *et al.*, 2001), and also stated that corticothalamic release is unreliable. Therefore, although the peripheral projection into thalamus is mediated by less synapses, it may be more effective at activating thalamocortical cells.

Nonetheless, were the first-order nuclei of the thalamus simply acting as passive relays of sensory information, it would be logical for their sensory inputs to far outweigh inputs from any other source, both in terms of efficacy and number of synapses. Furthermore, the feedback projection is specific with respect to topography (such that a cortical cell feeds back to the same group of thalamic cells that feed-forward to it), and other functional properties, as recent experiments have found. For example Murphy *et al.* (1999) showed, by recording, mapping and labelling cortical cells in cat V1 and examining the distributions of their axons with respect to the geniculate retinotopic map, that each cortical cell projects back to an anatomically overlaid set of thalamic cells that are aligned parallel or perpendicular to the cortical cell's orientation preference. Other recent results from paired in vivo recordings in the cat LGN and V1, suggest that a cortical cell with a given ON/OFF phase preference directly feeds back to thalamic cells that have the opposite central phase preference (Wang *et al.*, 2004). Therefore, feedback projections have been shown to be specific with respect to two major receptive field properties: phase and orientation. This precise wiring of projections indicates that feedback is serving some specialised role. Were this not the case then feedback projections could be arranged in a diffuse or random manner, which would be more straightforward for the nervous system to achieve.

1.2.2 The postulated role of feedback

Within neural systems, feedback is often responsible for fine tuning activity. Many studies have assigned such a modulatory role to the corticothalamic feedback projection. In this sense, an input can be classified as a modulator as opposed to a driver, and this scheme for describing the inputs to neurons was developed by Sherman & Guillery (1998). A driver plays a direct role in shaping the receptive field of a neuron, whilst a modulator affects the responses of a cell, but does not determine its receptive field properties. Therefore, while it is clear that corticothalamic feedback must have some effect on thalamic responses, it has not yet been shown whether this projection actually determines the form of thalamic receptive fields. In the following three sections, the role of the thalamus and the thalamocortical network in three different states is discussed: in the asleep state, in the awake state, and in the transition between these two states.

1.2.2.1 The asleep state

In the asleep state, the role of the thalamus and the thalamocortical network is understood to be central to the generation and maintenance of sleep oscillations, in particular sleep spindles. Spindle oscillations are observed in electroencephalogram (EEG) recordings during early sleep, and Sejnowski & Destexhe (2000) described spindles as being associated with the "loss of perceptual awareness". Studies have shown that these oscillations are no longer observed if the cortex is disconnected from the thalamus (Steriade *et al.*, 1985), which is not the case for other oscillatory activities such as the slow oscillation (Steriade *et al.*, 1993). Spindle oscillations have been well studied experimentally, and have also served as a favoured thalamocortical activity for theo-

retical studies. These studies are discussed at length in chapter 2, therefore at present it will suffice to say that it is generally accepted that a major role of corticothalamic feedback is to synchronise thalamic activity during spindling (Bal *et al.*, 2000; Contreras *et al.*, 1996; Destexhe *et al.*, 1998, 1999). As the discussion in chapter 2 will show, these previous modelling studies have concentrated more on the ionic properties that bring about the oscillations, and less on the underlying network dynamics intrinsic to the thalamocortical circuitry.

1.2.2.2 The awake state

Theoretical accounts of the role of the thalamocortical network have mostly been developed for sleep states. This is likely to be because its role in active sensory behaviour was assumed for a long time to be one of a passive relay, contributing nothing new to the processing of information. However, due to the new understanding about the potential potency of the cortical feedback projection, studies have appeared in recent years which consider that the thalamocortical network may have an active and dynamic role in sensory processing. In the visual system, many of the computational studies regarding the thalamocortical network have attempted to attribute high level feature extraction to thalamic neurons via feedback (Bickle *et al.*, 1999; Hayot & Tranchina, 2001; Sastry *et al.*, 1999). A more recent computational study by Bressloff & Cowan (2003b) used a mean-field approach to model the thalamocortical feedback circuit in order to investigate cortical orientation tuning. The results of their work indicate that corticogeniculate feedback modulates LGN activity in order to generate a faithful representation of the visual input. However despite this body of work, there remains a trend for the route from the retina to the primary visual cortex to be considered as a direct pathway, where the thalamus acts purely as a relay station.

Despite this trend, the influence of cortical feedback on the processing capabilities of thalamic neurons has started to be explored experimentally. In sensory systems, it is common to describe a neuronal response via a receptive field (RF). The receptive field can be defined as the region of stimulus space that directly modulates a cell's firing rate. There is growing evidence in the literature to suggest that corticothalamic feedback directly alters the RF properties of TC cells (Castro-Alamancos, 2002; Ergenzinger *et al.*, 1998; Ghazanfar *et al.*, 2001; Marrocco *et al.*, 1996; Nicolelis & Fanselow, 2002; Sillito & Jones, 2002), and consequently of cortical cells (Eyding *et al.*, 2003). This is despite the traditional view that TC RFs are determined entirely by feed-forward peripheral inputs. A number of these studies are briefly summarised below.

Much of corticothalamic feedback from the primate somatosensory cortex acts via N-methyl-D-aspartate (NMDA) receptors. In a study of the primate somatosensory system by Ergenzinger *et al.* (1998) the authors found that the chronic administration of an NMDA receptor antagonist into a cortical area responsible for hand representation, blocked much of the stimulus driven activity in this cortical area. They use this fact to investigate the effect of the corticofugal innervation of somatosensory thalamus. Their main finding is that in the somatosensory thalamus of experimental animals, RFs were greatly enlarged compared to in control animals. Therefore, the authors concluded that top-down projections from cortex can cause reorganisation of RFs, however they leave the mechanism for this effect unexplained.

In a later study by Castro-Alamancos (2002), the author investigates the rodent ventral posterior medial nucleus (VPM), a somatosensory nucleus to which input from the whiskers comes via lemniscal terminals. There are also neuromodulatory systems projecting to the VPM, such as cholinergic and noradrenergic fibers, and the concentrations of these neuromodulators are known to increase during activated states. Previous

studies have suggested that the lemniscal pathway may be modulated by these neuromodulators, as the relay of high-frequency activity is regulated by behavioural state. Therefore, the properties of lemniscal synapses in VPM slices were explored and the effects of acetylcholine (ACh) and noradrenaline (NE) were considered, by application of the appropriate antagonists. The neuromodulators were shown to have no direct effect on lemniscal synapses, but did reduce inhibitory post synaptic potentials (IPSPs), and corticothalamic EPSPs. Furthermore, when VPM neurons were at their resting membrane potential, suppression of lemniscal inputs was significant at frequencies greater than 10Hz. However in the presence of ACh or NE, lemniscal inputs at frequencies of up to 40Hz could be relayed. Therefore, the author concludes that these neuromodulators allow the transmission of high-frequency inputs by manipulating other thalamic afferents, particularly the corticothalamic input. Consideration of neuromodulators is beyond the scope of the current thesis, but the work by Castro-Alamancos highlights the ability of such inputs to manipulate the dynamics of the thalamocortical circuitry.

Sillito & Jones (2002) recently discussed to what extent corticothalamic feedback controls the state and transmission mode of thalamocortical cells, and whether the connections between thalamus and cortex are involved in specific sensory processing. They discuss various results from previous experiments. For example, layer 6 cells are known to innervate an area of LGN significantly beyond the location of their own RFs in retinotopic space, therefore they may influence inputs that lie outside of their classical receptive field. They discuss four specific hypotheses with reference to previous results: 1) Feedback enhances the inhibitory surround of the thalamic RF, causing TC cells to exhibit increased patch suppression and end-stopping; 2) Feedback increases stimulus driven synchronous firing between LGN cells; 3) Feedback switches LGN cells between firing modes; 4) Feedback from medial temporal (MT) cortex (an area implicated in

visual motion processing) may influence the transfer of retinal information through the LGN, and may introduce motion sensitivity; In summary, the authors believe that the feedback to the LGN changes the way in which cells respond to visual stimuli, and show that there is mounting evidence to support such a viewpoint.

In a study by Eyding *et al.* (2003), layer 6 corticothalamic projection neurons are eliminated by noninvasive laser illumination without affecting the underlying circuitry of the cat visual cortex. The authors then look at whether the visual responses during various EEG states are affected. They observe that the loss of the neurons causes an increase in activity both in the visual cortex and the LGN during synchronised EEG states, while in less synchronised states, the activity levels remained normal. LGN cells also exhibit less burst firing, which they relate to a decrease in inhibition, as feedback to inhibitory thalamic cells is simultaneously decreased. They also observe an activity-dependent increase in receptive field size in the experimental cortex, which they attribute to intra-cortical interactions as thalamic receptive fields remain unchanged. Therefore, this study also shows that the activity of the thalamocortical network is dynamically modified, this time depending on the EEG state of the animal.

Ghazanfar *et al.* (2001) previously proposed that cortical feedback is intimately involved in the formation of the temporal responses of TC cells. In the rat VPM, TC cells respond best to one whisker "at the earliest poststimulus time and then respond best to another whisker at a later time". Therefore, their spatiotemporal receptive fields (STRFs) are changing over time. The authors of this study investigate the effect of feedback from somatosensory cortex (SI cortex) by measuring VPM responses before and after SI inactivation in anaesthetised cats. While SI cortex was in tact, the STRFs of the VPM neurons are formed by a response pattern consisting of two temporal phases, an early phase and a late phase. When the activation of SI cortex was

effectively eliminated by infusion of muscimol (a GABA-agonist), one or both of these temporal phases may be reduced or eliminated. They propose that the early response of VPM neurons arises from ascending inputs plus the disynaptic pathway from the SI cortex via the TRN, while the late phase arises due to direct SI innervation of the VPM. This model fits their data, and once more suggests that cortical feedback has a key role in altering thalamic responses, but remains hypothetical. The issue of STRFs constitutes a major proportion of the current thesis and is discussed in more detail in chapter 4.

Another subset of studies have specifically shown that cortical feedback selectively enhances thalamic responses, so that particular aspects of feed-forward information are highlighted (Castro-Alamancos, 2004; Murphy & Sillito, 1987; Yan & Suga, 1996; Zhang *et al.*, 1997). This issue was reviewed by Alitto & Usrey (2003), who describe the evidence for such an effect in the three sensory pathways (visual, auditory, somatosensory). This particular idea is termed "egocentric selection" and is the hypothesised ability of cortical neurons to analyse their thalamic inputs and amplify the transmission of selected features via feedback. Therefore, cortical neurons would be able to adjust and improve their own inputs. Evidence for this has been shown in the auditory system of the bat by Suga *et al.* (2000). This has also been suggested to occur in the visual system (Sillito *et al.*, 1994), where feedback was observed to increase the temporal coherence between groups of LGN neurons that are co-activated by a common stimulus. Alitto & Usrey conclude that thalamic neurons are not simple relays of sensory information, but are the components of a complex circuit, which dynamically performs computations during sensory processing.

Therefore in sensory systems, there is a growing understanding that the thalamocortical network is more than a passive relay. However, the specific role of the

thalamocortical monosynaptic feedback loop remains largely unknown and disputed.

1.2.2.3 The transition from the asleep to the awake state

Throughout the sleep/wake cycle neural activity undergoes considerable changes, and the behaviour of the sensory thalamocortical network is no exception. These changes can be considered at different levels of descriptions: there is a switch from hyperpolarised to depolarised membrane potential levels in thalamocortical relay cells (Hirsch *et al.*, 1983); the firing mode of those cells changes from predominantly burst-firing during sleep, to predominantly tonic firing during wakefulness (McCarley *et al.*, 1983); at the functional level this behaviour is observed as oscillations during sleep, and the relay of afferent information during arousal. These changes are well understood in terms of the action of neuromodulators in the thalamus, and the consequent effects on cellular properties (McCormick & Bal, 1994). However, changes in the network dynamics have been less well studied. There have been theoretical studies that have considered the changes which occur in the thalamocortical network during the sleep to wake transition, but these have concentrated on the switch from slow wave sleep oscillations, to the fast non-synchronous activity of awake states (Bazhenov *et al.*, 2002; Hill & Tononi, 2005). These studies will be readdressed in chapter 5, and it is clear that the transition from awake visual processing to the early sleep spindle oscillation has thus far been neglected theoretically, and is consequently less well understood, particularly with respect to the role of corticothalamic feedback.

1.3 Investigating neuronal dynamics

A methodology that has up to now been almost entirely unexplored with respect to the thalamocortical network, is the use of population models to examine the dynamics intrinsic to the neuronal circuitry. This is despite the fact that a range of conductance-based modelling paradigms have been utilised for the analysis of this system, as reviewed in chapter 2. Population models have a useful place in the continuum of theoretical techniques, primarily as they deal with situations where conductance-based or compartmental models are too complex to represent a given level of network connectivity. More importantly, they allow exploration of the nonlinear dynamics of a system based solely on the connectivity. However, there are a number of significant drawbacks that ought to be considered, not only when deciding whether to use population models, but also when considering the results obtained from such models. These limitations will be addressed in detail in later chapters of this thesis.

The population-level approach to modelling has proven to be fruitful in many previous studies, looking at a variety of neuronal systems, and asking a variety of questions. Recent examples include Bressloff & Cowan (2003a); Deco & Rolls (2004); Denham & Borisyuk (2000); Husain *et al.* (2004); Lanyon & Denham (2004). Specifically, Denham & Borisyuk (2000) used such a paradigm to build a model of the septo-hippocampal circuitry and investigated network theta frequency oscillations. A more recent study by Lanyon & Denham (2004) used a population-level description to create a model which investigated the mechanisms that underlie visual attention. These examples show that despite lacking the biophysical details which are vital to the mechanisms at work in the nervous system, population descriptions provide a method of examining the dynamics of neuronal networks, which can explore systems and produce coherent and testable

hypotheses.

This thesis makes specific use of the work of Wilson & Cowan (1972), who derived a set of nonlinear ordinary differential equations to describe interacting populations of excitatory and inhibitory neurons. Wilson & Cowan start their derivation by stating that if "higher functions" of neuronal systems are to be considered, then looking at the level of single cells may not be appropriate. They go on to say that considering the time-varying activity across whole layers of cells is a more realistic approach. They make direct reference to the example of pattern recognition, stating that as this is a "global process" studying local interactions will not give much information. Therefore, they build a modelling paradigm that describes the properties of whole populations of neurons. The derivation of these equations, and the assumptions inherent to it, are discussed in chapter 3.

The major reason to utilise such models, is that they afford one the ability to analyse neuronal systems in terms of the nonlinear dynamics. This is the focus of the current work, and this property of the thalamocortical network has not been considered to this extent previously. However it is a useful first step in the investigation of a neuronal circuit, as it can reveal the dynamics intrinsic to that network. In this thesis, the aim is to consider the activity of the thalamocortical network in two different regimes: sleep and wakefulness. In terms of dynamics, these states translate to a steady state activity, which is oscillations, and transient activity, which are the sensory responses. Therefore the use of population models, which allow direct observation of the neuronal dynamics, is particularly appropriate.

1.3.1 Why computational modelling?

A wider question is why one should use theoretical models in neuroscience at all? Mathematical modelling has a long history in neuroscience, and some of the earliest of such work was undertaken by Hodgkin & Huxley when they proposed a set of equations in order to represent the process of action potential generation in the squid giant axon (Hodgkin & Huxley, 1952). They represented the electrochemical process of spiking in terms of three currents: the fast sodium current; the delayed-rectifier potassium current; and a leakage current. These equations are still widely used in models of neuronal processing, where the aim is to represent neurons generating spikes. From this detailed representation of neuronal activity, there has developed a wide array of modelling techniques for the theoretical analysis of the brain. However the reasons to utilise any such theoretical approach are important to understand, as they affect the choice of paradigm.

There are various reasons which may motivate the production of a model of neural behaviour. The most obvious seems to be in order to replicate the brain and it's functioning. This has interesting implications for discovering how the brain may achieve a behavioural goal, which could then be used for example to design an artificial system to achieve a similar goal. However, this approach has its limitations. A given outcome may be achieved in many ways, and this seems even more likely in the brain with its innumerable connections. Therefore, although a model may be able to show that a specific behaviour can be achieved in a given way, it must be remembered that the brain might produce this behaviour via other substrates, and these should at least be discussed in the context of a proposed model.

Simply to replicate the brain's activity is also not particularly fruitful, as the brain

itself is the best place to observe neuronal activity. However, models can allow experiments to be performed that are difficult practically, and can also allow many different permutations of experimental protocols to be tried in a relatively short amount of time. Therefore such models can prove useful to stimulate ideas, and potentially eliminate less fruitful lines of research. The aim of a study should clearly be used to direct the choice of paradigm, and it is then important to remember the assumptions which are integral to the chosen modelling paradigm, and not to infer too much from the results from a model. If these limitations are considered and the model is validated against experimental data, and other models which are based upon different assumptions, then this approach can be useful to make testable predictions about the activity and the function of the brain.

This thesis makes particular use of population level modelling. This approach is discussed in later chapters when each of the models is presented. Such models homogenise a large group of neurons and represent them via a single equation. This simplification immediately puts limits on the conclusions that can be drawn from such a paradigm. The models developed in this thesis are based upon the available information about the thalamocortical circuit, and the behaviour exhibited by the models is compared to what is seen experimentally and in other computational models of this network. The models' limitations are discussed alongside the results, and conclusions are drawn about the scope of the results. The short comings of the approach are also discussed in chapter 6, with reference to what cannot be explicitly represented. Such critique of the modelling paradigm helps to understand the results in this thesis, and shows what we can learn from the work.

1.4 Research questions

This thesis makes three specific hypotheses regarding the dynamics of the thalamocortical circuitry: 1) The first hypothesis is that the thalamocortical feedback circuit possesses an intrinsic resonant oscillation in the spindle frequency range. This would allow the network to maintain spindling once the oscillation has been generated through the conductances possessed by the thalamic cells; 2) The second hypothesis is that the receptive field properties of thalamocortical relay cells are not only formed by the feed-forward connections from the retina, but also by the feedback innervation from the cortex; 3) The third hypothesis is that a single description of the thalamocortical network can exhibit both spindle range oscillations, and receptive field properties. In order to address these hypotheses, three population-level computational models of the thalamocortical circuit were created. The first model is a simple representation of the thalamocortical network, and was used to investigate the oscillatory dynamics intrinsic to the circuitry. This model was extended to form the second model and to allow for receptive field formation. The third model is a reduction of the second model, as it was intended to find the minimal circuitry to account for the visual responses. Using population level models to answer these questions is useful, as the models are simple enough to contain a small number of parameters, and yet they are complex enough to allow the exploration of the nonlinear circuit dynamics.

The results of the simulations of the spindles model show that the nonlinear dynamics of the connectivity do support oscillations in the spindle frequency range. This basic thalamocortical network also replicates previous experimental findings through the manipulation of these dynamics. The receptive field model also uses a population-level approach, but utilises an extended architecture for the circuitry. Such a biologically

accurate (with respect to anatomical connections and parameter choices) population model of the sensory thalamocortical network has not been attempted in the past. The dynamics of the thalamocortical network in the extended receptive field model, particularly the pattern of anti-phase feedback connectivity found by Wang *et al.* (2004) and described in chapter 4, are shown to be involved in strengthening the thalamic temporal response. The third model replicates both the transient receptive field activity, and the sustained oscillatory activity in the spindle range. Furthermore, the model reveals that the circuitry must undergo a transition in order to link these two activities. This transition is related to a relative switch in the weight of cortical feedback to the thalamocortical, and the reticular cells, which is consistent with previous studies (Destexhe *et al.*, 1998; le Masson *et al.*, 2002). Therefore, this thesis demonstrates that the examination of the dynamics of the thalamocortical network provides robust answers to the questions that have surrounded this neural structure for decades.

1.5 Structure of the thesis

In order to present these results, the structure of this thesis is as follows: the next chapter will discuss the previous theoretical studies that have contributed to an understanding of the involvement of the thalamocortical network in spindle oscillations. In this chapter the deficiencies of these studies is also brought to light and the need for a population-level description is demonstrated. In chapter 3 the specific methodological approach used is described in detail. Following this, the results from the spindles model are presented and discussed. Chapter 4 considers studies which have measured the spatiotemporal receptive fields of thalamocortical relay cells. The failure of subsequent studies to fully explain this STRF is discussed, and the necessity for the receptive field

model is explicated. The description of the receptive field model is then given, and the results that arise from the behaviour of this model are presented and discussed. This model is then simplified in order to create the third model. The results from the simulations of this reduced model are also presented here. In chapter 5 the motivation for using the third model to look at both visual responses and sleep oscillations is presented, with reference to previous studies surrounding the sleep/wake transition in the thalamocortical network. This unified model is described, and the results of simulations in a transient receptive field mode and sustained spindle mode are presented and discussed. Finally, chapter 6 presents the general discussion and conclusions of the thesis, including section 6.5 which outlines the details of future work that could be undertaken to answer the specific questions that have arisen from this thesis.

Chapter 2

Theoretical background to the spindle oscillation

2.1 What are spindle oscillations?

Spindling is a periodic neural activity with a frequency in the range of 7 to 14 Hz. It has been observed both in the thalamus and the cortex during periods of early sleep and drowsiness. Spindles consist of rhythmic high-frequency (200Hz) bursts of action potentials, lasting for 1 to 3 seconds and recurring every 3 to 10 seconds. (Steriade & Deschenes, 1984). Hence they are often described as a waxing-and-waning oscillation. Spindle oscillations are thought to originate from intra-thalamic circuitry, primarily because decorticated thalamic slices exhibit spindles (von Krosigk *et al.*, 1993) as does the isolated TRN (Steriade *et al.*, 1987).

The mechanism behind spindling is now well understood due to various experimental and theoretical studies (for example see Bal *et al.* (1995b); Steriade *et al.* (1993); von Krosigk *et al.* (1993)). During spindle oscillations, neurons of the GABAergic thalamic reticular nucleus (TRN) generate rhythmic (7-14 Hz) spike-bursts that are

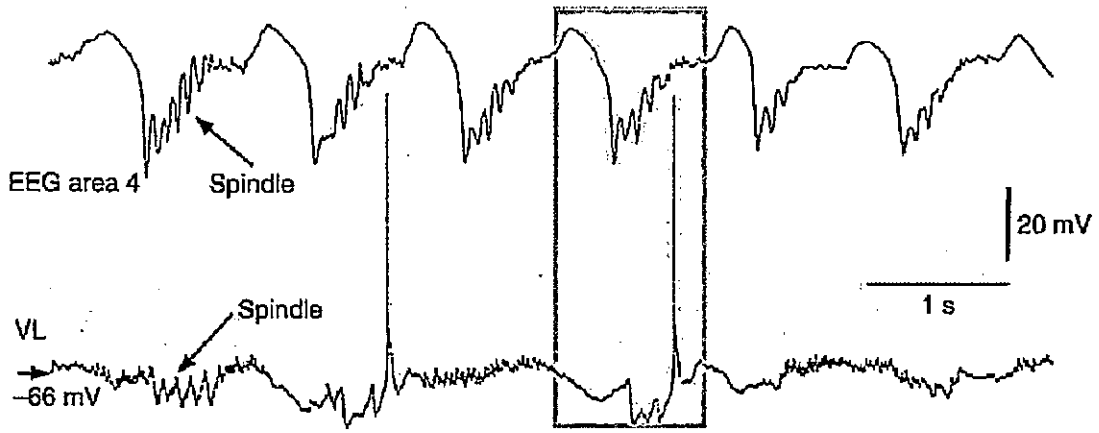

Figure 2.1: EEG recording and corresponding intracellular recording of spindle oscillations made from the ventrolateral (VL) nucleus of the cat thalamus. Reproduced from Timofeev & Steriade (1997).

superimposed on a depolarising envelope. When thalamocortical (TC) cells are sufficiently hyperpolarised, the low threshold Calcium (Ca^{2+}) current (I_T) is de-inactivated. Therefore, IPSPs generated by the reticular (RE) cells cause the TC cells to fire rebound bursts (which consist of action potentials crowning a Ca^{2+} spike). Once initiated in the thalamus, these oscillations are transmitted to the cortex where they induce rhythmic EPSPs, which are the origin of the spindle oscillations observed in the EEG. A typical EEG recording is shown in figure 2.1, and the high-frequency bursting is clearly seen.

There has been a great deal of speculation regarding the roles of the two firing modes of thalamic cells, the burst mode and the tonic mode. Burst firing occurs when a cell is hyperpolarised for a sufficiently long period of time, and this firing mode has historically been considered to occur during sleep states. Tonic firing occurs at depolarised membrane potentials and allows thalamic cells to respond linearly to an input (Reinagel *et al.*, 1999). Therefore, sleep spindle oscillations occur while the thalamic cells are in the burst firing mode, and tonic mode is dominant (though not

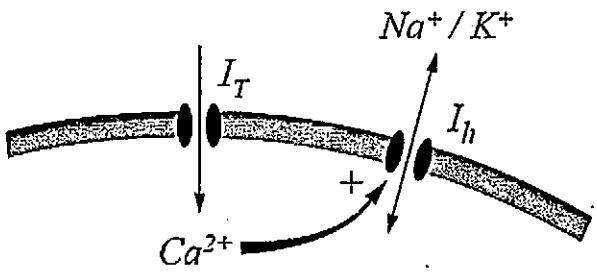

Figure 2.2: The inclusion of the I_T and I_h currents in a single compartment model by Destexhe *et al.* (1993) is schematised in this figure.

necessarily exclusive, see Sherman (2001); Swadlow & Gusev (2001)) during awake states, when the accurate relay of visual information is important.

Due to their appearance during early sleep, spindle oscillations were thought to be indicative of cortical inactivity, as while spindling thalamic cells do not faithfully relay the peripheral sensory input. However, recently it has been proposed by Steriade & Timofeev (2003) that sleep oscillations could represent periods of considerable mental processing and possibly also memory consolidation. Furthermore, studies of oscillatory brain states have implications for research into pathological conditions such as epilepsy (Suffczynski *et al.*, 2001). Therefore, the interest in spindle oscillations exists not just due to their use as a prototype thalamocortical activity, but also because of their role in the normal functioning of the brain.

The waxing-and-waning property of spindling was an unresolved issue for a long time. This property can be clearly seen in the recordings shown in figure 2.3. The cause for this phenomenon was predicted to be due to the regulation of the level of intracellular calcium in the TC cells by a modelling study by Destexhe *et al.* (1993). The model in this study consisted of a single-compartment model of a TC cell, which

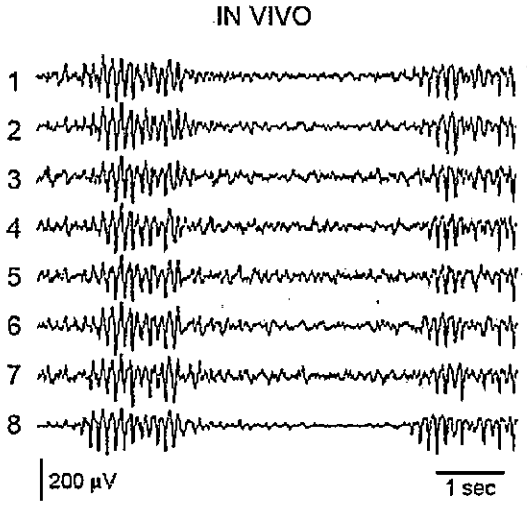

Figure 2.3: The waxing-and-waning of spindling can be seen in this figure of in vivo recordings from the intact cat thalamus. Reproduced from Contreras *et al.* (1996).

contained a number of different currents, in particular I_h and I_T, two currents which are considered to be crucial to the generation of spindles in thalamic cells. Figure 2.2 is taken from Destexhe *et al.* (1993), and this figure shows the arrangement of the currents in the model. This model showed how the I_T current allows calcium ions to enter the cell, and bind to the I_h channel, therefore changing its current voltage properties. At the time of this model there existed an alternative view which stated that the cause of the waxing-and-waning was due to the divergence of the connectivity between the thalamocortical cells and the reticular cells (Steriade *et al.*, 1993). Since the prediction of Destexhe *et al.* (1993) was verified experimentally by Luthi & McCormick (1998), there has been little further debate regarding this issue.

Since spindles are inseparable from the thalamic circuitry, it was thought that the cortex did not play a significant part in this oscillation. However, it has been proposed

that the role of the cortical feedback is to regulate and synchronise the oscillation (Bal *et al.*, 2000; Contreras *et al.*, 1997b; Destexhe *et al.*, 1998). Spontaneous spindle sequences appear almost simultaneously in both the thalamus and the neocortex. Therefore, it is likely that the spontaneous cortical activity imposes this near simultaneity of spindles throughout the thalamus (Contreras *et al.*, 1997a).

The discussion surrounding spindle oscillations has lead to both physiological and theoretical studies looking into the factors affecting the oscillation. The previous modelling studies have mainly used compartmental models containing various types of ionic conductances, and a number of such models are discussed below in more detail. The next section is not meant as an exhaustive survey of the literature, but rather a discussion of how models of the spindle oscillation have evolved, and to what extent the main features of spindling have been captured through such theoretical studies.

2.2 Previous theoretical studies of spindle oscillations

Spindle oscillations are a favoured thalamocortical activity for computational modellers, mainly because the mechanisms which underly this activity are well understood. As discussed above, early descriptions of this oscillation only considered the contribution of thalamic circuitry. One such theoretical model of spindling by von Krosigk *et al.* (1993), considered the dominant role of the TRN in particular, as the authors stated that "the dependence on the activity of relay neurons is unclear".

The authors first presented results from intra- and extra-cellular recordings of spindles in slices of ferret thalamus. They observed periodic inhibitory postsynaptic potentials (IPSPs) in relay cells, which are occasionally followed by rebound bursts. Figure 2.4 shows the occurrence of IPSPs in intracellular relay cell recordings by Steriade *et al.*

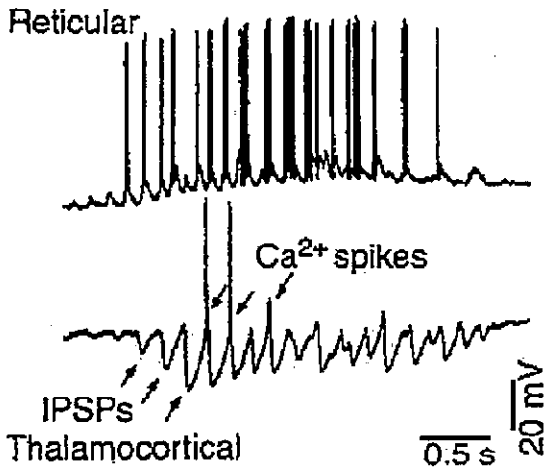

Figure 2.4: This figure, reproduced from Steriade *et al.* (1993), shows the intracellular recording of a single cycle of a spindle oscillation. The figure clearly indicates the occurrence of IPSPs in the TC cell recording, which are occasionally followed by a calcium spike.

(1993), some of which are followed by calcium spikes. When the recorded relay cells were depolarised by current injection, the bursts no longer appeared. This supports the idea that the bursts occur due to the low threshold calcium current I_T, which requires a hyperpolarised membrane in order to be de-inactivated (Jahnsen & Llinas, 1984a,b). Conversely, they measured excitatory postsynaptic potentials (EPSPs) in the RE cells, and these were synchronous with the bursts observed in the relay cells.

Hence, von Krosigk *et al.* proposed the following model for spindle generation: RE neurons become active and initiate IPSPs in TC cells. As a result of this inhibition, I_T is de-inactivated which allows relay cells to fire a low threshold calcium spike and a burst of action potentials at the offset of the IPSP. These bursting relay cells depolarise the RE cells, activating I_T, and triggering bursts of action potentials. They went on to propose that the waxing-and-waning of spindles is due to the hyperpolarisation of RE cells through a calcium sensitive potassium current. In addition, they suggested

that the synchronisation of this oscillation between neighbouring cells in PGN (the visual sector of the TRN) or neighbouring LGN laminae, results from a large overlap in afferent and efferent connections i.e. the convergence and divergence of connections.

This was a very influential study for the understanding of spindling. The authors accounted well for their experimental observations with a minimal model containing only thalamic elements, as was the expectation at the time. Furthermore, they also made predictions about the cause of the synchronisation of the oscillations, as well as the property of waxing-and-waning.

This theoretical model was soon simulated computationally by Destexhe *et al.* (1993), using two single-compartment neurons containing Hodgkin-Huxley type currents. In this paper, the authors showed that the model TC cell displays both slow oscillations (in the 0.5-4Hz range), and waxing-and-waning slow oscillations. Closer inspection showed that this occurs due to an interaction of the I_T and I_h currents, which is consistent with experimental observations, for example by Soltesz *et al.* (1991). I_h is a hyperpolarisation-activated inward rectifying current, and this current was hypothesised to play a major role in the generation of spindles, and particularly in the waxing-and-waning behaviour. Similarly, the RE cell model replicates experimentally observed (Avanzini *et al.*, 1989) periodic bursts at 8-12Hz, which occur due to I_T and a calcium dependent potassium current.

When these two model cells were mutually connected via inhibitory $GABA_A$ (for the RE to TC connections) and excitatory non-NMDA synapses (for the TC to RE connections), this network shows 8-10Hz spindle oscillations. The details of the spindling observed in the model, such as the "depolarising envelope" seen in the RE cell response and the "hyperpolarising envelope" in the TC cell, echoed the results presented by von Krosigk *et al.* (1993). This is a good indication that the modelling of

this network is accurate compared with the experimental results. The results of the von Krosigk *et al.* model, and in particular the observation of the cyclical pattern of rebound bursts between the TC and RE cells, proved to be a major step in showing how the spindle oscillation could be initiated in the RE nucleus and transmitted to the TC cells.

Another model which considered this two cell thalamic network, was produced by Wang *et al.* (1995). This model contained a population of single compartment TC cells, interconnected with a population of single-compartment RE-cells. Both populations contained a number of ionic currents. The authors showed that this large-scale model displays spindle range oscillations which are dependent on the reciprocal connectivity between the TC and RE cells. Furthermore, in the model the synchrony of the oscillation is dependent upon the convergence factor of the TC-RE connectivity. Hence, this model agrees with the predictions of von Krosigk *et al.* (1993) by showing that the oscillations in the model obtain synchrony when the amount of convergence in the RE to TC connections exceeds a threshold level.

The models discussed thus far have not considered the role of the cortex in the mechanism for spindling, even though Morison & Bassett (1945) proposed many years earlier that the cortex could be involved. It was not until a study by Contreras *et al.* (1996), that the authors asked what specific role the feedback from cortex to thalamus could have in spindling. By making recordings in the thalamus of cats under barbiturate anaesthesia, they found that with the cortex removed spindle oscillations no longer displayed long range synchrony within the thalamus, but only local synchrony between cells which were at close proximity to one another. The first model where this influence was considered appeared just a short time later in a study by Destexhe *et al.* (1998).

In this study, Destexhe *et al.* presented increasingly complex models of the spindling

thalamocortical network, and showed that in these models the synchronising effect of corticothalamic feedback is apparent. The models all contain single compartment neuronal elements, and they utilise four different cell types in total: excitatory cortical pyramidal (PY) cells, inhibitory cortical interneurons, TC cells, and RE cells. The main result of this paper is that cortical feedback is responsible for the observed coherence between individual TC cells of spindle oscillations. However, this effect only occurs if cortical feedback onto RE cells is stronger than that onto the TC cells. When this is the case, TC cell activity shows an IPSP-EPSP sequence that is crucial for the maintained synchrony of the oscillation. This idea of "dominant inhibition" recurs in later studies by the same authors, and also in other modelling studies (for example in le Masson *et al.* (2002), which is discussed below). The suggestion that this pattern of activation exists during spindling, was given credence by a study which measured the quantal amplitudes related to the synapses mediating feedback to TC and RE cells (Golshani *et al.*, 2001), which was discussed in chapter 1.

A later paper by Destexhe *et al.* (1999) that utilised a very similar network, also looked at the mechanisms underlying the large-scale synchrony of spindles within the thalamus during three different neural states: (1) natural sleep, (2) barbiturate anaesthesia, and (3) natural sleep with depressed cortex. The authors observed that during natural sleep there is good synchrony between the various neuronal populations, but in the latter two states there are multiple initiation sites for the oscillations within the TC cell layer, which results in less synchrony. They suggested that these differences are to do with the variable excitability of the cortex, such that the more excitable the cortex is, the more coherent the oscillations seem to be. This idea was pursued in a later paper by Bal *et al.* (2000), where an almost identical model is used, but feedback is modelled as an input to the thalamic cells and not explicitly by a layer of cortical

cells. They showed that increasing the strength of feedback in the model, results in an increase in the synchrony of oscillations. They went on to show that this is also observed in vitro, in thalamic slices from the ferret brain. Therefore, these studies collectively showed that corticothalamic feedback is intimately linked with the observed synchrony of spindle oscillations.

The studies discussed thus far have elucidated many features of the activity in the thalamocortical network during spindle oscillations. In the final studies reviewed here another important characteristic of the thalamocortical network is focussed upon, that is its ability to switch between different modes. A paper by Terman *et al.* (1996) describes a small-scale thalamocortical model, and investigates the transition from spindling to delta sleep rhythms. The delta rhythm is a 1-4Hz oscillation observed during deep sleep. The paper points out that as the same network of RE cells, TC cells, and cortical cells is thought to produce both of these sleep rhythms, the same mechanism ought to be responsible for the two oscillations, and that the switch between them occurs as a result of functional reorganisation within the circuitry.

The model consists of a population of 10 TC cells, a single RE cell and a cortex modelled by a single oscillator. All excitatory connections are mediated by AMPA synapses, and the inhibitory connections are mediated by both $GABA_A$ and $GABA_B$ synapses. The RE cell contains an I_T current, a long lasting after hyperpolarisation (AHP) current, and two leak currents. The TC cells contain I_T, I_h, and two leak currents. They show that a change in the intrinsic properties of the RE cells transforms the action of predominantly $GABA_A$ inhibition to predominantly $GABA_B$ inhibition, and consequently causes a switch from spindling to delta oscillations.

This issue of switching between spindles and slower frequency activity comes up often, both experimentally and in a subset of the studies discussed above. For example,

von Krosigk *et al.* showed that spindles are transformed into a slower (2 to 4Hz) activity if $GABA_A$ inhibition is reduced (by application of the $GABA_A$ antagonist bicuculline methiodide). By then applying a $GABA_B$ antagonist they go on to show that this occurs because $GABA_B$ inhibition, which acts over longer time scales, becomes the dominant form of inhibition. This behaviour was also replicated in two of the modelling studies discussed above (Bal *et al.*, 2000; Destexhe *et al.*, 1993).

Finally, le Masson *et al.* (2002) recently used an interesting combination of experimental and theoretical methods to investigate the thalamocortical network. Their hybrid network consisted of a thalamocortical cell recorded in vitro from guinea-pig or ferret slice preparations, attached to a computational model of an RE cell. They demonstrate that there is a selective relay of sensory information through the TC cell, which depends upon inhibition from the RE cell. When the inhibitory feedback loop between the TC and RE cell has a gain greater than a critical value, the circuit tends towards oscillations resembling spindles. This causes a decorrelation of retinal input and TC cell output, hence the cortex is effectively cut-off from sensory input. However, low feedback gain in the TC-RE loop and the action of noradrenaline, work together to relay sensory information to the cortex faithfully. This occurs when the TC cells fire predominantly in tonic mode, therefore are able to code their inputs linearly in their firing rates. This model therefore predicts that strong intra-thalamic inhibition is necessary for spindles, and the authors propose that this intra-thalamic inhibition may be driven by cortical afferents, therefore agreeing with the requirement for dominant inhibition, and predicting that dominant excitation is required for the relay of sensory information.

There have been other studies in which the theoretical treatment of the 7-12 Hz spindle oscillation has formed a constituent part. However, those that have been re-

counted here show the development of the main issues regarding spindles using similar computational paradigms. These reports have gone far in aiding and inspiring experimental research of this early sleep oscillation. However, the next section discusses whether a different approach could inject a fresh perspective into this matter.

2.2.1 The gap in the literature

The studies discussed above have explained the mechanism behind spindling extremely well, from the initial proposal of interconnected RE and TC cells, to a putative role for corticothalamic feedback. However, the spindle oscillation could also be examined at a different level of complexity, that is via population-level modelling. Doing so would allow the investigation of the intrinsic nonlinear dynamics of the thalamocortical loop to become easily accessible. The structure of this feedback loop could be examined to see whether it is able to support spindle frequency oscillations by the interaction of its component excitatory and inhibitory cell populations.

Population models, were originally developed to minimise the amount of complexity inherent to conductance-based dynamics in compartmental neuronal models. It was also thought that, due to the large numbers of neurons involved in neural activity, systems ought to be modelled by large-scale populations rather than considering the effect of a small number of detailed components. Such models have previously been successfully used in numerous studies of neuronal systems to both test and expand upon experimental hypotheses (for example see Bressloff & Cowan (2003a); Deco & Rolls (2004) and section 1.3).

Having established which neuronal properties contribute to the initiation and propagation of the spindle oscillation, the use of such population modelling of the thalamocortical network can allow larger scale questions to be addressed. The most central

of these questions is whether or not spindles are supported by the dynamics of a basic thalamocortical network. That is, once they are generated by the ionic mechanisms outlined in the studies discussed above, does the thalamocortical network resonate at this frequency and help to sustain this oscillation?

Other questions involve the relative importance of the various connectivities within the circuit. Although these questions could all be addressed in compartmental models, a population model allows the global effect of the manipulation of connections to be observed. An advantage of population-level models is also their much lower computational cost, as well as the possibility of connecting a number of such models to form large-scale, high-level representations of neural activity. Another major benefit is the ability to utilise bifurcation analysis to investigate the nonlinear dynamics of the model within the parameter space. This is an additional way to consider the relative effects of connections on the network behaviour, and also provides a good indication of the robustness of the activity with respect to parameter manipulations. This last point is discussed in more detail in the next chapter.

In order to address and answer these questions, the Wilson-Cowan equations for the dynamics of neuronal populations were used to describe a thalamocortical network (Wilson & Cowan, 1972). This is the simplest representation of the thalamocortical feedback network that could address these questions. Such population dynamics have been used previously to look at oscillatory behaviour, in different network configurations, and this issue is re-addressed in the next chapter after the presentation of the proposed model (see section 3.2.6). A recent study by Robinson *et al.* (2002) also used a purely population-level approach to investigate a variety of pathological oscillatory activities in the thalamocortical network. Though this study used a similar approach to that proposed here, it differs significantly from the aim of this work, as here the

interest is in the intrinsic resonant behaviour of the healthy thalamocortical network. In the next chapter, the methodology is outlined, with respect to the specific form and equations for the model. This is followed by presentation and discussion of the results of the simulations of this model.

2.3 Summary

In this chapter it has been shown that previous computational models of the spindle oscillation have used conductance-based descriptions. These studies have been invaluable for uncovering the ionic details of the mechanisms that are central to spindling, but are too detailed to consider the network dynamics. Population models are a useful method of looking at the nonlinear dynamics involved in neuronal activity. In the following chapter, the thalamocortical feedback circuit is represented by a set of Wilson-Cowan equations, and the nonlinear dynamics of such a system are tested to see if they support oscillations in the 7-14Hz spindle range.

Chapter 3

A model of the spindle oscillation

3.1 Introduction

A number of previous theoretical studies of the spindling thalamocortical network have exclusively used ionic models, and concentrated on elucidating the conductances underlying spindling (as reviewed in section 2.2). Although these models have been extremely successful at achieving this aim, they have not addressed a fundamental question regarding this neural activity: that is, whether the intrinsic nonlinear dynamics of the thalamocortical network possess a resonant oscillatory activity within the 7-14Hz spindle range.

In order to address this issue, the existence of a spindle range oscillation was examined as an activity supported solely by the dynamics of a simple thalamo-reticulocortical circuit model, which is described in the next section. Using a population-level description of neuronal dynamics means that the major factor influencing the behaviour of this circuit model is the interaction between the excitatory and inhibitory cell populations and not ionic mechanisms. Furthermore, only the essential cell types and details of connectivity are preserved in the architecture of the model. In the current chapter,

results from the simulations of such a model show that a 7-14Hz range oscillation is supported by this network, and that the attributes and manipulations of this oscillation are consistent with previous results from both experimental and theoretical studies.

3.2 Methods

3.2.1 Architecture of the spindles model

The cell types that are involved in the generation and maintenance of spindle oscillations, were clearly outlined in a review paper by Steriade *et al.* (1993). The paper discusses various types of thalamocortical oscillations and their underlying mechanisms. When describing spindling the authors refer to the "main players" as two types of thalamic cells: thalamocortical relay cells, and thalamic reticular cells. In addition, they stress that cortical pyramidal cells are an important component of the circuitry. Although the cortex was not always thought to be crucial for spindle oscillations, the current knowledge clearly indicates that cortical cells have a central role in the spatiotemporal properties of the spindle oscillation (as discussed chapter 2). Hence, the neuronal classes that were considered for the present model are in accordance with those described above: TC cells, cortical pyramidal (PY) cells and RE cells. No other cell types were considered, as this study aimed to elucidate the minimal circuit required to support spindles.

The thalamus contains two types of nuclei, as classified by Sherman & Gullery (2001). First-order nuclei are the sensory nuclei that receive information from peripheral sensors and relay it to the cortex. Higher-order nuclei are involved in transmitting information within circuits between various cortical areas. Most of the data available about spindling in the thalamus and the thalamocortical circuit originates from ex-

periments performed in the cat lateral geniculate nucleus (LGN). Therefore, the LGN, visual TRN (or perigeniculate nucleus), and layer 6 of cortical area V1 are the specific components of the model thalamocortical system described here. Hence, in the following description the term "thalamus" refers specifically to the LGN.

Having defined the cell types (and particular nuclei) that are considered to be important for this study, the connections between the various populations must also be defined. The structure and connectivity of first order nuclei has been described previously (Jones, 1985; Sherman & Guillery, 2002), and is now extremely well known. The TRN surrounds much of the dorsolateral and anterior thalamus. The GABAergic cells in this nucleus receive collaterals from both thalamocortical and corticothalamic projections. In turn, RE cells innervate the excitatory cells of the LGN. The TRN has been considered to have a crucial, yet unknown role in mediating the activity in the thalamocortical network (for example Crick (1984); McAlonan & Brown (2002); Montero (2000)). The central position it holds, monitoring both the ascending and descending flow of information, is the main reason that such views exist.

In addition to this intra-thalamic circuitry, there is the feedback loop between the LGN and V1. The connections to, from, and within V1 have also been clearly mapped, as described by Thomson & Bannister (2003). The TC cells of the LGN, feed visual information forward to both layers 4 and 6 of the primary visual cortex. The thalamic innervation of layer 4 is synaptically more numerous than that of layer 6 (Bannister *et al.*, 2002). After traversing the intra-cortical circuitry, thalamic information reaches layer 6 via an alternative route: the information is passed from layer 4 to layers 2/3, from layers 2/3 to layer 5, and finally from layer 5 to layer 6. The LGN receives a feedback projection from V1, from the corticothalamic cells found in layer 6. In this study, finding the minimal model required to support spindle range oscillations is of

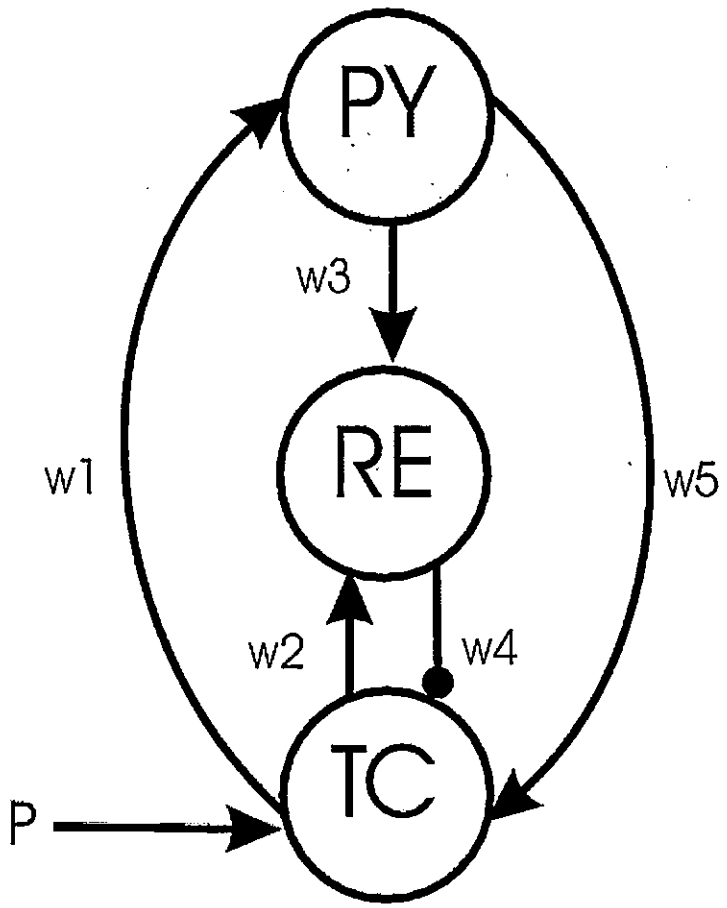

Figure 3.1: The minimal architecture required to represent the thalamocortical network. Three cell types are represented: excitatory cortical pyramidal cells (PY), inhibitory thalamic reticular cells (RE), and excitatory thalamocortical relay cells (TC). Connections between cell populations have an associated weight parameter, and are all excitatory (labelled by a triangular arrowhead $\rightarrow$) except for a single inhibitory connection (labelled by a circular arrowhead $-\bullet$).

interest. Therefore only the monosynaptic feedback loop between TC cells in the LGN and the excitatory cells in layer 6 of V1 is considered, in addition to the TRN, and this circuit is schematised in figure 3.1.

The model contains a single population to represent each type of neuron. Again this is to keep the model as simple as possible, in order to examine the intrinsic dynamics of the network. The figure also shows a driving force, which acts upon the TC cells and is labelled "P". P represents an intrinsic membrane property of TC cells, which is the ability of the TC cells to fire rebound bursts following hyperpolarisation (Deschenes *et al.*, 1984). The use of the input P ensures that the TC cell population becomes depolarised following the decay of inhibition by the RE cell population. Therefore, it acts in the same way as de-inactivation of the low threshold calcium current I_T, which brings the TC cell to firing threshold so that it may fire bursts of action potentials crowning a low-threshold calcium spike (Jahnsen & Llinas, 1984a,b).

In summary, the model architecture takes into account only those neuronal types that have been shown to be essential for the initiation and maintenance of spindle oscillations. These are layer 6 pyramidal cells in V1, inhibitory cells of the TRN and the excitatory thalamic relay cells of the LGN. The architecture defined here, is similar to many of the previous theoretical models of spindling, as discussed in section 2.2. However, in its deliberate sparseness, the model described here deviates sharply from its predecessors.

3.2.2 The Wilson-Cowan equations

The Wilson-Cowan equations for the nonlinear dynamics of the activity of neural populations (Wilson & Cowan, 1972) have been used to represent the thalamocortical network presented above. A full mathematical derivation of these equations will not

be relayed here, but the main steps highlighting the crucial assumptions that the authors made, are recounted in this section. The starting premise is that in the analysis of higher level activities of the brain, the properties of interacting populations of neurons are of interest. In particular, Wilson & Cowan state that information in the sensory modalities is relayed via "large-scale spatiotemporal activity in sheets of cells", therefore their aim is to describe a model that accounts for these global population dynamics of neural activity.

The initial assumptions are outlined here:

1. Cells within a population are assumed to be in close spatial proximity. Their interconnections are assumed to be random but dense enough so there is at least one path (direct or via interneurons) between any two cells in a population.

2. Spatial interactions within populations are overlooked, therefore the model deals only with the temporal dynamics of a population.

3. Wilson & Cowan chose the relevant variable to be the proportion of cells in a population which become active per unit time. Therefore, single cell activity is represented by a rate code and not by the timing of individual spikes.

4. Finally, they assume that all neural activity of any complexity is dependent upon the mutual interaction between excitatory and inhibitory cells.

Hence, they define the dynamic variables representing the activity of populations to be $E(t)$ and $I(t)$, for excitatory and inhibitory populations respectively. By definition, $E(t)=0$ and $I(t)=0$ are resting states, which represent a low-level background firing or a spontaneous firing rate. Therefore, small negative values of these variables represent a suppression of resting activity.

Wilson & Cowan derive the functions $Z_p(x)$ (where $p{=}i$ for inhibitory, or $p{=}e$ for excitatory populations) which are called the response functions. These functions represent the proportion of cells firing in a population for a given level of input activity x. The response functions can be derived by assuming that the population has a distribution of neural thresholds, and that all cells receive the same average excitation $x(t)$. Alternatively, $Z_p(x)$ can be found by assuming that the cells in a population all have the same threshold, but that there is a distribution of the number of afferent synapses per cell. Either approach leads to the response function having the form of a monotonically non-decreasing sigmoid function as shown in Wilson & Cowan (1972), and as defined by equation 3.1.

$$Z_p(x) = \frac{1}{1+\exp(-b_p(x-\theta_p))} - \frac{1}{1+\exp(b_p\theta_p)} \tag{3.1}$$

Here θ_p and b_p are constants, and x is the level of input activity. Following Wilson & Cowan, the following values are used for these constants throughout this thesis: $\theta_e = 1.3$, $b_e = 4$, $\theta_i = 2.0$, and $b_i = 3.7$.

Wilson & Cowan assume that cells sum their inputs and that the effect of stimulation decays over time. They introduce the idea of "connectivity coefficients" (c_n) where n is the number labelling a given connection. Effectively these are the weights (or strengths) associated with each connection. In practice these parameters are chosen using various types of experimental data, as described in section 3.2.4 below.

The authors consider what proportion of cells are sensitive in the period (t+τ), and subsequently receive supra-threshold excitation at time t. The next main assumption is that the probability that a cell population is sensitive, meaning not refractory, is independent of the probability that it is excited above threshold. This allows them

to neglect the inclusion of a term to account for this correlation. There are then two final steps in the derivation. The first involves time coarse-graining, which averages out rapid temporal variations over a time-scale of τ. The second entails stating that the steady state solution (i.e. the solution in the absence of external inputs) ought to be zero, which is satisfied by defining $Z_p(0) = 0$. Hence, they arrive at equations 3.2 and 3.3, for the dynamics of an excitatory and an inhibitory population respectively.

$$\tau_e \frac{dE}{dt} = -E + (k_e - r_e E) \cdot Z_e(c_1 E - c_2 I + P) \tag{3.2}$$

$$\tau_i \frac{dI}{dt} = -I + (k_i - r_i I) \cdot Z_i(c_3 E - c_4 I + Q) \tag{3.3}$$

The constant r_p (where p=e or p=i) is set to be equal to 1, where $r_p P$ (P=E or P=I) represents the probability that a cell is refractory. k_p is defined to be the maximal value of the functions Z_p, such that $k_p = Z_p(\infty)$.

Therefore, the Wilson and Cowan type equations for the three cell populations that are considered in this study (as described in section 3.2.1), are shown in equations 3.4 to 3.6. Where E_{PY}, I_{RE}, and E_{TC} are the dynamic variables representing the neural

activity of the PY, RE and TC populations respectively.

$$\tau_1 \frac{dE_{PY}}{dt} = -E_{PY}(t) + (k_e - E_{PY}(t)) \cdot Z_e(w1 \cdot E_{TC}(t)) \tag{3.4}$$

$$\tau_2 \frac{dI_{RE}}{dt} = -I_{RE}(t) + (k_i - I_{RE}(t)) \cdot Z_i(w2 \cdot E_{TC}(t) + w3 \cdot E_{PY}(t)) \tag{3.5}$$

$$\tau_3 \frac{dE_{TC}}{dt} = -E_{TC}(t) + (k_e - E_{TC}(t)) \cdot Z_e(-w4 \cdot I_{RE}(t) + w5 \cdot E_{PY6}(t) + P) \tag{3.6}$$

Here τ_n, where n is 1 to 3, are the time constants of the PY, RE, and TC populations respectively. $w1$ is the TC to PY connection weight, $w2$ is the TC to RE connection weight, $w3$ is the PY to RE connection weight, $w4$ is the RE to TC connection weight, and $w5$ is the PY to TC connection weight, as schematised in figure 3.1.

3.2.3 Criticism of the Wilson-Cowan paradigm

Although in the previous section the assumptions made during the derivation of the equations were explained, this section highlights the main criticism of this modelling paradigm, which lies with the parameters. The Wilson-Cowan equations contain two main types of parameters that must be defined by the user: τ and w.

τ represents the time constant of the change in the proportion of non-refractory cells which are firing in a population, in response to the change in the average membrane potential activity of the cells. The τ parameter has been assumed in previous studies to be equivalent to the membrane time constant of the particular cell type, as in Tsodyks *et al.* (1997) and Denham & Borisyuk (2000). However, the time required for a change

in the firing of a cell, also relies upon synaptic delays and synaptic time constants, and such effects are not considered if τ is equal to the membrane time constant.

Similarly, the weight parameters w are assigned values relative to the other weight parameters in the model, based on various types of physiological data (as described in section 3.2.4 below), but there is no direct physiologically measurable value which is equivalent to w. Furthermore there is often insufficient data about the numbers of synapses, strengths of synapses, and reliability of synaptic transmission, which mediate the various connections in the brain.

The fact that the parameter choices will to some extent be fairly arbitrary, can be defended against criticism if the user takes appropriate measures. For example, in the current study the relative parameter choices have been chosen (section 3.2.4) using a variety of physiological data, and are therefore linked to the relative strengths of these connections in the brain. Furthermore, given that parameter choices are subject to error, the range of parameters for which a given result is observed can be tested. If the result is robust then parameter perturbations within these ranges do not affect the observation of the result. In the current study, parameter ranges were tested by bifurcation analysis, which is explained in section 3.2.5.

3.2.4 The choice of parameters

As stated in the previous section, the τ parameter is usually set to be equal to the membrane time constant, and is therefore set within 10 and 20ms (Tsodyks *et al.*, 1997). For thalamic cells a wide range of values for the membrane time constant have been measured. For TC cells, the observed range is 5 to 64ms (Turner *et al.*, 1997; Ulrich & Huguenard, 1996), for RE cells it is 13 to 53ms (Landisman *et al.*, 2002; Ulrich & Huguenard, 1996), and for cortical cells it is 7 to 22ms (Anderson *et al.*, 2000; Hirsch

et al., 1998, 2002). The time constants that were chosen for the populations lie within each observed range.

The weights of each connection type also need to be assigned. There is a great deal of evidence from physiological experiments that can be used to determine the relative connection strengths. For example, the number of synapses serving a connection type, and the efficacy of synaptic transmission between populations. The data that was used in this study is as follows: the corticothalamic (CT) projections to RE cells are stronger than the CT projections to TC cells (Golshani *et al.*, 2001); the strength and reliability of TC to RE projections (Contreras *et al.*, 1993; Gentet & Ulrich, 2003); the relative strength of the thalamocortical projections (TC to PY cells) compared to the feedback corticothalamic projections (Castro-Alamancos & Calcagnotto, 2001); studies which specify the numbers of synapses from each afferent, for example van Horn *et al.* (2000), show that the greatest number of synaptic contacts onto TC cells are cortical in origin; the fact that RE cells send most of their outputs to innervate TC cells (Wang *et al.*, 2001). Hence, the selected parameter values for the model reflect the above findings in respect of their relative magnitudes.

3.2.5 Bifurcation analysis

The Wilson-Cowan model discussed in section 3.2.2 is described by a system of coupled ordinary differential equations (ODEs). These equations contain a number of free parameters, which can be fixed by considering the evidence from the literature, as described in the previous section. However, the effect of parameter changes on the evolution of dynamical regimes in the model is an important consideration. For such a system of nonlinear ODEs, the point at which the right-hand side of the system is equal to zero, is called a fixed point (also known as an equilibrium point, the steady

state, etc). If we consider the following set of autonomous ODEs:

$$\dot{x} = f(x, \alpha) \tag{3.7}$$

where $f(x, \alpha)$ is a nonlinear vector function; x represents the dynamic variables; α represents the parameters of the system; $x \in \mathbb{R}^n$; $\alpha \in \mathbb{R}^k$.

To find a fixed point, the following equations have to be solved for fixed α:

$$f(x_0, \alpha) = 0 \tag{3.8}$$

where x_0 is a fixed point of the system. If we consider a small neighbourhood around x_0, the nature of the fixed point's stability can be accurately defined. The fixed point is asymptotically stable if there exists a sphere around x_0, such that all trajectories starting within this sphere tend to x_0, as time tends to infinity.

To formulate a criterion of stability, the system of nonlinear ODEs in equation 3.7 can be linearised in the region $x_0 + h$, where h represents a small perturbation from x_0, in the following way:

$$\begin{aligned} h &= x - x_0 \\ so \quad \dot{h} &= \dot{x} \\ &= f(x_0 + h, \alpha) = f(x_0, \alpha) + \left(\left(\frac{\partial f_i}{\partial x_j} \right)_{ij} \right)_{x_0} \cdot h + higher\ order\ terms \end{aligned}$$

If we neglect all higher order terms, then the following linear equation governs the system dynamics, near x_0:

$$\dot{h} = Ah \tag{3.9}$$

where A is the Jacobian matrix of the system at the fixed point. We can assume a solution of the form $h = h_0 e^{-\lambda t}$, and substitute this into equation 3.9 to obtain $\lambda h_0 e^{\lambda t} = A h_0 e^{\lambda t}$, or $\lambda h_0 = A h_0$, and the latter is the standard eigenvalue equation. Here λ represents the eigenvalues of the Jacobian matrix, and h_0 represents the corresponding eigenvectors. Therefore, if the eigenvalues of the Jacobian matrix are less than zero, $e^{-\lambda t}$ tends to zero, and the trajectory tends to x_0. Hence the fixed point is asymptotically stable (see Strogatz (1994) for more details).

For a given system of equations, the nature of such fixed points can change as the parameters of the system are varied. If a fixed point changes stability, appears, or disappears we say that a bifurcation has occurred. At points of bifurcation the behaviour of a system changes in a way that depends upon which type of bifurcation has happened. There are a number of types of bifurcations possible, and the type of simple bifurcations that may occur can be classified by the eigenvalues of the linearised system.

This study considers whether a nonlinear, autonomous system can support oscillations. An important type of bifurcation to consider when looking at oscillatory behaviour, is the Andronov-Hopf (A-H) bifurcation. This type of bifurcation is characterised by a pair of eigenvalues crossing the imaginary axis on a complex plane. For example at a stable fixed point of the system, the eigenvalues all have negative real parts. As the parameters of the system vary, an Andronov-Hopf bifurcation may occur, and the fixed point will become unstable due to the two eigenvalues (which crossed the imaginary axis) having positive real parts after the bifurcation occurs. At the point of an Andronov-Hopf bifurcation, a particular type of trajectory can appear in the neighbourhood of the fixed point. This trajectory is called a limit cycle, which is an isolated closed curve. Rotation along the limit cycle is periodic, and hence oscillatory

behaviour is encountered.

Let us suppose that α_{cr} denotes the value of the parameter which corresponds to an A-H bifurcation, such that for $\alpha < \alpha_{cr}$ the fixed point is stable. If the Andronov-Hopf bifurcation is super-critical, then for $\alpha > \alpha_{cr}$ the fixed point is unstable and a stable limit cycle appears. If the A-H bifurcation is sub-critical, then for $\alpha > \alpha_{cr}$ the fixed point is unstable, and an unstable limit cycle appears in the region where $\alpha < \alpha_{cr}$.

Note that oscillatory behaviour can also arise when a saddle-node on an invariant circle (SNIC) bifurcation occurs. In the latter case, the frequency of oscillations tends to infinity near the critical bifurcation point. This type of bifurcation will not be discussed at length here, as the thalamocortical circuit investigated was not observed to encounter a SNIC bifurcation in the parameter space. However more details about this type of bifurcation can be found in Kuznetsov (1998); Strogatz (1994).

Computational methods of finding bifurcations are often based on the center manifold theory. This theory allows an n-dimensional system to be reduced to two-dimensions, nearby of an Andronov-Hopf bifurcation point. This theory will not be discussed here, but more details can be found in chapter 5 of Kuznetsov (1998). Based on this theory, we can plot bifurcation curves of an autonomous system by exploring the stability of equilibrium points. One way of doing this is to use an automated system for bifurcation analysis such as LOCBIF (Khibnik *et al.*, 1993). This package starts by finding a fixed point in the system equations, and can then vary a single parameter systematically whilst keeping all other parameters static. The parameter space can be assessed in this way to find bifurcation points. If a bifurcation point is located, it can be taken as the new starting point of the system. Through another procedure of systematic parameter variations, this time varying pairs of parameters at a time, we can define parameter sets which are critical for that bifurcation to occur. If this is done

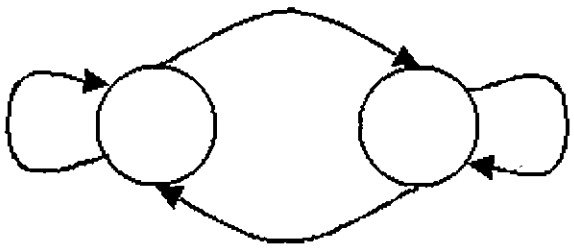

Figure 3.2: This figure shows a schematic figure of the two population excitatory-inhibitory model which constitutes the Wilson-Cowan oscillator.

for an Andronov-Hopf bifurcation, the oscillatory regions within the parameter space can be found. Hence, this can be used to analyse a given oscillating system, and test the robustness of this particular behaviour.

3.2.6 Previous population models of oscillations

A final step before presenting the results from the proposed model, is to consider additional theoretical studies of oscillations. There are previous population-type models which have investigated oscillatory behaviour arising in such networks. The simplest of which is often referred to as the "Wilson-Cowan oscillator", and this network consists of an excitatory-inhibitory pair of interconnected populations, which Wilson & Cowan based the derivation of their equations upon (see section 3.2.2). This network is shown schematically in figure 3.2, and has been examined in the subsequent literature. One particular example is presented in Dayan & Abbott (2001), where this model is analysed with specific reference to oscillatory activity. The authors discuss how the existence of oscillations can be examined by linearising the system in the neighbourhood of a fixed point, as explained in the previous section (3.2.5). The dependence of the dynamics on parameter values are then explored with reference to the eigenvalues of the Jacobian matrix.

The equations that Dayan & Abbott analyse are similar to the original Wilson-Cowan equations, except that a threshold is used in place of a sigmoid function. The parameters are set at initial values, and setting the right-hand side of the equations to zero allows the authors to find the equilibrium points of the system of equations. They therefore show that there exists a single equilibrium point. The authors maintain the weight parameters at constant values and look at the effect of varying the time constant of the inhibitory population on the activity. They present the "stability" matrix for the system, which is equivalent to the Jacobian matrix defined in the previous section. They describe how the eigenvalues of the Jacobian reflect the activity of the network, such that if the real part of all of the eigenvalues are negative the equilibrium point is stable. If the stability of the equilibrium point changes, a bifurcation occurs. By examining the eigenvalues of this system, they show that increasing the time constant of the inhibitory population from its initial value causes the system to undergo an Andronov-Hopf bifurcation, and display oscillations.

Dayan & Abbott go on to discuss a model of the olfactory bulb by Li & Hopfield (1989). This model consists of a layer of inhibitory cells and a layer of excitatory cells which are interconnected. There are ascending excitatory sensory inputs to the excitatory cells, and top-down excitatory cortical inputs to the inhibitory cells. Li & Hopfield represent this network by two coupled ODEs, and show that the oscillatory behaviour seen in the olfactory bulb can be replicated by the dynamically changing value of cortical innervation. These two previous studies clearly show how linearising a system of ODEs near an equilibrium point yields useful information about the dynamic behaviour of that system. Both these examples used two coupled equations, and therefore analysed a 2 by 2 Jacobian matrix.

The current model contains three populations, and therefore linearising in the region

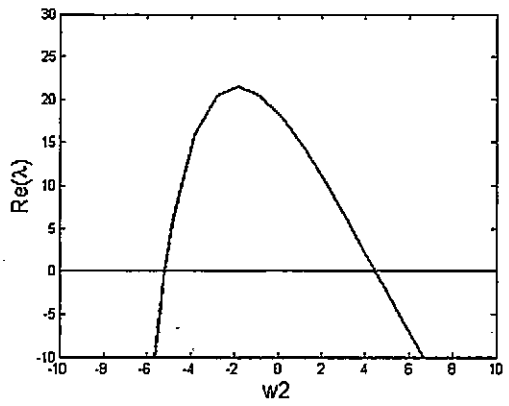

Figure 3.3: This figure shows the relationship between the real part of an eigenvalue, and the weight parameter w2. The equilibrium point is unstable ($Re(\lambda)$ is positive) if w2 is less than approximately 4.

of an equilibrium point gives a 3 by 3 Jacobian matrix. This is more complex to determine and find trends for the eigenvalues with respect to the parameters. Therefore, the current study used LOCBIF (see previous section) to numerically find the Jacobian and its eigenvalues for equations 3.4 to 3.6. As LOCBIF calculates the eigenvalues at each point whilst varying one or two parameters, it is possible to observe the change in dynamics as a change in the stability of the linearised system as done by Dayan & Abbott (2001), and Li & Hopfield (1989). An example of this is shown in figure 3.3 where the real part of one of the eigenvalues changes from negative (indicating a stable equilibrium point) to positive (indicating that the equilibrium point has lost stability) as the parameter w2 changes. This loss of stability is indicative of the occurrence of the Andronov-Hopf bifurcation, and therefore oscillations. It is interesting to observe the change in eigenvalues when examining a change in the activity of the model, and therefore this theoretical approach will be used to alongside the experimental results in section 3.3.8.

3.3 Results

3.3.1 Main result - a 7-14 Hz oscillation

As described in the previous section, the architecture of the model, involves a simple thalamo-reticulo-cortical network (see figure 3.1) consisting of only three cell populations: an excitatory cortical pyramidal cell population (PY cells), an inhibitory thalamic reticular cell population (RE cells), and an excitatory thalamocortical relay cell population (TC cells). Hence, the network is represented by three coupled differential equations (equations 3.4 to 3.6). The parameters, representing both the time constants of each cell population and the weight of each connection, were set such that the constraints outlined in section 3.2.4 were adhered to. These parameters were then explored within the ranges permitted by these constraints, and oscillatory activity was observed. At this point the model parameters were set at the values shown in table 3.1. From here onwards this set of parameters will be referred to as the control parameters for this model.

The oscillation observed had a frequency of approximately 10Hz, which is within the spindle range of 7-14Hz. The activities of the three populations are shown separately and on a single plot in figure 3.4. Figure 3.5 shows a close-up view of the activity, and it is clear that the populations are almost in phase with one another. The peaks marked by straight lines in figure 3.5 show that the populations are within 18ms of one another. Previous studies have reported that cortical and thalamic activity during spindling, is simultaneous within up to 100ms (Destexhe *et al.*, 1998; Verzeano & Negishi, 1960).

This synchronous oscillatory behaviour seen throughout the thalamocortical network is consistent with previous experimental (Contreras *et al.*, 1996, 1997a) and modelling studies (Destexhe *et al.*, 1998, 1999). These earlier studies reported that the

Parameter name	Value
τ_1	20ms
τ_2	20ms
τ_3	20ms
w1	12
w2	4
w3	14
w4	8
w5	10
P	3

Table 3.1: The table shows the parameters used in the spindles model. These parameters are in line with the constraints set by physiological studies, as described in section 3.2.4.

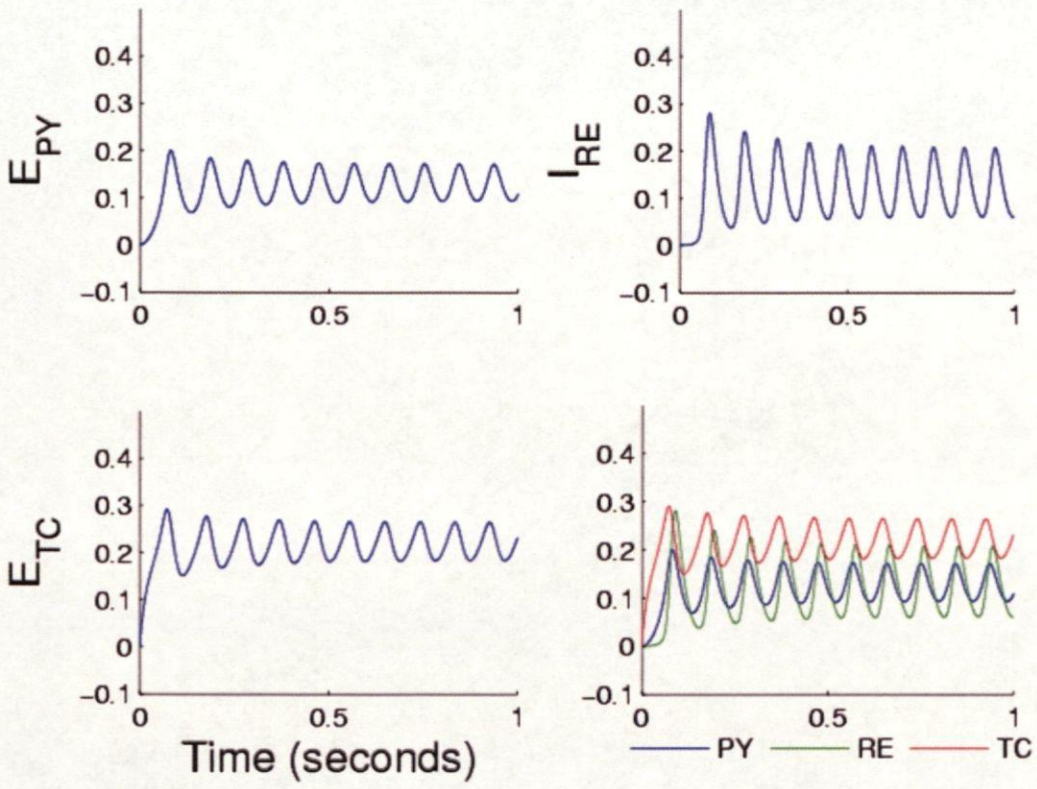

Figure 3.4: The model displayed robust oscillatory behaviour with a frequency of approximately 10Hz. All populations oscillated at the same frequency as shown here.

spindle oscillation is synchronised across cortical and thalamic cell populations, which is attributed to the influence of cortical innervation of thalamic cells. Furthermore, in the current model the TC cell population leads the oscillation. This is also consistent with previous simulation results, as can be seen in figure 4 of Destexhe *et al.* (1998), and figure 5 of Destexhe *et al.* (1999). This result also agrees with the idea that spindles are instigated by "initiator" TC cells, as proposed by Destexhe *et al.* (1998).

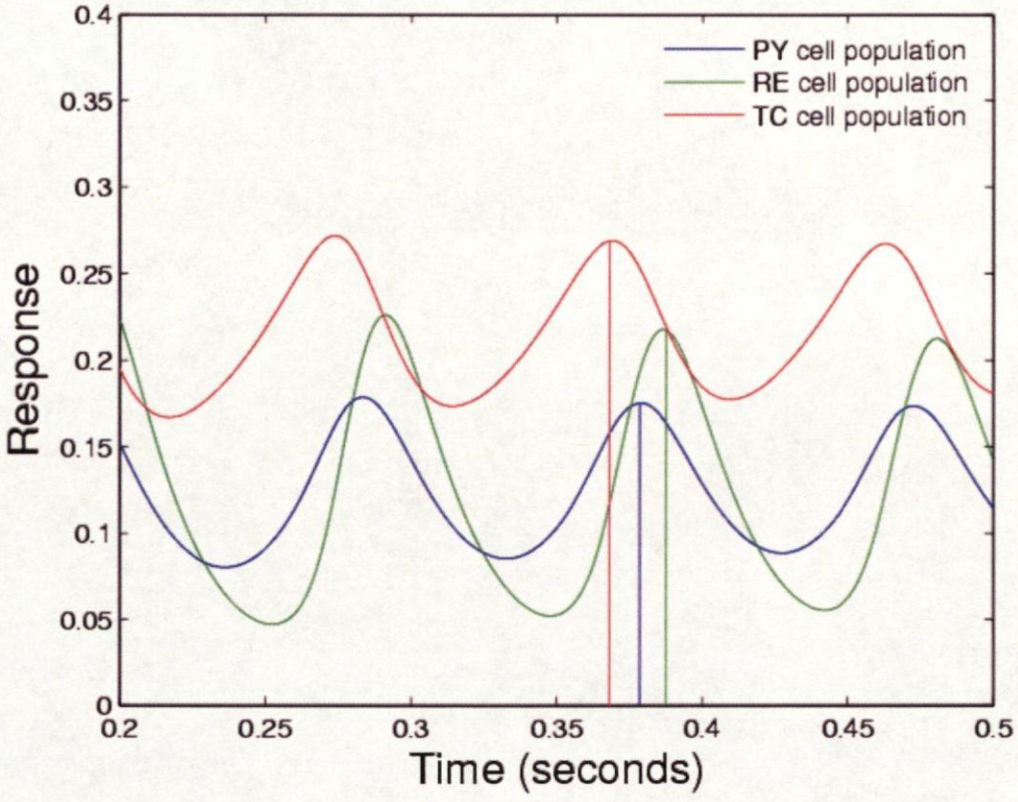

Figure 3.5: The oscillatory behaviour displayed by the three cell populations in the model was almost in phase. The figure shows that their activity was separated by less than 18ms overall (where response refers to E_{PY}, I_{RE} or E_{TC}).

3.3.2 Bifurcation analysis results

This spindle range oscillatory activity was observed for a large range of parameter values. Therefore, it was necessary to quantify the robustness of the oscillation with respect to variations from the control parameters (shown in table 3.1). This was done by using bifurcation analysis to investigate the differential equations that describe the network (equations 3.4 to 3.6). An automated package called LOCBIF (Khibnik *et al.*, 1993) was used, which finds equilibrium points in the phase space of a system of nonlinear differential equations, and investigates the effect of varying parameters on the nature of such points, as described in section 3.2.5.

Through the use of this software, it became clear that oscillatory activity in the model arises when an Andronov-Hopf bifurcation occurs in the parameter space. The software can trace the curves of Andronov-Hopf points, which will be referred to as bifurcation diagrams. In order to do this, the software first locates a single Andronov-Hopf bifurcation point of the system whilst varying a single parameter and tracing a curve of equilibrium points. The eigenvalues of the system are calculated at each equilibrium point on the plotted curve. The eigenvalues at the critical point of an Andronov-Hopf bifurcation, must fulfil the following requirements: the real parts of two of the three eigenvalues are zero, and the imaginary parts (of the same two eigenvalues) are equal and opposite. That is, they are a complex conjugate pair, with zero real part. Therefore the software checks for the existence of such a point, by testing whether the sum of a pair of purely imaginary eigenvalues is zero. These conditions are summarised

in equations 3.10 to equations 3.12 below:

$$\lambda_1 = +i\beta \tag{3.10}$$

$$\lambda_2 = -i\beta \tag{3.11}$$

$$\lambda_1 + \lambda_2 = 0 \tag{3.12}$$

Starting from the located Andronov-Hopf point, the bifurcation curves can then be traced as required. Two parameters are varied simultaneously, whilst all other parameters are kept at control values (table 3.1). In this way, still using the condition set out in equation 3.12, a curve of Andronov-Hopf bifurcation points can be traced. All points on one side of such a curve represent a stable equilibrium and the points on the other represent an unstable equilibrium. Depending on whether the bifurcation is subcritical or supercritical, there either exists an unstable limit cycle nearby of the curve on the side of the stable equilibrium, or a stable limit cycle on the side of the unstable equilibrium. During the analysis of the model, the software reports that a supercritical Andronov-Hopf bifurcation has occurred. Therefore, a bifurcation curve separates the oscillatory region from the non-oscillatory region of the parameter space, because there exists stable limit cycles near the bifurcation curve. Note that it is also necessary to check the oscillatory regions by trial of parameter pairs, to investigate whether the entire region is oscillatory, or if only regions near the curve are oscillatory.

Bifurcation curves for all combinations of the model's connection weight parameters, are shown in figures 3.6 and 3.7, and for the time constant parameters in figure 3.8. Pairs of parameters within the regions were tested, and it was found that not all regions were oscillatory. This issue is re-addressed in section 3.3.3, where it is shown that this is due to the occurrence of another type of bifurcation. Generally, the plots show that the

parameters are not tightly confined around their control values. Hence, within feasible parameter ranges the values can vary and the network will still produce oscillations. This is an important consideration for the robustness of the result, showing that the oscillations do not only occur for one fixed set of parameters, but for a flexible range of values.

When these plots are considered in more detail, a number of interesting features of the model's behaviour come to light, and the plots in figure 3.6 show the most interesting relationships between the model's weight parameters. The time constant plots show that oscillations are possible for a wide range of physiologically viable values of τ_2 and τ_3. However, this is not the case for τ_1 which is the time constant for the cortical pyramidal cell population. This can be clearly seen in the (τ_1, τ_3) plot (figure 3.8(c)) where τ_1 is constrained to a value of less than approximately 22ms. This suggests that pyramidal cells, which are believed to have a central role in the control of spindling (see section 2.2), have a relatively restricted range for their time constant parameter. Hence, the oscillatory behaviour in this model is dependent upon the temporal properties of the cortical cells. This is consistent with the idea that PY6 cells have an influence on the temporal properties of spindling, as reviewed in section 2.2.

w2 is the weight parameter of the TC to RE connection, and w3 mediates the PY to RE connection. In the (w2, w3) parameter space, the oscillatory region is bound by the w3 axis, as shown in figure 3.6(b). While w3 can take a reasonably wide range of values, w2 is tightly constrained to be less than a value of approximately 5. w2 and w3 are the two excitatory inputs to the inhibitory RE population. The limited range of values that these parameters can take shows a necessity for a controlled level of inhibition in the network. This plot also shows the dispensability of w2, as while it is clear that w2 can be set to zero and oscillations are maintained, this is not the case

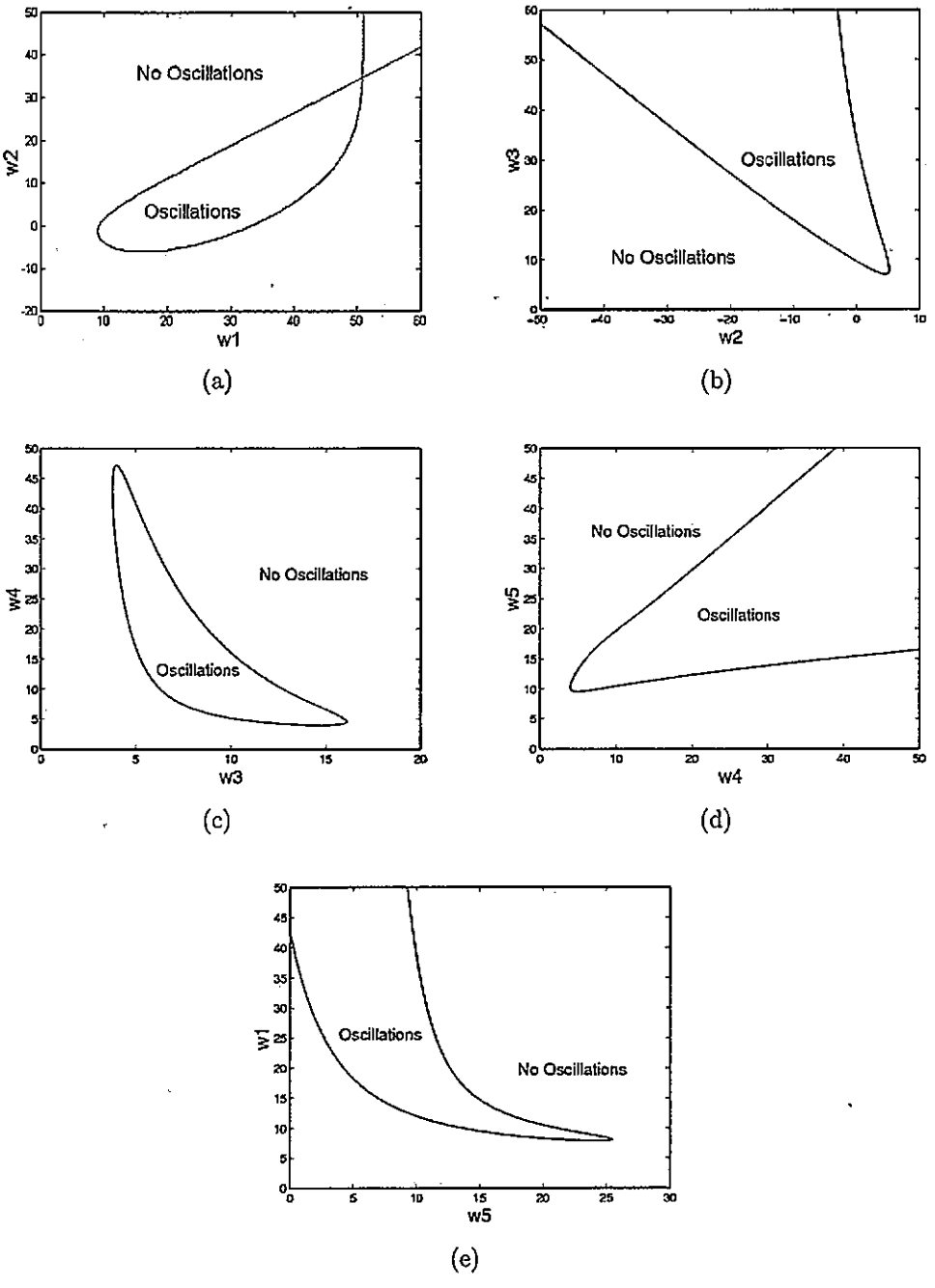

Figure 3.6: Bifurcation curves in the parameter planes of the following pairs of connection weights: (a) w1 and w2, (b) w2 and w3, (c) w3 and w4, (d) w4 and w5, and (e) w5 and w1. These plots show the curves of parameter pairs for which an Andronov-Hopf bifurcation occurs in the system, and therefore they separate the oscillatory from the non-oscillatory regions as labelled.

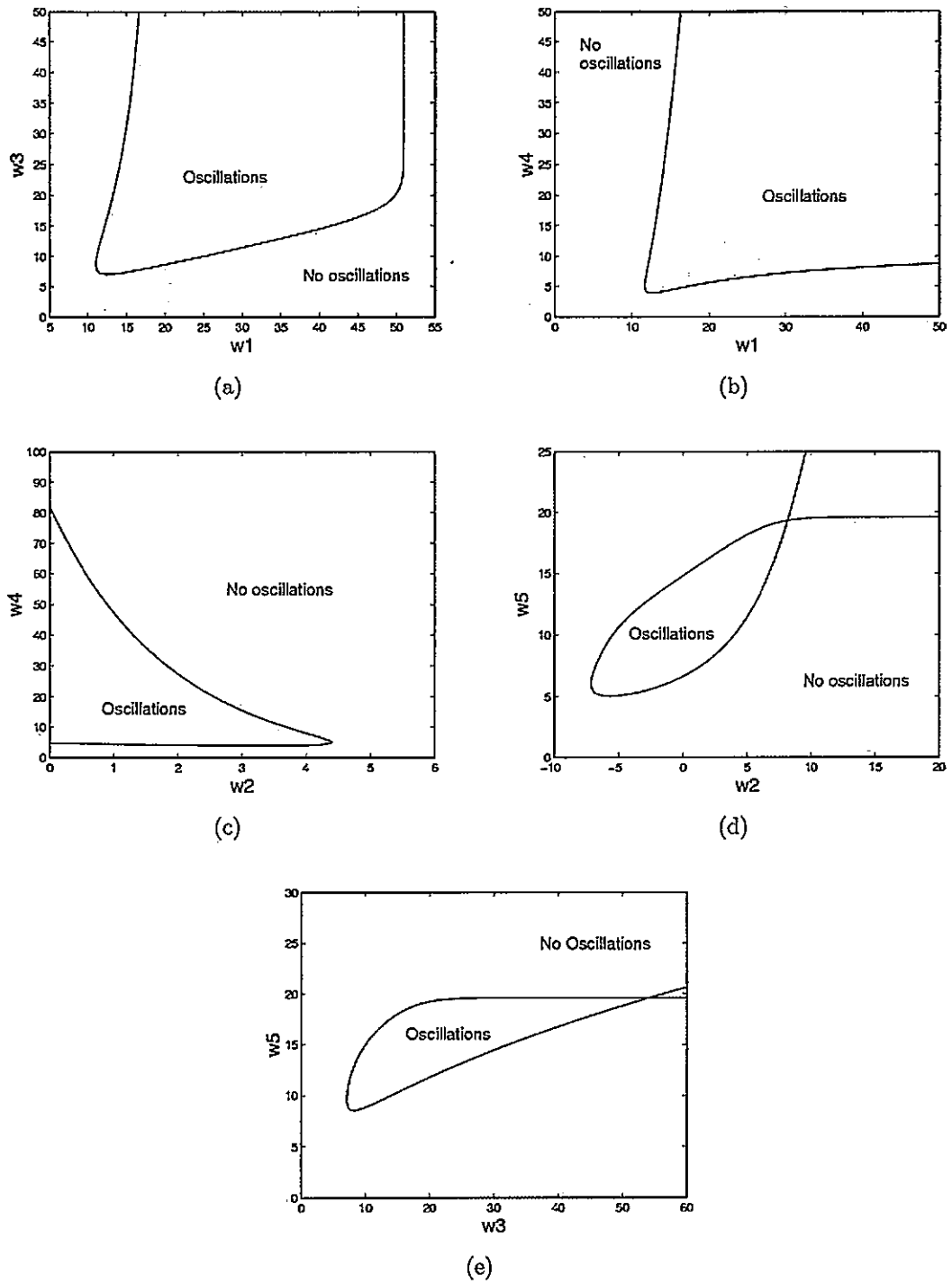

Figure 3.7: Bifurcation curves in the parameter planes of the following pairs of connection weights: (a) w1 and w3, (b) w1 and w4, (c) w2 and w4, (d) w2 and w5, and (e) w3 and w5.

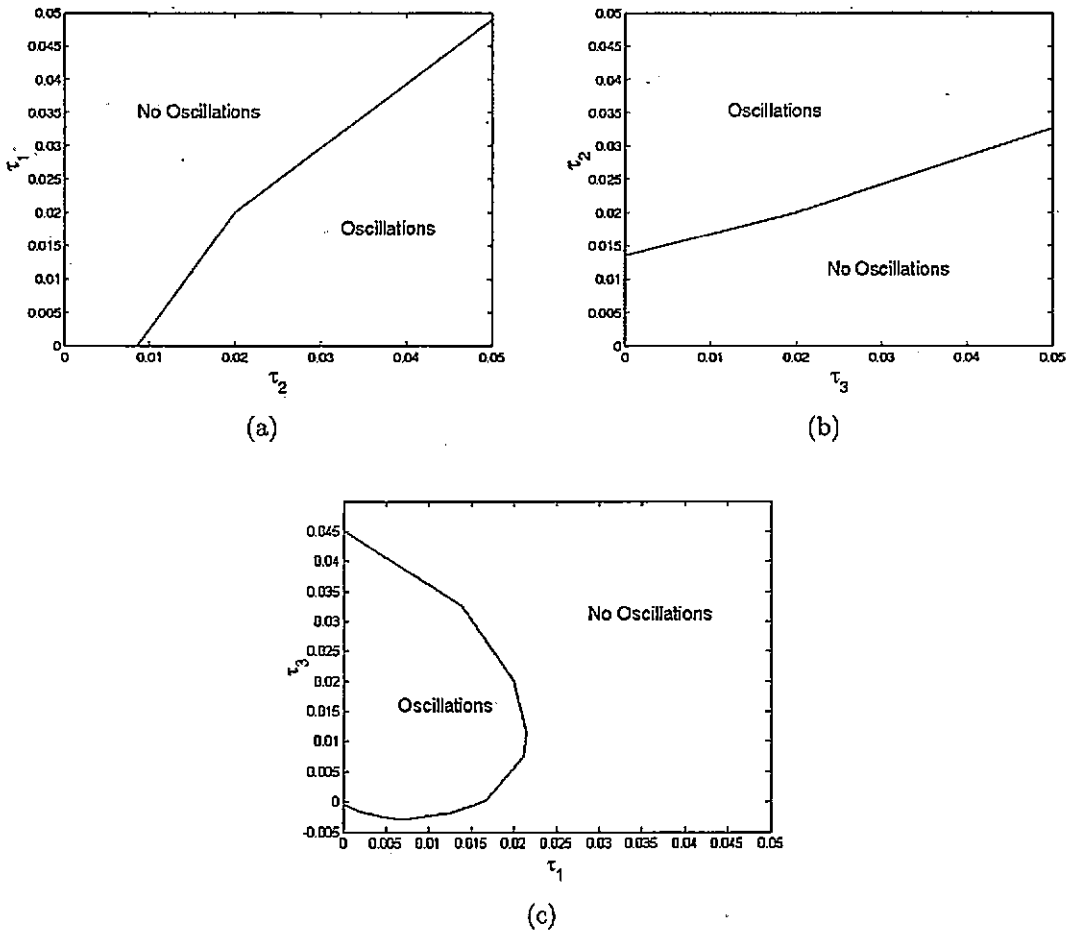

Figure 3.8: Bifurcation curves in the parameter spaces of the following pairs of time constants: (a) τ_1 and τ_2, (b) τ_2 and τ_3, (c) τ_3 and τ_1. These plots only show the bifurcation curves for positive values of the time constants.

for w3. This can also be seen in the (w2, w4) and (w2, w5) parameter spaces (figure 3.7). No other parameter is expendable in this way, and this is discussed in more detail below.

The w2 parameter may also be responsible for constraining activity in the (w1, w2) parameter space. From figure 3.6(a) it is clear that w1 and w2, which represent the strength of the excitatory connections from the TC population to the cortical PY and reticular RE populations respectively, are constrained to a relatively small range of values. This indicates that the strengths of TC cell projections may play a significant role in determining whether or not spindle oscillations occur. TC cells, and therefore the strength of their projections, are modified during arousal through the action of neuromodulators such as acetylcholine (Steriade *et al.*, 1997). This cholinergic innervation causes increased firing rates and greater excitability in the TC cells, and therefore also in their cortical targets (Dossi *et al.*, 1991; Steriade, 2000). Hence, it may be that the increased excitation of TC cells and consequently of the cortical and reticular cells, is a major factor in terminating spindling activity in the network during the transition from sleep to awake states.

Related to this idea is the relationship that exists between the strength of the cortical excitation of the RE cells, (w3 referred to as the corticoreticular projection) and the strength of the RE cell inhibition of the TC cells (w4). The reciprocal relationship between these parameters, which is necessary for maintaining oscillatory activity in the model, is shown by the bifurcation diagram in figure 3.6(c). Therefore, the model suggests that the hyperpolarising effect of cholinergic innervation of RE cells (Steriade *et al.*, 1997) which would decrease RE firing and therefore decrease the strength of the reticular innervation of the TC cells (and so less w4), would need to be accompanied by an increase in corticoreticular excitation in order for spindle oscillations to be

maintained.

w4 and w5 represent the two inputs (from the RE and PY cell populations respectively) to the TC cell population. The bifurcation diagram for the parameter space defined by these two weights shows that they are not restricted a great deal with respect to one another (figure 3.6(d)). Hence, relative to the control set of parameters shown in table 3.1, w4 and w5 can take much bigger values compared to the rest of the parameters, and oscillations will be maintained (provided that the two parameters are increased simultaneously). However for fixed w4, w5 is limited in the range of values it can take. Hence the balance between these two inputs is important for the existence of oscillations, such that too much cortical feedback to the TC cell population without a corresponding increase in inhibition from the reticular cell population, would eliminate spindling. This is related to the requirement for dominant inhibition, which was discussed in section 2.2 in relation to previous studies, and will be dealt with below.

w1 and w5 are the two parameters that mediate the connections between the TC cells in the thalamus and the cortical PY cells. w1 is the feed-forward, TC to PY, connection weight, and w5 is the feedback, PY to TC, connection weight. The (w5, w1) parameter plot shows that for small positive values of w5, w1 can be large (and can be greater than the range shown in figure 3.6(e)). However, for a fixed value of w1, w5 is constrained to a limited range of values. Similarly, for larger values of w5 there is a tight control over the range of values that w1 can take. The reciprocal relationship between these parameters indicates the importance of a balanced monosynaptic feedback loop for spindling in the model, and therefore in the dynamics of the entire network.

A major theme to emerge from these results is that of balance. In several cases, the two parameters represented within a plot impose some form of restriction on one another. This concept of balance is crucial to the maintenance of the spindle frequency

oscillation in the model, and indicates that though the parameters can vary, they can only vary relatively to one another. This in turn implies that there is a specific region in the multi-dimensional parameter space where spindle range oscillatory activity is maintained. This is expected as the oscillatory parameter space should be restricted to physiologically acceptable ranges, and not encompass all possible values. This link between the individual bifurcation plots and the experimental data that was presented in section 3.2.4, is discussed in detail in section 3.3.5 below.

3.3.3 Bogdanov-Takens bifurcations

The (w1, w3) parameter space contains a cross-over point. This feature is anomalous, as it is inconsistent with the idea that the line of bifurcation separate oscillatory from non-oscillatory regions of the parameter space. Furthermore, when surveying the parameter space, it was clear that there existed regions of the parameter space that were labelled oscillatory, though oscillations were not observed. This prompted further examination of the system using the bifurcation analysis software, and it was found that a point exists along some of the Andronov-Hopf bifurcation curves where the system undergoes a Bogdanov-Takens (B-T) bifurcation. This means that the curve of Andronov-Hopf bifurcation points comes into contact with a fold bifurcation and a saddle separatrix simultaneously in the parameter space, see Kuznetsov (1998) for more information.

After this point, the Andronov-Hopf curve which the software identifies is no longer a true line of bifurcation. The reason for this is that LOCBIF uses the condition in equation 3.12 to test for the existence of an Andronov-Hopf bifurcation, i.e. that the sum of two of the eigenvalues is zero. However there are three ways that this condition can be satisfied. Either by the two eigenvalues being a pair of complex conjugates with real parts equal to zero, as the further two conditions in equations 3.10 and 3.11 specify.

Alternatively, if a pair of the eigenvalues are real, equal, and of opposite sign they will also sum to zero. Finally, the pair of eigenvalues can both be equal to zero to fulfil the requirement. At a B-T point, the eigenvalues that were complex conjugates (on the line of Andronov-Hopf points) become precisely equal to zero. After this point, the pair of eigenvalues are real, with equal and opposite values. Hence, although LOCBIF's requirement for an Andronov-Hopf bifurcation is met along the curve, after a B-T point the plotted curve is not a true line of Andronov-Hopf bifurcation.

Therefore, the region bound by the Andronov-Hopf curve after a B-T bifurcation point is not necessarily oscillatory. The actual reductions in the oscillatory regions which are shown in figure 3.6, were found by testing various pairs of parameters in the vicinity of a B-T point to see whether they resulted in oscillatory behaviour or not. The results are shown in figure 3.9. In the (w1, w2) plot in particular, this new bifurcation results in a considerably smaller oscillatory area than the enclosed loop of the Andronov-Hopf bifurcation curve. This area is reduced even further when the $w2 = 0$ line is plotted, in order to exclude the region of negative parameter space. It is worth noting that w1 and w2 represent the connections made by the TC cell population onto the pyramidal and reticular populations respectively. As discussed earlier, these connections may be important in the conformational changes that the network undergoes in the transition from sleep to arousal.

Note that although a B-T point occurred in the (w2, w3) plot, it lies in the negative region of w2 parameter space and is therefore not considered to affect the results here, and is not shown in figure 3.9. Such occurrences of B-T points at negative parameter values also happen in the time constant plots, and are also not shown here. Finally, there was no occurrence of a B-T point in the closed curve of Andronov-Hopf points in the (w3, w4) parameter space. It is important to note that despite the occurrence

of this additional bifurcation, the relationships between the connection weights which were discussed in section 3.3.2 remain valid.

3.3.4 Three dimensional considerations

The bifurcation curves shown thus far enclose the oscillatory regions in two-dimensions of the parameter space, and therefore give an indication about the situation in the multi-dimensional parameter space. While it becomes increasingly difficult to consider higher dimensions, it is possible to visualise the oscillatory regions in three-dimensions by producing a given bifurcation curve for a pair of parameters while systematically varying a third parameter. This analysis can show how the oscillatory region of two parameters depends on a third. While it is superfluous to the aims of the current investigation to produce and analyse such plots for all possible combinations of parameters, this analysis was done for two interesting cases. The results, shown in figures 3.10 and 3.11 indicate the following:

- w4 is the RE to TC connection weight, and this parameter manipulates the (w1,w2) bifurcation curve by restricting the oscillatory region at values smaller than its control value (of 8), and expanding the oscillatory region at values larger than its control value. Considering the occurrence of B-T points along the bifurcation curves shows that this effect is perpetuated, such that at smaller values the limit of the oscillatory region is very tightly constrained. At higher values of w4, the oscillatory region is less constrained. Therefore, as the inhibitory innervation of the TC population increases, the strength of TC innervation of both the PY and RE populations can also increase while oscillatory behaviour is maintained. This is an interesting result, as it suggests that the inhibition of the

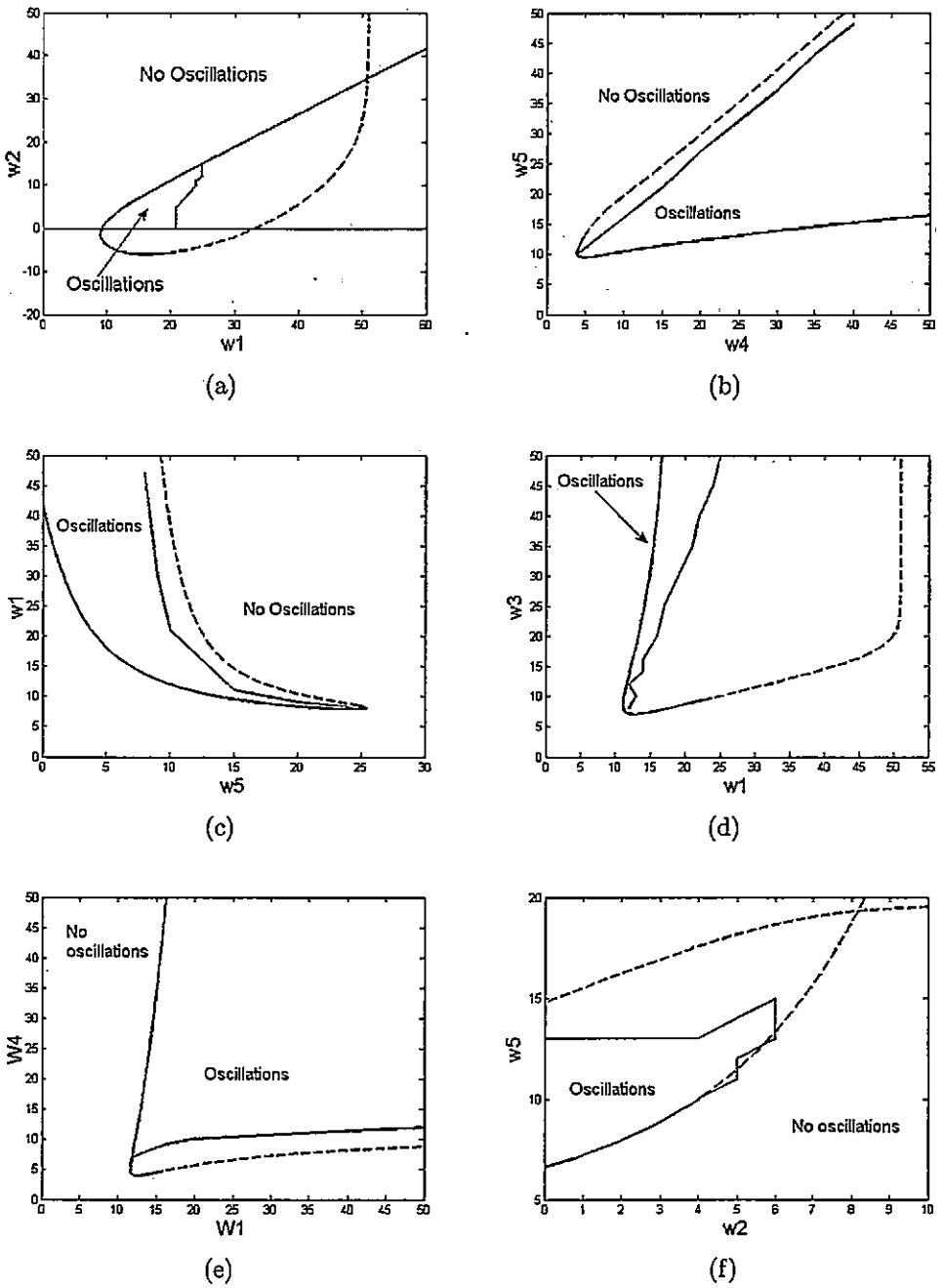

Figure 3.9: Bifurcation curves in the parameter spaces of the following pairs of parameters: (a) w1 and w2, (b) w4 and w5, (c) w5 and w1, (d) w1 and w3, (e) w1 and w4, and (f) w2 and w5. The plots show the reduced oscillatory area due to the occurrence of a Bogdanov-Takens point. In each plot, the dashed blue line shows the continued A-H curve beyond the B-T point, and the red line shows the limit of oscillatory behaviour, which was found by trial of parameter pairs.

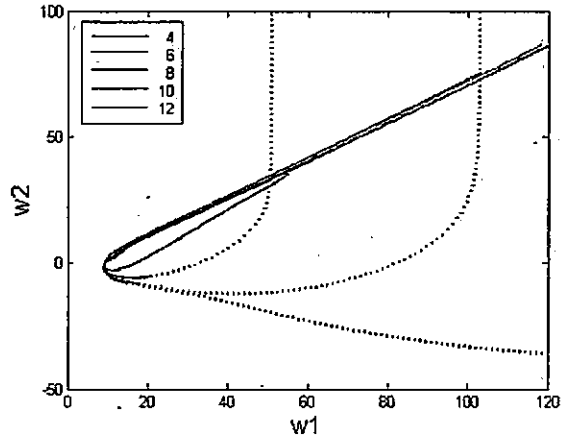

(a)

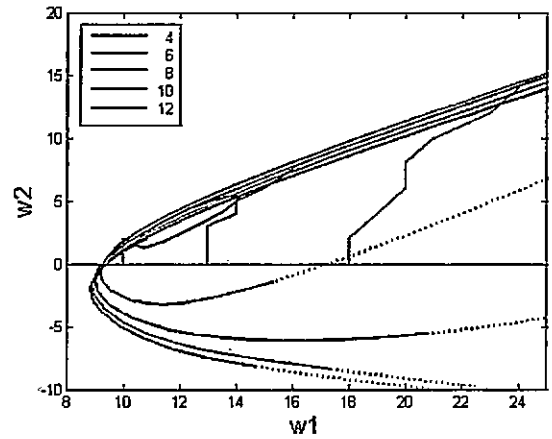

(b)

Figure 3.10: These figures show a representation of the three-dimensional parameter space of w1, w2 and w4. The figures show how the (w1, w2) bifurcation curve varies with w4, by displaying the (w1, w2) curve at different values of w4, as shown in the legend. (a) shows the overall picture, and (b) shows a detailed view including B-T points and limits of oscillatory behaviour. Note that at w4=12 the limit of the oscillatory region goes beyond the scope of the figure and therefore no line is shown.

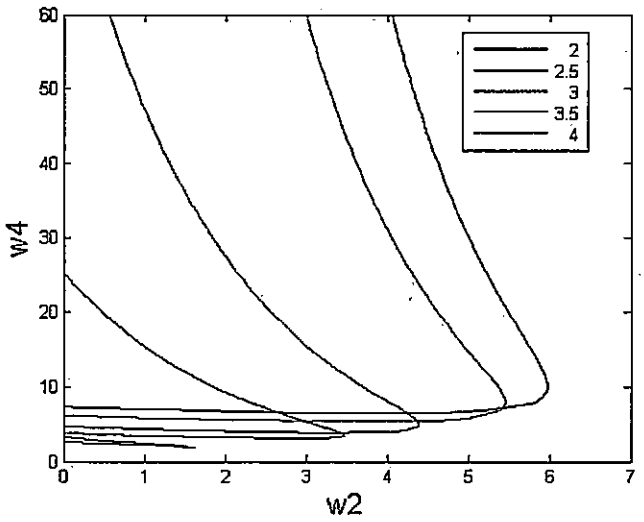

Figure 3.11: This figure shows a representation of the three-dimensional parameter space of w2, w4 and P. The figure shows how the (w2, w4) bifurcation curve varies with P, whose values are given in the legend.

TC cell population by the RE cell population, is facilitatory for the existence of oscillations.

- P is the parameter which represents the ability of the TC population to rebound from inhibition. Its control value is three, and it was varied between two and four, while the (w2, w4) bifurcation curve was plotted. It is clear that as P increases the oscillatory region also expands. Primarily this indicates the importance of the P parameter, because as P decreases the oscillatory region of the parameter space decreases. w2 and w4 mediate the TC to RE and RE to TC connections respectively. The increase in P is specifically accompanied by an increase in the range of values that w2 can take. Therefore an increased ability of the TC population to rebound from inhibition allows the TC population to have a greater impact on the RE population, which is an intuitive result.

3.3.5 Comparison to experimental results

If the bifurcation curves are directly compared to the experimental evidence given in section 3.2.4, a number of interesting similarities are highlighted. Four pieces of evidence from section 3.2.4 are referred to here:

1. Castro-Alamancos & Calcagnotto (2001) showed that the strength of feed-forward thalamocortical projections out-weighs that of feedback projections. In the model, these connections are represented by the weight parameters w1 and w5 respectively. In the (w5, w1) parameter plane, figure 3.6(e), the majority of the oscillatory parameter space lies in the region where w1>w5, and therefore the model reflects this experimental result well.

2. van Horn *et al.* (2000) showed that the greatest number of synaptic contacts onto TC cells are cortical in origin. In the model there are two synaptic inputs into the TC cell population, the RE input labelled w4, and the cortical input labelled w5. The bifurcation curve in the (w4, w5) parameter space shown in figure 3.6(d) does not appear to be consistent with this view. However, once the B-T point is included in this figure, and the limited oscillatory region is taken into account (figure 3.9(b)), it appears that most of the oscillatory region is within the region where w5>w4, and hence the model is consistent with the data in the literature.

3. Golshani *et al.* (2001) show that the strength of cortical feedback to RE cells is stronger than that to TC cells. This relationship is examined in detail in a later section, where it is shown that the model also reflects this experimental result.

4. Finally, Wang *et al.* (2001) show that RE cells send most of their projections to TC cells. In the model the RE population only projects to the TC population,

Parameter	Upper limit	Lower limit
w1	20%	3%
w2	10%	20%
w3	10%	20%
w4	20%	20%
w5	20%	5%
P	20%	3%
τ_1	20%	20%
τ_2	20%	10%
τ_3	20%	20%

Table 3.2: The table shows the upper and lower limits that each parameter used in the model can take, while oscillatory behaviour is maintained in the model. These limits are given as percentages of their control values, which are shown in table 3.1.

and so this condition cannot be tested directly.

3.3.6 Individual parameter ranges

As shown above, LOCBIF allows investigation of the parameter space by manipulating two parameters at a time. It is also useful to look at the range of values of a single parameter, which allow the network to maintain oscillations. Therefore, these ranges were explored between ±20% of the control values shown in table 3.1. The limits for each parameter are shown in table 3.2.

If ±5% is considered to be the minimum accepted variability that a parameter can have, then from the figures in table 3.2 there is one main result seen. That is that P and w1 are effectively at minimum values when they are at their control values (as

shown in table 3.1). The P parameter represents an intrinsic property of the TC cell population, which is required for spindling to occur (see section 3.2.1). That is the ability of the TC population to rebound from inhibition. Without this parameter, as soon as the TC population receives inhibition from the RE population, its activity would be suppressed and therefore oscillations could not persist. This property is directly comparable to the ability of TC cells to fire post-inhibitory rebound bursts, which they do during oscillatory behaviour Steriade *et al.* (1993); von Krosigk *et al.* (1993). Hence the dependence of the model on its value is not surprising. w1 is the weight of the TC population to PY population connection, and this value also has to exceed a minimum for the oscillations to persist. This demonstrates the importance of the inclusion of the cortical population, and therefore of corticothalamic feedback in supporting the spindle-range oscillatory behaviour in this network model.

3.3.7 Weight manipulations

Similar manipulations were performed to look at which connections in the network could be spared while the network continues to oscillate. Each weight was set to zero in turn, whilst keeping all others at their control level. It was clear that all connections are essential for oscillatory behaviour to exist, except for the relay cell population to reticular cell population connection. This has been discussed above in relation to the bifurcation diagrams. To reiterate it seems that the TC input to the RE cell population is not vital for oscillations to exist in the model's behaviour, whereas the RE input to the TC population and the PY to TC input both are required. This is likely to be because the TC to PY to RE pathway can compensate for the direct TC to RE projection.

The bifurcation diagrams can also show whether oscillations remain when severed

connections are compensated for by increasing other connection weights. If the weight of the connection between the PY and the TC populations is set to zero, and no other changes are made, the oscillations cease. However, if feedback is severed while the TC to PY connection is increased to a value greater than approximately 43, then oscillations remain. Hence, although the monosynaptic feedback loop is important for oscillations, one part of this loop can compensate for the other. In this way, a balance between the two major excitatory pathways is apparent and is the only case where such compensation can be seen.

The connection weights were not only set to zero, but also halved and doubled to further examine the dependence of the oscillatory activity on the parameters. The full results are shown in figure 3.12. There were some particularly interesting manipulations, which are highlighted here:

1. If either w3 (PY to RE connection weight) or w5 (PY to TC) were halved, the oscillation did not disappear entirely but was damped. This shows that the cortical input to both the TC and RE cell populations is important for the preservation of oscillations.

2. If w2 (TC to RE), w3 or w4 (RE to TC) were doubled, the oscillation was not abolished but was damped. This clearly indicates that too much inhibition is perilous for the maintenance of oscillations.

3.3.8 The 5-dimension parameter space

Bifurcation analysis in two and three dimensions can give a good insight into the behaviour of the model with respect to the oscillatory regions of the five-dimensional

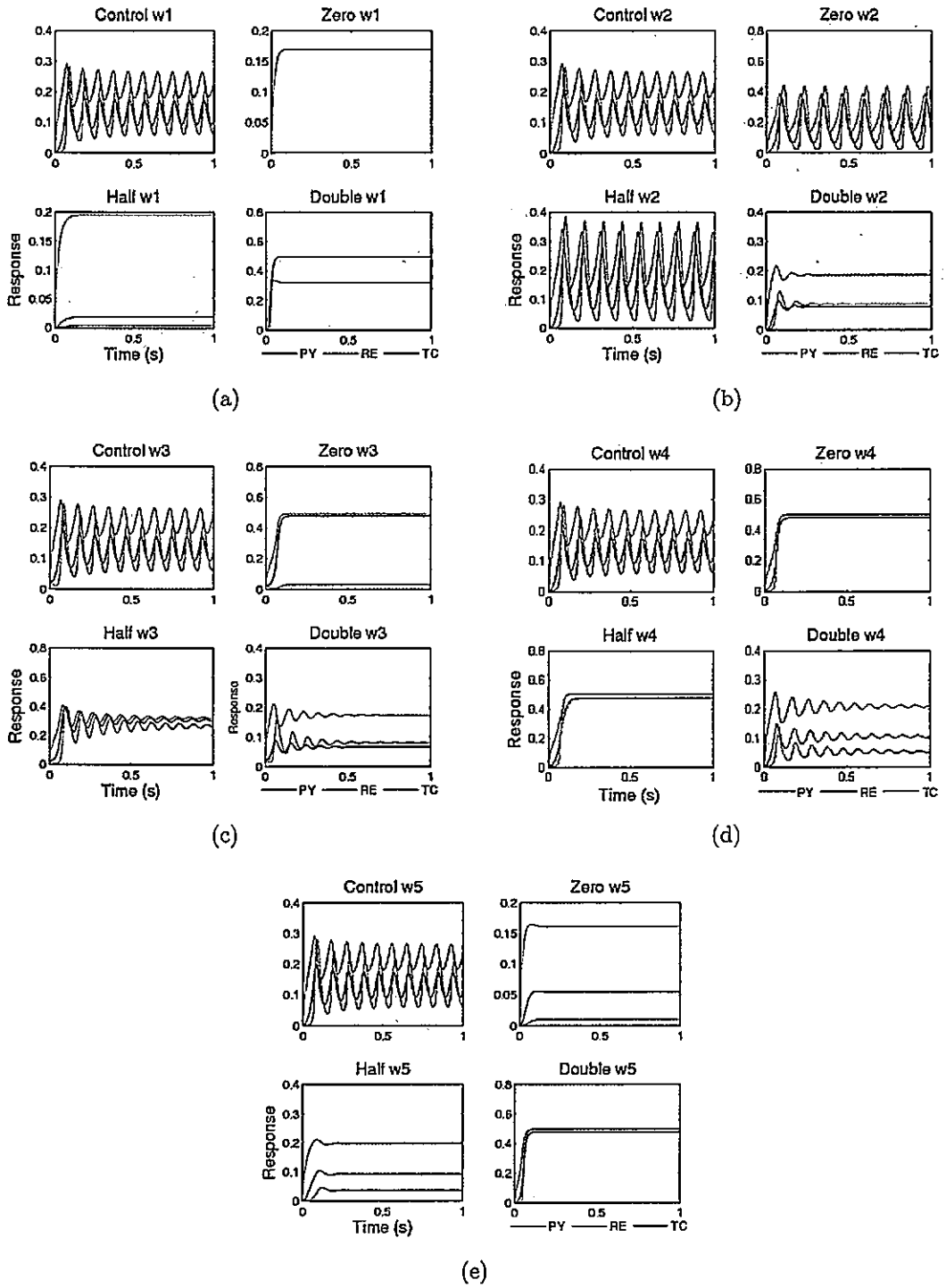

Figure 3.12: This figure shows the effect on the oscillatory activity when each weight parameter is put to zero, halved, and doubled. (a) w1, (b) w2, (c) w3, (d) w4, and (e) w5. Note that the activity with control parameters is also shown for reference.

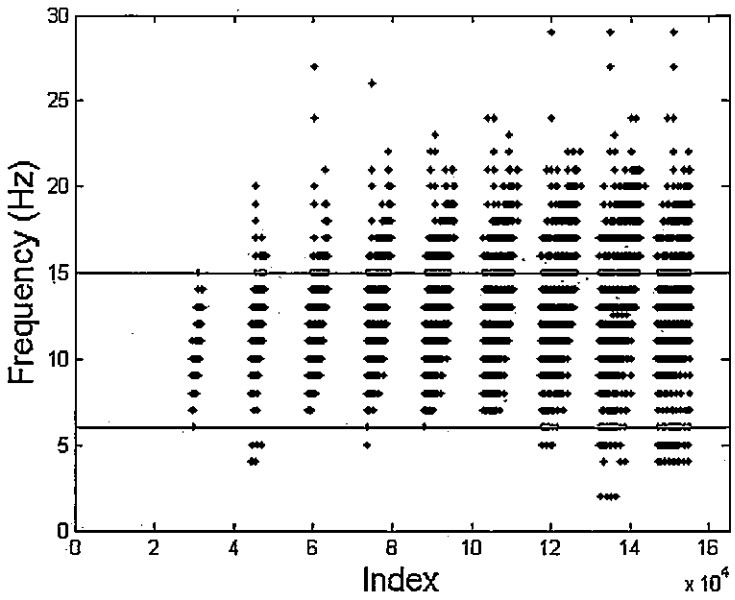

Figure 3.13: This figure shows the results of the simulations which examined the 5 dimensions of the parameter space. Each point in the figure is a point where oscillations occur, plotted against the frequency of oscillations at that point.

parameter space. However, as discussed previously this is a simplification of the reality, as all five weight parameters interact dynamically to effect the behaviour of the system. In order to understand how this occurs, the five-dimensional parameter space was assessed by observing the activity of the network while all 5 weight parameters were simultaneously varied. The visualisation of a 5-dimensional space is not straightforward, however figure 3.13 plots the points, from the 161,051 points tested, at which oscillatory behaviour occurs.

Examining the regions where oscillations are not present shows that these points often relate to unphysical regions of the parameter space with respect to the connectivity of the network. For example, no oscillations occur during the first 29,559 points

tested. These points relate to the parameter space where w1 has not yet reached a large enough value to allow for oscillations. This reinforces the results in section 3.3.7, which showed that when w1 was set to zero, oscillatory behaviour was no longer observed. Throughout the rest of the points tested, oscillations appear to die away regularly, which can be seen in figure 3.13 as the recurring vertical spaces where no points are plotted. The parameter values in these regions were studied, and it was found that the following relationships between weight parameters are important for the maintenance of oscillations.

- Each time that w3, w4 and w5 are reset to zero oscillations cease. This is understandable in terms of the model architecture, as all but two of the connections (w1 and w2) are severed at these points.

- There also exists a fine balance between w4 and w5, such that oscillations are often inhibited if w5 becomes greater than w4. Some degree of "balance" between these parameters can be seen in the two-dimensional bifurcation diagram (figure 3.6(d)). Furthermore, although the bifurcation diagram including the B-T point (figure 3.9(b)) shows that more of the oscillatory region exists where w4 is greater than w5, the 5-dimensional simulations show the significance of this relationship much more clearly.

- The simulations show that at a number of points where w5 becomes zero, oscillations do not cease if a particular relationship between w1, w3 and w4 is adhered to. Figure 3.14(a) shows the values of these three parameters plotted in three-dimensions, for all the oscillatory points where w5 is zero. These points form a plane in the (w3, w4) space at w1=35. Figure 3.14(b) shows that w3 and w4 can take almost any pair of values, with w3 always greater than 10. This relationship

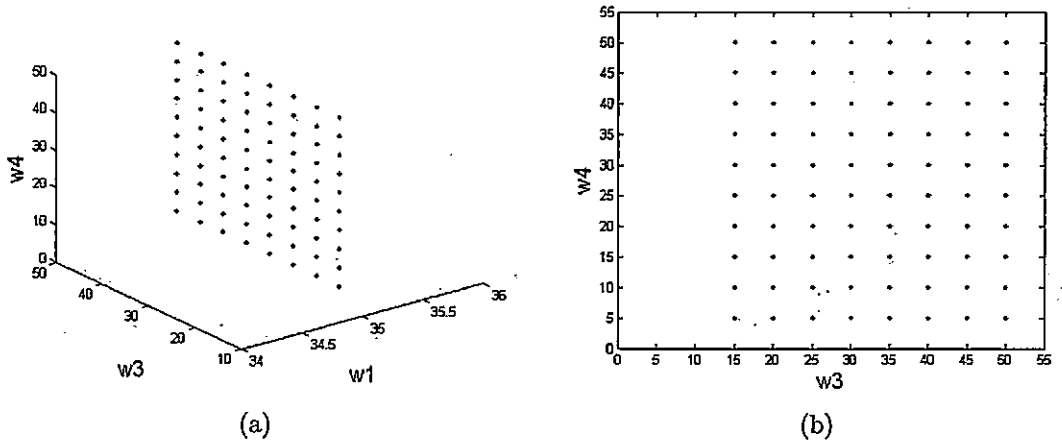

Figure 3.14: These plots show the relationships between the parameters (a) w1, w3, and w4, and (b) w3 and w4, for all points where w5=0 and oscillations continue.

would not be observable in two or three-dimensions, but in the five-dimensional space it is possible.

Relating these observations to the theoretical analysis of the system, as discussed in section 3.2.6, we can see the changes reflected in the eigenvalues of the system. Recalling that an Andronov-Hopf bifurcation can be detected by the real part of at least one of the eigenvalues becoming positive (Dayan & Abbott, 2001), it is possible to use LOCBIF to plot the eigenvalue against the changing parameter value in a particular region of interest. For example, figure 3.13 shows that oscillations do not start to occur until w1 is large enough. The first point at which oscillations are observed, is when w1=10, w2=0, w3=10, w4=15, and w5=10. Using LOCBIF to examine the eigenvalues around this point, while varying w1 produces the plot seen in figure 3.15(a). This plot shows that for w1 less than 10, the eigenvalue has a negative real part, indicating that the equilibrium point is stable and therefore no oscillations will occur. However, as w1

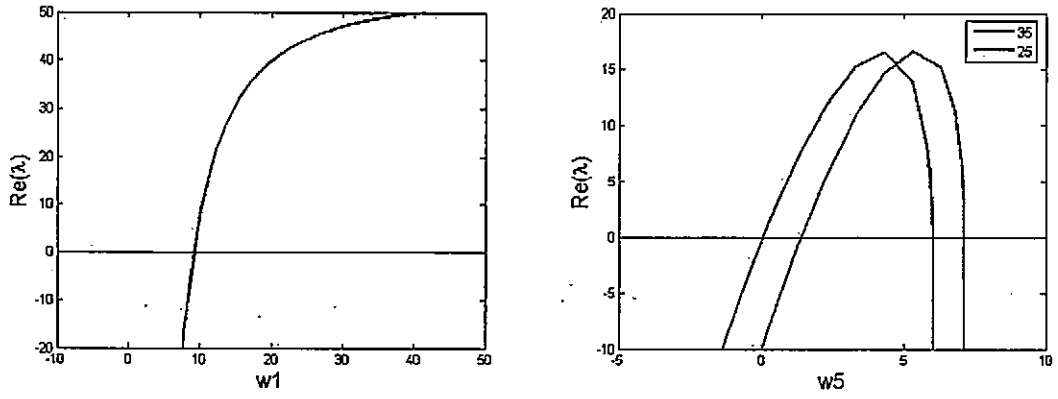

Figure 3.15: This figure shows how the real part of one of the eigenvalues (λ) in the system changes as (a) w1, and (b) w5 and w1 change for two specific points in the 5 dimensional space.

becomes greater than 10 the real part of the eigenvalue becomes positive, hence the equilibrium point is unstable and oscillations are possible.

A second example is when w5 is zero, oscillations are possible at only one value of w1. Looking at the eigenvalues in this case, as shown in figure 3.15(b), shows that when w1 is at the desired value of 35, the eigenvalue becomes positive at w5=0 therefore allowing oscillations at this point. However, at a different value of w1 (in figure 3.15(b) w1=25), the eigenvalue becomes real at approximately w5=1. Therefore the theoretical analysis of the eigenvalues, as performed by LOCBIF, matches the simulations well.

Other interesting results to emerge from these experiments, are related to the frequency of oscillations. The two horizontal lines in figure 3.13, show the limit of the spindle frequency range. It is readily seen that most of the oscillatory points lie within this range. However, there are oscillatory points which lie in the 2-5 Hz, and the 15-30 Hz ranges. Such slow oscillations are related to paroxysmal activity, as discussed

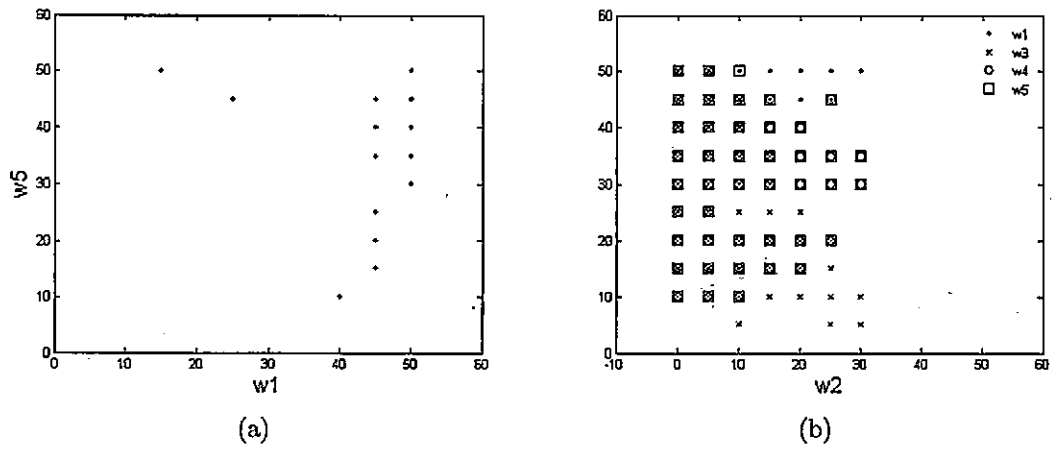

Figure 3.16: These figures plot the relationship between (a) w1 and w5, and (b) w2 and the remaining four parameters, for the points where the frequency of observed oscillations is less than 6Hz, in order to observe any correlations between these parameters.

below (section 3.3.9.1). The higher frequency range is called the beta band, which is associated with concentration and perceptual awareness. These points were analysed with respect to the parameter values which are required to cause the activity.

Figure 3.16(a) shows the relationship between w1 and w5 when oscillations are in the 2-5 Hz range. This figure shows no definitive relationship, although not all points in the space are sampled, and it seems that there is a degree of balance required between these two parameters as seen previously (see section 3.3.2). Figure 3.16(b) shows that w2 is always relatively smaller than the other 4 parameters, and this is consistent with the restricted range of w2 that was seen in previous sections.

For regions of the parameter space which result in 15-30 Hz oscillations, figure 3.17(a) shows that w1 is in general large compared with the other parameters, while once again w2 is small. w1 mediates the connection from the TC cell population to the PY cell population, and if beta oscillations are related to perception, then this is

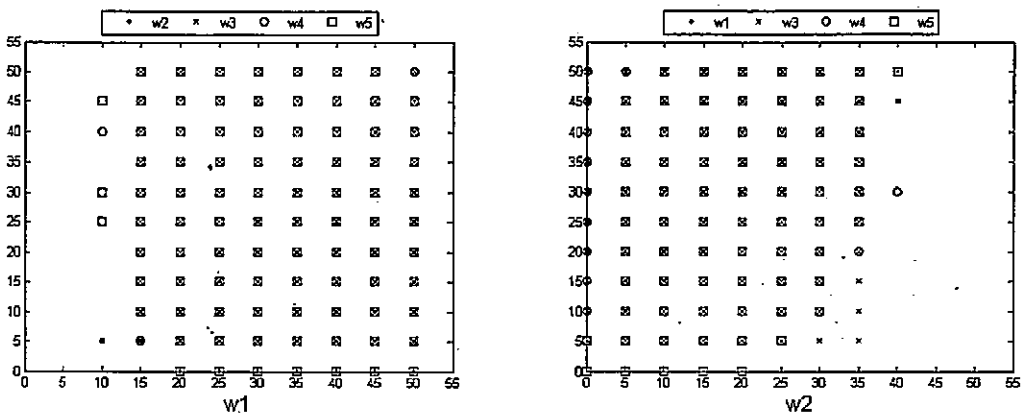

Figure 3.17: These figures plot the relationship between (a) w1, and (b) w2, and the remaining four parameters, for the points where the frequency of observed oscillations is more than 14Hz, in order to observe any correlations between these parameters.

consistent with a requirement for a strong feed-forward pathway through the thalamus.

The simulations in the 5-dimensional space have proven useful for the further understanding of the system, particularly when considering the effect of the parameter changes on the changes in the eigenvalues of the equations. Furthermore the frequency changes observed provide more insight into the behaviour of the model. This consideration of frequency is considered in more detail in the next sections.

3.3.9 Frequency considerations

So far in this chapter, the parameter ranges that support the existence of oscillatory behaviour have been shown, and these ranges are generally quite broad. An additional consideration is whether the frequency of the oscillatory activity remains within the 7-14Hz range, while parameters are changing. There are two ways that we can assess whether the frequency of oscillations is robust to parameter changes or not. The first

is to try pairs of values within each parameter space and check the frequency at each point. For almost all oscillatory regions of weight parameter space investigated in this way, the oscillations remained within the spindle frequency range (7-14Hz). The main exception is when w2$\leq$0, which is not physiologically meaningful. For varying time constants this robust frequency value is also not maintained, and this is discussed below in more detail.

The second option for monitoring frequency involves utilising LOCBIF further. Whilst tracing bifurcation curves, it is possible to simultaneously monitor the frequency of oscillations. As described above, while the curve is being traced the eigenvalues are calculated at each point. As explained previously, two of the eigenvalues at an Andronov-Hopf bifurcation are $\pm i\beta$, and β is equal to the frequency of the oscillations in radians per second. Therefore, if the frequency is required to remain within a range of 7-14Hz, this relates to an angular frequency range of 44-88 rads^{-1}. Therefore, the value of this angular frequency (relating to the frequency around the limit cycle) can be observed whilst tracing the bifurcation curves in order to assess how well the oscillatory parameter space represents spindle range oscillations. This analysis also showed that within physically reasonable ranges of parameters, the frequency remains within the spindle range of 7-14Hz. The exceptions are near B-T points where the amplitude of oscillations tends to zero.

Investigation of the time constant parameter spaces are considered in more detail below, by the manual trial of various pairs of parameter points.

3.3.9.1 Transition to a slow frequency oscillation

Simulations showed that modifying the values of τ_1 or τ_3 within the oscillatory range of parameter values (as defined by the bifurcation curve in figure 3.8(c)) has little effect on

the frequency of the oscillations, such that the frequency remains fairly constant within the 7-14Hz spindle range. However with increased τ_2, the time constant for the reticular cell (RE) population, the frequency of the oscillatory activity in the entire network changes. In particular, for the case when τ_2 is increased from it's control value of 20ms, the frequency of oscillations is dramatically reduced. This change in network activity is illustrated in figure 3.18, where τ_2 is increased to 60ms and the frequency drops to approximately 4Hz (exactly 3.90Hz in all three cell populations). It is proposed here that this change in τ_2 is comparable to the pharmacological manipulation of thalamic slices by application of bicuculline methiodide, a $GABA_A$ antagonist.

This manipulation has been carried out in a number of previous studies (for example Bal *et al.* (1995a,b); Kim *et al.* (1997); von Krosigk *et al.* (1993)). In Kim *et al.* (1997), it was shown that the normal interaction of RE and TC cells in generating spindle oscillations was disrupted by the application of bicuculline to their slice preparation. Specifically, the bursting in RE cells was prolonged due to disinhibition from other RE cells. This in turn resulted in the activation of slow bicuculline-resistant IPSPs in TC cells. Application of a $GABA_B$ receptor antagonist resulted in the abolition of this slow IPSP, confirming that these IPSPs are mediated by $GABA_B$ receptors. The IPSPs mediated by $GABA_A$ and $GABA_B$ receptors were also observed to differ significantly in their delay to onset. Bursts of action potentials in single RE cells resulted in the activation of $GABA_A$-receptor-mediated IPSPs with a delay to onset of <1 ms, whereas the activation of prolonged burst discharges resulted in the activation of $GABA_B$-receptor-mediated IPSPs at a delay of 30 to 42 ms. Application of bicuculline therefore resulted in the abolition of spindle wave associated IPSPs in TC cells, resulting in a synchronised 2-4 Hz "paroxysmal" oscillation.

In the present model an equivalent manipulation to the application of bicuculline

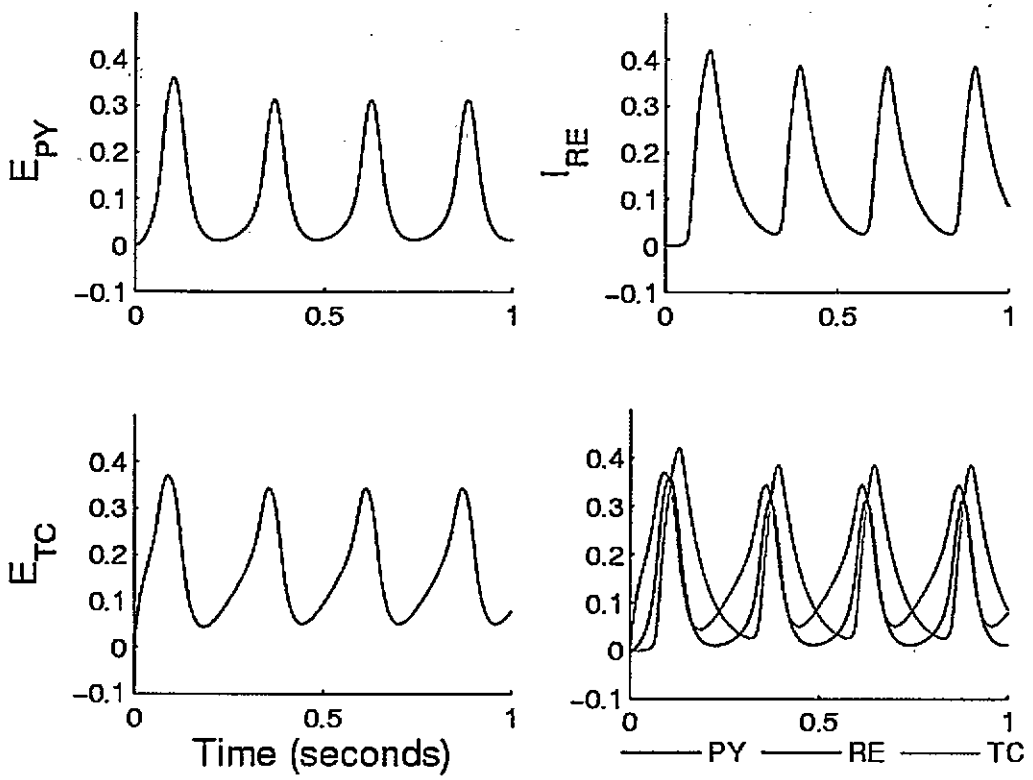

Figure 3.18: The oscillatory activity in the model shows a 4Hz frequency when the time constant of the reticular cell populations is increased to 60ms. Note that the frequency of oscillation is very similar in all populations, and the populations are well synchronised.

would have to slow the rate at which inhibition acts on the TC cells, in order to mimic a slower (compared to normal) IPSP. This can be achieved by increasing the time constant of the RE cell population, which therefore increases the time course that inhibition acts over. Simulating the considerably slowed inhibitory effect of this population on the TC cell population gives the result shown in figure 3.18, which shows that the frequency is dramatically reduced. This was observed for a range of physiologically feasible increases in τ_2 (20 to 100ms) and the accompanying change in frequency was measured and can be seen in figure 3.19(a). This figure demonstrates that as τ_2 increases, the frequency rapidly decreases to around 2-4Hz, and that in this range the frequency asymptotically approaches 2Hz.

Such slow oscillations are also identified by an increase in synchrony (Bal *et al.*, 1995b). In the Wilson-Cowan model, higher synchrony within a population can be interpreted as a higher proportion of the population being active during the oscillation, and therefore the amplitude of oscillation will be greater. Therefore, τ_2 was increased, while the amplitude of the resulting oscillation was measured at each step. Figure 3.19(b) shows that as the oscillations become slower, they also become more synchronised, which is consistent with experimental results. Thus the behaviour of the model indicates that the transition from spindle to synchronised "paroxysmal" oscillations, may be part due to the slower $GABA_B$-mediated inhibition of the TC cells causing a change in the nonlinear dynamics of the thalamocortical network.

3.3.10 Dominant inhibition

There has been some speculation in the literature regarding the importance of the corticoreticular feedback connection, and it has been suggested that the strength of this innervation compared with that from cortex to the LGN, must be greater for

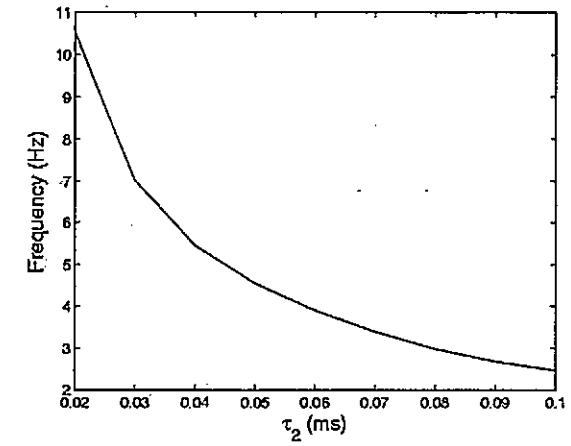

(a)

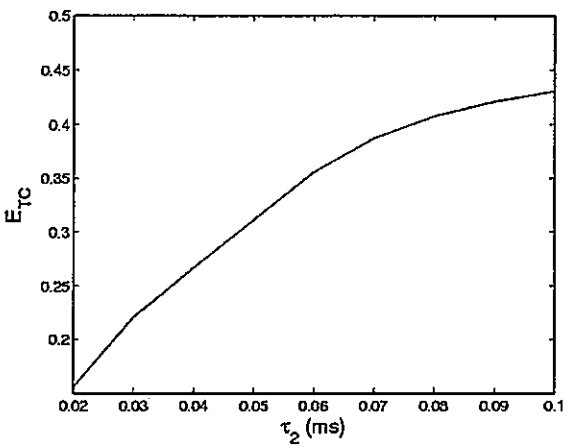

(b)

Figure 3.19: (a) The frequency of oscillations has a strong dependence on the time constant of the reticular cell populations, as shown here. With increasing τ_2, the frequency drops to around 2-4Hz. (b) The synchrony of oscillations also has a dependence on the time constant of the reticular cell populations, as shown here. With increasing τ_2, the amplitude of oscillations (and therefore the synchrony) increases steadily.

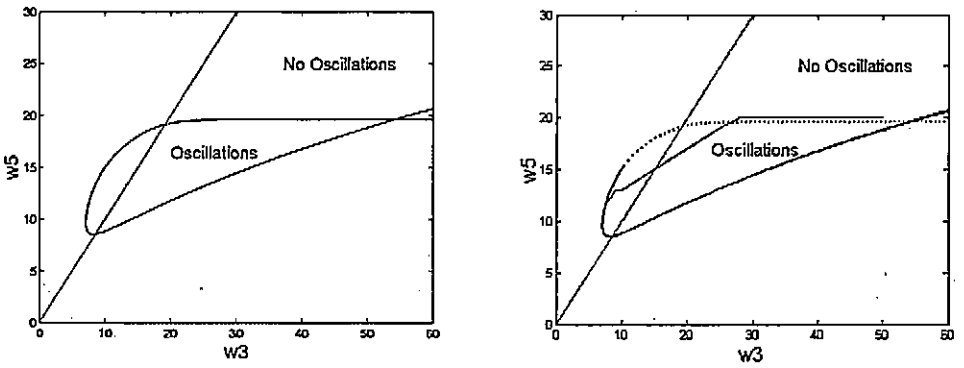

(a) (b)

Figure 3.20: The bifurcation diagram for the parameters representing the corticoreticular (PY to RE) projection, w3, and the corticothalamic (PY to TC) projection, w5. Both the original Andronov-Hopf bifurcation curve (a), and the curve including the Bogdanov-Takens point (b) are shown. In (b) the dashed blue line is the continuation of the Andronov-Hopf point following a B-T point, and the red line is the limit of the oscillatory parameter space, found by trial of parameter pairs.

spindling to occur (Destexhe *et al.*, 1998). As discussed in section 2.2, based on detailed conductance-based modelling studies it was proposed that the conductance of the AMPA-mediated cortical drive on RE cells must be substantially greater than that on TC cells, in order for cortical stimulation to evoke spindle oscillations, and to replicate a number of important features of this oscillation. The IPSP/EPSP sequence seen in model TC cells was indicated by Destexhe *et al.* to be consistent with several experimental observations (e.g. those of Contreras & Steriade (1996)). To investigate this idea further, the oscillatory region in the (w3, w5) parameter space was examined and the results are shown in figure 3.20(a). In figure 3.20(a), the line of equality (w3=w5) is also plotted, and it is clear that much more of the oscillatory region lies in the space which satisfies $w_3 > w_5$.

Furthermore, this parameter plot indicates that the corticothalamic feedback has

to be balanced in order for oscillations to continue. This is seen in the shape of the oscillatory region, which is a contained area. Therefore, corticothalamic feedback cannot be increased without an accompanying increase in corticoreticular feedback. Also for a given value of w3, w5 is very much restricted to a given set of values, and this effect is enhanced once we consider the true oscillatory region after identifying a B-T point, as shown in figure 3.20(b). This is also consistent with the view that corticothalamic feedback, both via the TRN and directly to the LGN, controls the oscillations.

The idea of dominant inhibition was first suggested by Destexhe *et al.* (1998), when they presented a number of models of spindling in the thalamocortical network. This paper is reviewed in section 2.2 of chapter 2. The authors found that in order to achieve the correct EPSP-IPSP pattern, which is required to generated rebound bursts and therefore spindles, a large difference in AMPA-conductances between PY to TC and PY to RE connections was needed. This population model does not reflect the 20-fold difference in AMPA-conductances between the TC and RE cells, as was implemented in the model by Destexhe *et al.* (1998). However, this is understandable as the weight parameters in this population model are not equivalent to synaptic conductances.

3.3.11 Synchrony of oscillations

Finally, to further investigate the role of cortical feedback in the model, the effect of feedback on the synchrony of the oscillatory behaviour within the TC population was investigated. Previous studies have proposed that the role of cortical feedback is to synchronise activity within the thalamus during spindle oscillations, which was discussed in section 2.2. Once more, higher synchrony is interpreted as a higher proportion of the population being active, and therefore a greater amplitude of oscillation.

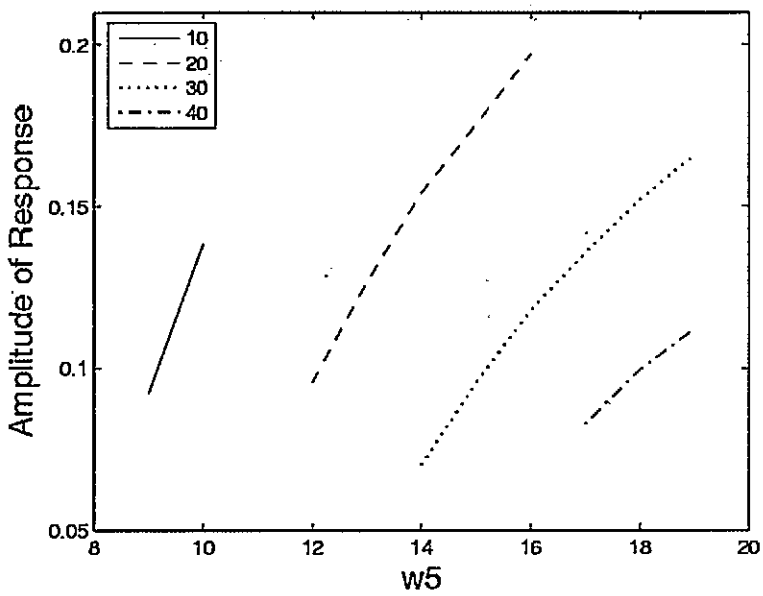

Figure 3.21: To consider the effect of cortical feedback on the synchrony of oscillations, the plot shows the amplitude of the oscillatory response (which is a measure of synchrony) varying with feedback weight. In all plots w3 is kept constant at the level shown in the legend, while w5 is varied. Each plot shows that synchrony increases with increasing feedback.

Figure 3.21 shows that increasing corticothalamic (w5) feedback strengths, while corticoreticular (w3) feedback is kept constant, yields an almost linear relationship between feedback and amplitude. Hence, the model supports the hypothesis that the effect of corticothalamic feedback is to increase synchrony within thalamic populations during the spindle oscillation.

3.4 Discussion

The main result of this present chapter is that based on the simulations of a population model, the thalamocortical network possesses an intrinsic oscillatory activity. With the

weights of the connections set at values that reflect the relative strengths of the actual connections in the brain, the frequency of this oscillation lies within the 7-14Hz spindle range. Modelling spindling activity has previously depended upon the inclusion of various currents, the most important of these being I_T (Deschenes *et al.*, 1984), and I_h (Destexhe *et al.*, 1993). The model presented here depends only upon the dynamics of the excitatory and inhibitory populations and connections within the circuit (Wilson & Cowan, 1972), an this has been shown to be enough to sustain a natural oscillation.

The bifurcation curves, which display the Andronov-Hopf bifurcation points in the various parameter planes of the system, clearly show that the oscillatory behaviour of the network is robust to a range of parameter variations, which are consistent with the biological constraints. Not only do oscillations occur for ranges of weight and time constant parameter values, but the frequency of oscillations remains within the spindle frequency range for almost all parameter values tried. The only exception to this frequency robustness occurs with respect to τ_2, the time constant of the reticular cell population. When this parameter increases the frequency of oscillations decreases, and this effect is discussed below with specific reference to previous experimental work.

The bifurcation curves also show that in general, there must be a balance of connection weights in the model if oscillations are to be maintained. Either reciprocal or linear relationships between pairs of parameters can be seen in parameter planes such as (w1, w2), (w3, w4), (w5, w1), (w4, w5) and (w2, w5). There is a range of experimental evidence which has shown specific relationships between the connections represented in the model. Therefore it is reasonable to see such relationships in the model's bifurcation curves, and the analysis shows that such relationships are reflected by the model. In particular, the w2 parameter, which mediates the TC to RE connection, is tightly constrained and can even be set to zero. It is hypothesised that the

TC to RE connection can be compensated for by the disynaptic loop through the PY population. The importance of this disynaptic pathway can be seen in the (w1, w3) bifurcation curve, which shows that the oscillatory region is tightly constrained to a region where w3 (the weight of cortico-reticular feedback) is large compared to w1.

Other interesting results include the following: The (w1, w2) curve, which are the output connections of the TC population, shows how the TC population may control spindling in transitions between sleep and awake states via its innervation of the other cell populations; w4 and w5 are the inputs to the TC populations, and the curve in their parameter plane shows that they are generally not constrained, though again there is some degree of balance required; The first of the three-dimensional plots shows that increased inhibition of the TC population allows the TC innervation of the PY and RE populations to act over a greater range of values; The second showed that the increased ability of the TC population to rebound from inhibition allows the TC population to have a greater impact on the RE population. Taken together these results show that there are a number of interesting relationships between the model's parameters.

These relationships also show how the model's parameter choices can be validated by bifurcation analysis. The curves reflect previous experimental results, which suggests that the model's behaviour is accurate. Due to the biological constraints as discussed above, it is reasonable to assume that there is a specific region in the multi-dimensional parameter space of the model which is oscillatory. Therefore, the fact that both the two-dimensional and 3-dimensional plots show that the parameters constrain one another is intuitive. The importance of the monosynaptic feedback loop, which is mediated by the feed-forward w1, and the feedback w5 weight, is also reflected in many of the bifurcation curves and is consistent with experimental results.

The control that is exerted over spindle oscillations by cortical feedback has been

shown in previous studies, both experimentally (Bal *et al.*, 2000; Blumenfeld & McCormick, 2000; Contreras *et al.*, 1997a) and in conductance-based models (Bal *et al.*, 2000; Destexhe *et al.*, 1998, 1999). Here this effect is highlighted in the (w3, w5) bifurcation curve, which shows that these two paths for cortical feedback must be balanced in order for oscillations to be maintained. Furthermore, feedback weights w3 and w5 also impose restrictions on other connection weights, which can be seen from the other bifurcation curves involving w3 or w5.

The plot of the oscillatory region in the (w3, w5) parameter space further shows that much more of the oscillatory region lies in the region where w3 is greater than w5. This agrees with the idea that the PY-RE connection needs to outweigh the PY-TC connection in order to achieve spindling (Destexhe *et al.*, 1998). This idea has emerged from previous modelling studies using conductance-based models. However, this population level model also indicates that a similar mechanism is at work, at the level of the nonlinear dynamics of the network.

A specific role for corticothalamic feedback in spindling has been previously proposed. The massive feedback projection from the cortex to the thalamus has been hypothesised to be responsible for synchronising the activity during oscillatory behaviour. The current model also shows that if feedback to the LGN is outweighed by that to the TRN, then as feedback increases so does the amplitude of oscillations. With the modelling paradigm used here, a greater amplitude of oscillation is a direct indication of a larger number of simultaneously active cells, and therefore higher synchrony within populations. Hence, the results support the suggestion that corticothalamic feedback synchronises oscillatory activity in the thalamocortical network.

The 5-d parameter manipulations proved to be extremely insightful, particularly when examining the eigenvalue changes at the same time. Although the visualisation

of all 5 of the weight parameters changing simultaneously is not easy to achieve, the results clearly reflected the relationships identified in the bifurcation diagrams in less dimensions. Relating the results to the changes in the eigenvalues reinforced the theoretical analysis, and supported the use of LOCBIF for numerically determining the eigenvalues of the system. Furthermore, the changes in the oscillation frequency provide a further insight into the thalamocortical network, showing that the speeding up of oscillations into the attentive beta range is associated with a strong feed-forward thalamic projection into the cortex.

The slowing effect of the reticular time constant is comparable to that seen when bicuculline methiodide is applied to thalamic slices (e.g. by von Krosigk *et al.* (1993)). Bicuculline blocks $GABA_A$ receptors in the LGN, therefore $GABA_B$-mediated inhibition becomes dominant. Therefore, inhibitory inputs from the TRN induce slower IPSPs in TC cells, which was observed to result in spindles being transformed into slow paroxysmal 3-4 Hz oscillations. In the model, reducing τ_2 means that the inhibitory effect of the RE cell population acts over a longer time scale, and is therefore consistent with the effect of the application of bicuculline. This manipulation causes a slowing of the oscillation frequency to a similar 2-4Hz range. Furthermore, the synchrony within the TC cell population also increases as the frequency decreases, which is also consistent with previous findings (Bal *et al.*, 1995b). It is interesting that the transformation of spindles into slow, synchronised oscillations is replicated in this population model.

It is clear that in the circuit all included connections bar one are essential for the maintenance of oscillatory behaviour. Therefore the model does not support the experimental evidence, which shows that spindles exist in thalamic circuits. However, the model does not attempt to explain the generation of spindling, but to consider whether the thalamocortical network can support spindles which have been generated by ionic

interactions in the thalamic circuit. In addition, P is required to be greater than zero in order for the oscillations to exist. Therefore the included architecture of the model is validated by this result. The spindle frequency oscillation is not dependent on the TC-RE connection, which is inconsistent with the known circuitry of the thalamus, and with previous studies showing that disconnection of TC cells from RE cells abolishes spindling in thalamic slices (von Krosigk *et al.*, 1993). However, in the model it is likely that the lack of direct excitation from the TC cell population is compensated for by indirect excitation from the PY cell population. This compensatory pathway would not be present in the experiments as they were performed in thalamic slices, i.e. disconnected from the cortex.

In the current model, the existence of spindling is dependent upon the presence of the cortical population. This is not the case in the real system, as it has been shown experimentally that thalamic slices exhibit spindle oscillations in absence of the cortex (for example see von Krosigk *et al.* (1993)). The current model does not offer an alternative mechanism for the generation of spindling, as this phenomenon and its generation by the intrinsic properties of the RE and TC cells and their reciprocal connections is well established and fully described in previous experimental and modelling literature (for example Bal *et al.* (1995b); Steriade *et al.* (1993); von Krosigk *et al.* (1993)). Instead, the present model is used to investigate whether a model of the nonlinear population dynamics in thalamocortical network possesses a robust oscillatory activity in the spindles range, and therefore whether the structure of the network contributes to the maintenance of this behaviour once it is generated by the TC-RE network. Therefore, the necessity for the inclusion of the cortical population indicates that the cortex is involved in this maintenance of the oscillatory activity.

The approach used here is an extremely simplified one, such that ionic properties

are not explicitly represented by the model. Therefore this model fails to fully represent characteristics of spindle oscillations, such as waxing-and-waning. However, as discussed in chapter 6 extensions to the current model could involve including ionic neuronal properties, and would be interesting future work. Furthermore, each Wilson & Cowan equation represents a homogenous population of neurons with no spatial dimension. In reality, neurons in any giyen group are not perfectly identical and therefore the condition of homogeneity does not hold. As discussed in chapter 6, section 6.4.1, although homogeneity within a population of neurons is not perfect, within a localised region of a specific brain area, one can assume that neurons of the same type are similar.

The lack of spatial differentiation means that interesting phenomena such as the effect of cortical feedback on the synchrony of spindling between TC neurons across a region of thalamus cannot be measured, as done experimentally (Destexhe *et al.*, 1999). These limitations are important to understand, as they effect the questions that can be answered using such a representation. Therefore, this model should be considered as a tool in understanding thalamocortical spindling, which should be used in conjunction with other models, and experimental data. As the aim of this study was to investigate the oscillatory capabilities based on the dynamics of this simple thalamocortical network, this approach was well suited to address the hypothesis.

3.5 Summary and contributions

Using a population-based model of the thalamocortical network, it has been shown that the nonlinear dynamics intrinsic to this feedback circuit instil an ability to support oscillatory activity in the 7-14Hz spindling frequency range. The architecture of

the network is the simplest possible representation of the thalamocortical loop; a TC cell population, a cortical population and a reticular cell population. The connections between these populations were only included if they have been observed experimentally. The parameters for the network were also determined from experimental data, and the dependence of the network activity upon these parameters was evaluated using bifurcation analysis. This analysis indicated that the oscillatory activity in the 7-14Hz range is a robust property in relation to the model parameter space. However, it has also shown how a few parameters, relating either to specific connection strengths between populations or to the activation time constants for specific populations, exercise a close control over both the existence and frequency of the network oscillations. In this way, the results show a remarkable consistency with both experimental results and with results from other modelling studies, which used conductance-based models and emphasised the intrinsic membrane properties of the cells involved. A major prediction of the model is that the switch from normal spindle (7-14 Hz) to paroxysmal (2-4 Hz) oscillations may be a result of the change in the inherent thalamocortical circuit dynamics. This change is caused by the switch from a mainly $GABA_A$-mediated to a more slowly activating, $GABA_B$-mediated inhibition of the TC population by the RE population. The study of population-based models of neuronal networks may have particular value in neuroscience, since such models emphasise the importance of nonlinear dynamics in network behaviour.

Chapter 4

A model of receptive fields in the Lateral Geniculate Nucleus

4.1 Introduction

The hierarchy of the mammalian visual system has formed the basis of our understanding of visual processing, as well as being the foundation of most of the research in this area, for decades. However this hierarchical rule, which predicts that at each subsequent step through the visual system the level of processing should become increasingly complex, is broken as early as at the lateral geniculate nucleus (LGN), the primary visual nucleus of the thalamus. The thalamocortical (TC) relay cells of the LGN receive their driving input (as defined by Sherman & Guillery (1998)) from retinal ganglion cells. In turn, they send driving projections directly to the primary visual cortex (V1). TC cells have receptive field (RF) structures that are almost identical, in spatial terms, to those of their retinal inputs (Bullier & Norton, 1979; Hirsch, 2003; Hubel & Wiesel, 1961; Kuffler, 1953). In fact, the only reported difference is an increased inhibitory effect of the surround (Hubel & Wiesel, 1961; Levick *et al.*, 1972; Singer & Creutzfeldt,

1970; Solomon *et al.*, 2002). Therefore there appears to be no significant increase in the level of complexity of the thalamic RFs, which clearly challenges the idea of hierarchy.

Furthermore, TC cells in the LGN receive only 7% to 12% of their synaptic inputs from retinal sources (Montero, 1991; van Horn *et al.*, 2000). In contrast, TC cells receive feedback projections originating from excitatory cells in layer 6 of V1 which constitute approximately 30% of their inputs (Montero, 1991; van Horn *et al.*, 2000). It has been proposed in earlier studies that cortical feedback modulates thalamic responses (Destexhe, 2000; Montero, 1997; Rivadulla *et al.*, 2002), but the specific role of this input in sensory processing remains something of a mystery. Intuitively the magnitude of the cortical innervation suggests that the responses of thalamic TC cells should be driven by their cortical inputs as well as their retinal inputs. However, thalamic static responses to visual stimuli do not agree with this view, as they almost precisely replicate those responses seen in the retina (Bullier & Norton, 1979; Hirsch, 2003; Hubel & Wiesel, 1961; Kuffler, 1953).

However, when the temporal response properties of TC cells are considered, they tell a different story. The mapping of spatiotemporal receptive fields (STRFs) using a technique called reverse correlation (Jones *et al.*, 1987), has been an important tool in visual neuroscience for some time (for a review see DeAngelis *et al.* (1995)). For example, Cai *et al.* (1997) mapped the time-varying structure of TC cell receptive fields. STRFs have also been mapped in earlier studies using different experimental paradigms (Bullier & Norton, 1979; Stevens & Gerstein, 1976; Wolfe & Palmer, 1998), particularly the response plane technique (also reviewed in DeAngelis *et al.* (1995)). The results of Cai *et al.* (1997) confirm that TC cells do have a spatially concentric receptive field structure that is almost identical to those of retinal ganglion cells. However, they also show that this spatial structure reverses in polarity over time.

Cai *et al.* stimulated cat LGN TC cells with continuous sequences of bright and dark bars, which were presented at randomly selected positions across a cell's receptive field. Each time a cell fires a spike, the authors look backwards in time to find the stimulus (position and polarity) which triggered that spike (within a given time interval). The stimulus histogram is incremented at that spatial position, and separate histograms for light and dark stimuli are constructed. The final step involves subtracting the dark histogram from the light histogram to yield a composite STRF. This process is schematised in figure 1 of Cai *et al.* (1997), which is reproduced here in figure 4.1. These measured STRFs were shown to be biphasic in time, such that an ON-centre cell is bright-excitatory (in response to a stimulus presented in the centre of its RF) in the first phase of its response, and in the second phase the cell is dark-excitatory.

This time-varying property of TC cell phase preference, was also observed by (Reid *et al.*, 1997). These authors also performed a reverse correlation study, in this case with m-sequences, to estimate the RF structure of an OFF-centre Y cell in the cat LGN. As reviewed by Ringach & Shapley (2004), an m-sequence is a stimulus that is often used in reverse-correlation studies, and is effectively a "string of -1's and 1's", which approximates white noise. Reid *et al.* recorded what they called a "seemingly paradoxical feature of the receptive field", that the RF centre exhibits light-excitation at delays longer than 39 ms, peaking at around 65 ms. The expected dark-excitation was observed within a latency of 7.4 ms, peaking at ~22ms.

In both of these studies, a TC cell responds as expected in the first $\sim$ 50ms post-stimulus, but will produce the response expected from a cell of the opposite polarity in the subsequent $\sim$ 50ms. This is depicted in figure 4.2, which shows a typical ON-centre TC cell STRF as measured by Cai *et al.* (1997). A study which followed Cai *et al.* and Reid *et al.* measured the responses of connected retinal and geniculate

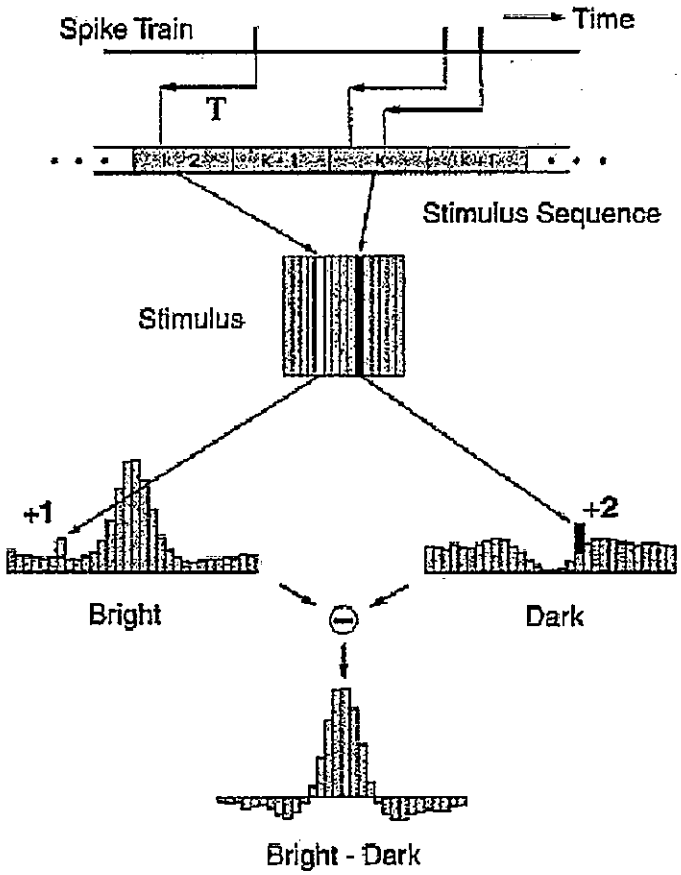

Figure 4.1: This figure is reproduced from Cai *et al.* (1997), and shows the reverse correlation algorithm which was used in that study in order to find the spatiotemporal receptive field structure of geniculate relay cells.

cells by an identical reverse correlation method (Usrey *et al.*, 1999). This was the first study to simultaneously use reverse correlation to measure the STRFs of pairs of monosynaptically connected retinal ganglion cells (RGCs) and TC cells.

Usrey *et al.* found that RGCs and TC cells both display a biphasic temporal response as shown previously (Cai *et al.*, 1997; Citron *et al.*, 1981; Reid *et al.*, 1997). However, they also show that the second phase of the TC cell response has a larger amplitude than that of the retinal response, when normalised with respect to the amplitude of the first phase. In some cases the amplitudes differed by three-fold. Therefore, although retinal inputs are in part responsible for the formation of TC temporal responses, this study highlights the fact that thalamic responses differ significantly from those of their retinal counterparts. This mismatch is not explained by Usrey *et al.*, nor in the subsequent literature.

One plausible explanation for the difference in the magnitude of the thalamic and retinal second-phase, is that the increased late dark-excitation exhibited by ON-centre TC cells (or the light-excitation by OFF-centre cells) is an offset response. That is, an excitatory response to the bright stimulus being switched off or leaving the receptive field. Considering the latencies involved allows the investigation of this proposal. Bair *et al.* (2002) recently made measurements of onset and offset responses in the LGN of macaque monkey. The results show that the latencies of offset responses are in the range of 18-27ms. Previous studies made in cat LGN, found the offset response to have a mean of 38ms (Mastronarde, 1987). Cai *et al.* (1997) used stimuli that were 13ms long, and the peak of the dark-excitation that Cai *et al.* measure occurs between 60-100ms. Therefore the biphasic response of Cai *et al.* occurs in the period of time after an expected offset response would be observed. *Therefore, the mechanism underlying the appearance of this biphasic response remains unknown.*

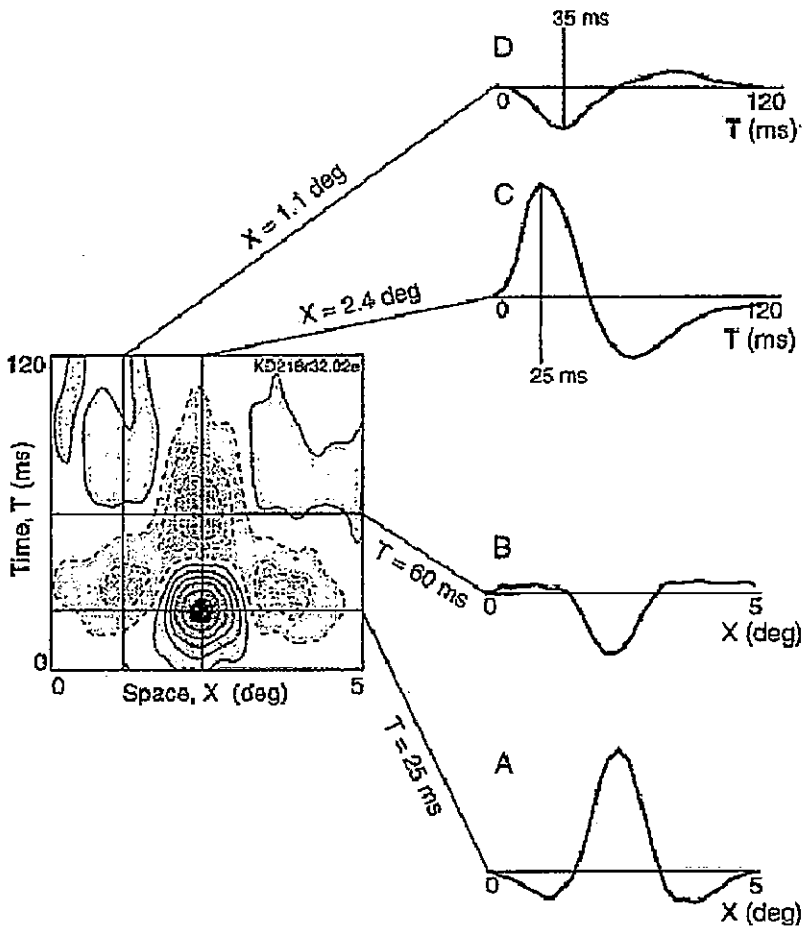

Figure 4.2: This figure, which is reproduced from Cai *et al.* (1997), shows a typical spatiotemporal receptive field of an LGN relay cell. The cell, which is classified as an ON-centre cell, shows the expected centre-surround receptive field at 25 ms post-stimulus onset. However at 60ms this response has reversed in polarity over time.

Therefore the retinal input to TC cells determines their spatial centre-surround receptive field properties, and to some extent accounts for the formation of the biphasic temporal receptive field. However, it is not clear what purpose the numerically large cortical innervation of TC cells serves. This poses a particular conundrum as corticothalamic feedback is specific with respect to a number of cell properties, as discussed in chapter 1, section 1.2.1. The most interesting of these properties are topography, cortical orientation preference (Murphy *et al.*, 1999), and phase preference (Wang *et al.*, 2004). Given that the results of Cai *et al.* (1997) are related to the phase properties of TC cells, it is logical that if feedback has an effect on thalamic temporal receptive fields, the phase relationship will be of particular importance. Wang *et al.* (2004) performed paired, in vivo recordings in the cat LGN and V1. Their results, which are based on the changes in firing mode of TC cells when the gain of the cortical feedback is manipulated, indicate that a cortical cell with a given ON or OFF preference directly feeds back to thalamic cells that have the opposite central phase preference. In the present work, a population-level model of the thalamocortical feedback circuit was constructed in order to investigate the influence of such anti-phase cortical feedback on thalamocortical cell response dynamics and receptive fields. It is hypothesised that this property plays a major role in the formation of thalamic temporal responses, and in particular in the strengthening of the second phase, therefore accounting for the difference between TC cells and RGCs measured by Usrey *et al.* (1999).

As described previously in section 1.2.2.2, Ghazanfar *et al.* (2001) proposed that cortical feedback is intimately involved in the formation of temporal responses in rat TC cells. The authors investigated the effect that inactivating the somatosensory cortex (SI) has on thalamic responses. They proposed that the early response displayed by VPM neurons arises from ascending inputs plus the disynaptic pathway from the SI

cortex via the TRN, while the late phase arises due to direct SI innervation of the VPM. Hence, they provide empirical evidence that corticothalamic feedback contributes to the temporal RF structure of TC cells. It is intended that theoretical evidence in support of this experimental study will be obtained in this part of this thesis.

As for the spindles model presented in the previous chapters, the Wilson-Cowan equations were used to create an extended population model of the thalamocortical network (Wilson & Cowan, 1972). Such models allow the analysis of the network behaviour in terms of the dynamics of the connectivity. The model network's architecture is described in section 4.2.1, and is based solely on connections that have been biologically proven to exist. A recent study by Casti *et al.* (2002) investigated a population-level model of LGN cells, but this was based on a population of integrate-and-fire-or-burst neurons, and is therefore at a higher level of complexity than that of the Wilson & Cowan equations. Here only spatial receptive fields are applied through the connectivity, and therefore the effect that the network dynamics have on temporal response properties can be determined. In the subsequent sections the model is described in detail, in particular the equations, architecture, and receptive field properties. Following this, the results of simulating this model are presented and discussed. It is shown that this network allows the thalamocortical relay cell populations to display temporal responses consistent with those observed experimentally, only when feedback is arranged in anti-phase.

4.2 Methods

4.2.1 Architecture of the receptive field model

In the sensory thalamocortical network there is evidence for a topographic mapping of connections (Sherman & Gullery, 2001), hence this rule was the underlying premise for specifying the model's architecture. The model involves a feedback loop between the TC cell populations of the LGN and the excitatory cell populations in layer 6 of the primary visual cortex (Amitai, 2001; Kaplan, 2004; Thomson & Bannister, 2003). This is the main component of the thalamocortical network that will be examined. The excitatory cortical cell populations receive inputs from the TC cell populations in order to form receptive fields that consist of three elongated subregions, a central subregion of one polarity flanked by two subregions of the opposite polarity. This receptive field connectivity is described in detail in section 4.2.4. In total the model contains four types of excitatory cortical cell populations: (1) horizontal ON, (2) horizontal OFF, (3) vertical ON, and (4) vertical OFF cell populations. The orientation refers to the preferred orientation of the cell population (as determined by the connectivity), and the ON or OFF refers to the polarity of the dominant central subregion.

In addition, there is the involvement of the thalamic reticular nucleus (TRN). As described previously in section 3.2.1, the TRN receives collaterals from both thalamocortical and corticothalamic projections, and sends its own projections to the TC relay cells (Liu & Jones, 1999; Wang *et al.*, 2001). There are also inhibitory interneurons present both in the cortex and the LGN, and such local inhibitory interneurons are assumed to be essential to normal neuronal functions. Similar architectures have been represented in previous models of the thalamocortical network (Bal *et al.*, 2000; Bickle *et al.*, 1999; Destexhe, 1999; Destexhe *et al.*, 1998; Hayot & Tranchina, 2001; Kirkland

et al., 2000; le Masson *et al.*, 2002; Suffczynski *et al.*, 2001; Terman *et al.*, 1996), although these previous studies usually neglect one or other of the inhibitory thalamic cell classes. However, as these two separate sources of inhibition in the thalamus have been postulated to serve distinct roles (Uhlrich & Cucchiaro, 1992), both were included in the current model. This anatomical connectivity is summarised schematically in figure 4.3.

The specific connectivity of the model can be seen in figure 4.4. This figure shows the connections between all cell types except the detailed structure of the inputs to the TC cell populations, which are shown separately in figure 4.5. Note that figure 4.5 shows the feedback connections arranged in anti-phase, which is the first of the three feedback arrangements that are examined in this model (see below and section 4.2.5 for more details). The connections are arranged so that populations are retinotopically connected. More specifically, many of these are point to point connections. The main exception is the connection between TC cell populations and cortical cell populations, where nine TC cell populations feed into each cortical cell population (except at the boundaries of the layers). This is due to the method adopted for the feed-forward formation of layer 6 cortical cell population RFs, which is explained in detail in section 4.2.4. In a number of cases, a presynaptic population is also connected to its retinotopically nearest neighbours in the postsynaptic population.

Between all cell populations of the same type, except the TC cell populations, there are horizontal nearest neighbour connections. Within thalamic nuclei no such horizontal connections between TC cells have been found (Contreras *et al.*, 1997b), and were therefore not included. In cortical excitatory layers and the RE layer there are also next to nearest neighbour connections. This is because there is evidence for long-range horizontal connectivity between the pyramidal layer 6 cells (Bolz & Gilbert,

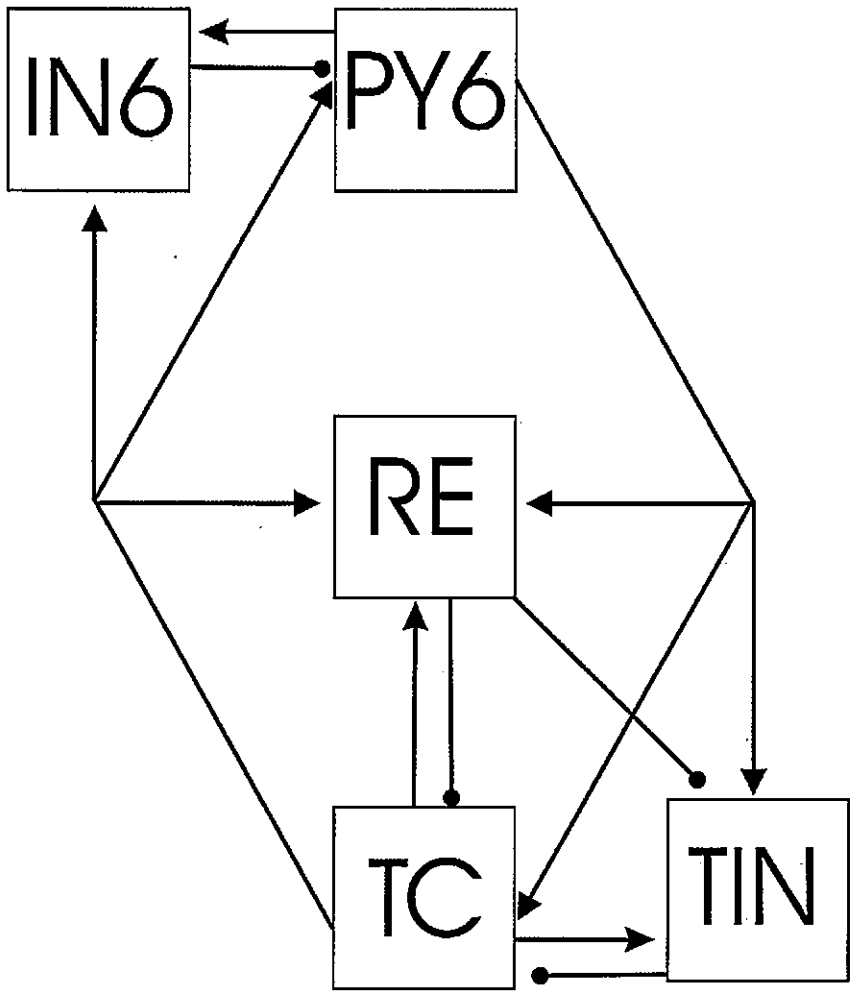

Figure 4.3: This figure shows the anatomical connectivity of the TC feedback network based on the physiological data from the literature. This figure presents the cell types and connections that were included in the architecture of the receptive field model. Excitatory connections are labelled by a triangular arrowhead $\rightarrow$, and inhibitory connections by a circular arrowhead $-\bullet$. Note that PY6 = Layer 6 cortical pyramidal cells, IN6 = Layer 6 cortical interneurons, RE = cells of the thalamic reticular nucleus, TC = thalamocortical relay cells, and TIN = thalamic interneurons.

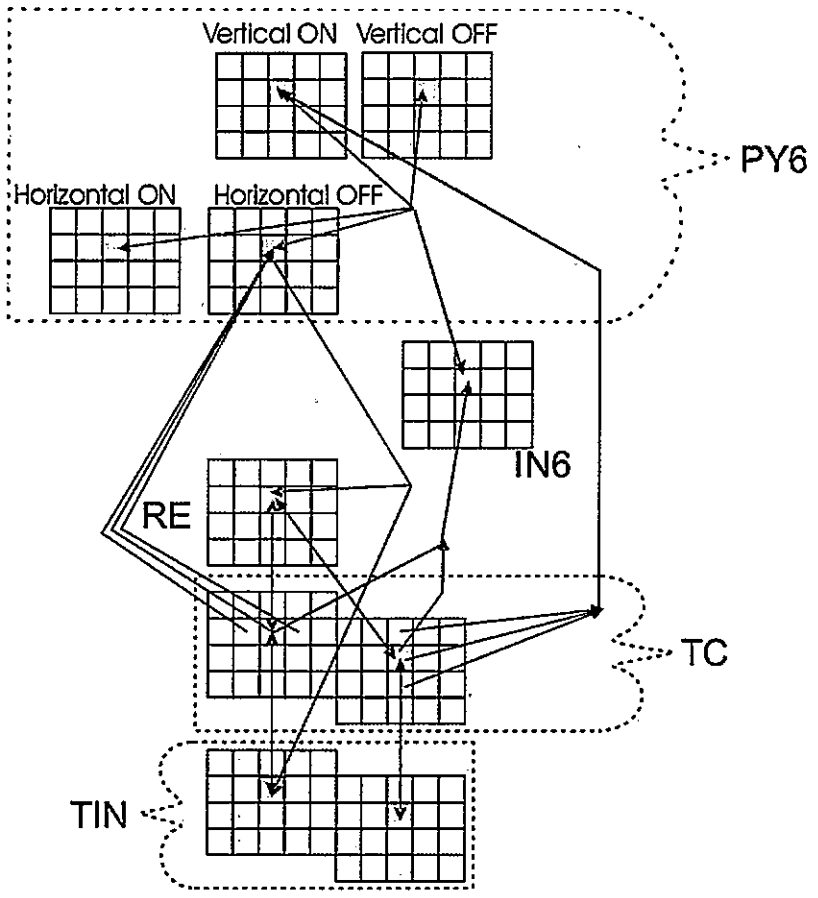

Figure 4.4: This figure shows the detailed connectivity between the populations in the model. In each of the PY6, IN6, and RE layers there are 20 populations of each cell sub-type. The TC and TIN populations have 40 populations to allow for 20 ON-centre and 20 OFF-centre populations. The details of the connectivity can be found in the main text.

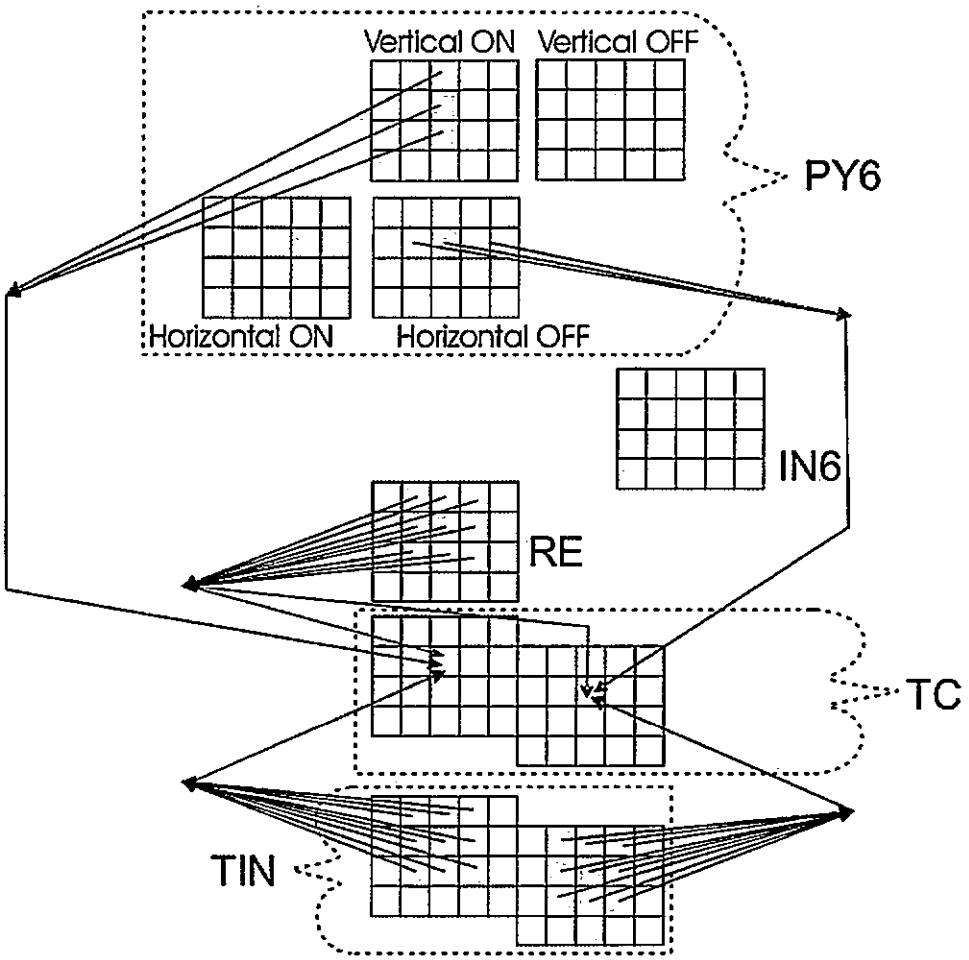

Figure 4.5: Detailed connectivity of the inputs to the TC cell populations. PY6 populations innervate a row of TC cell populations, which are parallel to the orientation preference of the PY6 cell population. This is consistent with the findings of Murphy *et al.* (1999). Thalamic inhibitory inputs from RE and interneuron populations come from retinotopically matching and nearest neighbour populations.

1986; van Brederode & Snyder, 1992). For the reticular cell populations, this is because horizontal connections have been proposed to have functional significance (Sherman & Gullery, 2001).

Studies have shown that TC cell to cortical cell connections join cells of the same phase type (Alonso *et al.*, 2001; Alonso, 2002). This means that an ON-centre TC cell will feed forward to an ON dominant cortical cell. This idea is also a major factor in the Hubel and Wiesel model for the formation of cortical receptive fields (Hubel & Wiesel, 1962), and consequently this strategy was adopted in the current model. However, a recent study by Wang *et al.* (2004) suggests that this in-phase connectivity may not be maintained for feedback connections. The authors initially propose a number of connectivity patterns that may be present between the thalamus and the cortex. Their experiments measure the change in thalamic firing mode when cortical feedback is focally enhanced. With enhanced feedback, the authors report that a larger proportion of TC cells increase the burst/tonic ratio, compared to those with a decrease in burst/tonic ratio. As burst firing requires hyperpolarisation to activate the I_T current, it is proposed that feedback must either occur between the same polarity cells via an inhibitory interneuron, or between cells of the opposite polarity. Figure 4.6 shows the proposed circuitry, from Wang *et al.* (2004), for clarification. That is, when a TC cell receives input from the visual cortex it comes from a cell which has the opposite ON/OFF phase preference. Therefore, three feedback architectures of the model are investigated: one containing anti-phase feedback, one without cortical feedback, and one with in-phase feedback. The STRF results shown in section 4.3.2 were produced for these three model architectures.

In summary, there are 5 main cell types (and a total of 10 sub-types) represented in the model. There are 20 populations of each sub-type, therefore there is a total of

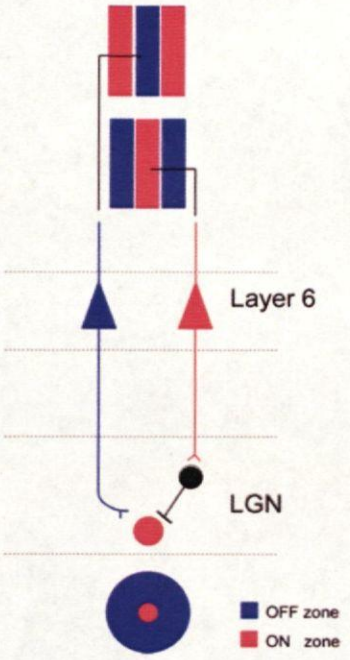

Figure 4.6: This figure shows the circuitry which the results from Wang *et al.* (2004) suggest exists between the thalamus and the cortex. A given ON centre TC cell is shown at the bottom of the figure, and this cell receives feedback either directly from a cortical cell of the opposite polarity or indirectly from a cell of the same polarity via an inhibitory interneuron. This connectivity pattern is termed anti-phase or phase reversed feedback.

200 cell populations:

1. Layer 6 cortical pyramidal cells in four sub-types, called PY6 cell populations: horizontal ON cell populations, horizontal OFF cell populations, vertical ON cell populations, and vertical OFF cell populations.

2. Layer 6 cortical inhibitory interneurons, called IN6 cell populations.

3. Cells of the thalamic reticular nucleus, called RE cell populations.

4. Thalamocortical relay cells in the LGN, called TC cell populations: ON-centre populations, and OFF-centre populations.

5. Inhibitory interneurons in the LGN, called TIN cell populations: ON-centre populations, and OFF-centre populations.

4.2.2 The Wilson-Cowan equations

As before, the Wilson-Cowan equations for the nonlinear dynamics of neural populations were used to represent the thalamocortical network described above (Wilson & Cowan, 1972). The equations for each of the five main cell types are presented in equations 4.1 to 4.5. Whilst only one of each connection type appears in the equations shown here, there may be more than one connection from a given type of presynaptic cell population innervating the postsynaptic population, as described in the previous section (section 4.2.1) and as shown in figures 4.4 and 4.5. Note that both TC cell populations and TIN cell populations receive retinal input (Sherman & Gullery, 2001).

$$\tau PY6\frac{dE_{PY6}}{dt} = -E_{PY6}(t) + (k_e - E_{PY6}(t)) \cdot Z_e(-wIN6PY6 \cdot I_{IN6}(t) + wTCPY6 \cdot E_{TC}(t)) \quad (4.1)$$

$$\tau IN6\frac{dI_{IN6}}{dt} = -I_{IN6}(t) + (k_i - I_{IN6}(t)) \cdot Z_i(wPY6IN6 \cdot E_{PY6}(t) + wTCIN6 \cdot E_{TC}(t)) \quad (4.2)$$

$$\tau RE\frac{dI_{RE}}{dt} = -I_{RE}(t) + (k_i - I_{RE}(t)) \cdot Z_i(wPY6RE \cdot E_{PY6}(t) + wTCRE \cdot E_{TC}(t)) \quad (4.3)$$

$$\tau TC\frac{dE_{TC}}{dt} = -E_{TC}(t) + (k_e - E_{TC}(t)) \cdot Z_e(wPY6TC \cdot E_{PY6}(t) - wRETC \cdot I_{RE}(t) - wTINTC \cdot I_{TIN}(t) + Retinal) \quad (4.4)$$

$$\tau TIN\frac{dI_{TIN}}{dt} = -I_{TIN}(t) + (k_i - I_{TIN}(t)) \cdot Z_i(wPY6TIN \cdot E_{PY6}(t) + wTCTIN \cdot E_{TC}(t) - wRETIN \cdot I_{RE}(t) + Retinal) \quad (4.5)$$

In summary, the main features of the Wilson & Cowan model are as follows:

1. The functional variable is the fraction of cells in a population that are firing per unit time, at time t. For example, E_{PY6}, or I_{IN6}.

2. The model ignores spatial interactions within populations and deals only with the temporal dynamics of that population.

3. The strength of the connection from a given presynaptic population (Pre) to a postsynaptic population (Post) is denoted by wPrePost.

4. The functions $Z_p(x)$ (where p=i for inhibitory populations or p=e for excitatory populations) are called the response functions. These represent the proportion of cells firing in a population for a given level of input activity x. They are defined by equation 3.1 in chapter 3.

4.2.3 The choice of parameters

In equations 4.1 to 4.5, as described previously in section 3.2.2, each of the parameters τ represents the time constant of the change in the proportion of non-refractory cells which are firing in a population, in response to the change in the average membrane potential activity of the cells. As before, experimental data from the literature was used to determine the range of values that these parameters could take. For TC cells, the observed range τ is 5 to 64ms (Turner *et al.*, 1997; Ulrich & Huguenard, 1996); for RE cells it is 13 to 53ms (Landisman *et al.*, 2002; Ulrich & Huguenard, 1996); for TIN cells, membrane time constants as high as 94ms have been reported (Zhu *et al.*, 1999); for cortical cells the range is within 7 and 22ms (Anderson *et al.*, 2000; Hirsch *et al.*, 1998, 2002). Therefore, the time constants were chosen to be within these ranges.

The weights of each connection type also need to be defined, and once more there is a great deal of evidence from physiological experiments that can be used to determine the relative connection strengths, for example the number of synapses mediating a connection, or the efficacy of synaptic transmission between populations. For the current study the evidence described in section 3.2.4 was used in partnership with the additional following data: thalamic interneurons receive their greatest number of

synaptic inputs from retinal sources (van Horn *et al.*, 2000); the strength of thalamocortical innervation is greater than the intra-cortical innervation of a cortical cell (Amitai, 2001; Beierlein & Connors, 2002); there is a larger number of intra-cortical connections compared with thalamocortical connections (Usrey, 2002); the fact that RE cells send most of their outputs to innervate TC cells (Wang *et al.*, 2001). The selected parameter values were chosen to reflect the above findings as described below.

4.2.4 Receptive field structures

The aim of this model was to look at the effect of cortical feedback on the temporal receptive field properties of thalamic cells. By imposing only spatial receptive fields, the effect of network dynamics on the arising temporal responses can be examined. Therefore, it was assumed that the visual field is a 2-D space uniformly divided into pixels, and each TC and TIN (Dubin & Cleland, 1977) cell population receives input from a 4x4 pixel portion of the space. A centre-surround receptive field is created by taking as input to the population the sum of 4 central pixels and the 12 peripheral pixels. For an ON-centre cell population, the centre four pixels give a positive input and the peripheral pixels a scaled negative input. Therefore, a light stimulus (positive contrast relative to a zero background) flashed in the RF centre will elicit a positive input, but a light in the surround produces a negative input. The opposite situation exists for OFF-centre, ON-surround populations. In this way 20 TC and 20 TIN ON-centre, OFF-surround populations, and 20 TC and 20 TIN OFF-centre, ON-surround populations were obtained. These have spatially overlapping surrounds at each point in the visual space. This process is depicted in figure 4.7.

Simple cortical cell RFs were originally proposed by Hubel & Wiesel (1962) to be constructed through a purely feed-forward scheme. This involves aligned TC cells with

overlapping centre/surround RFs feeding information to a single simple cell to form a RF with alternating ON and OFF subregions. This mechanism does not allow for contrast invariant orientation tuning of cortical cells, as described in a review by Ferster & Miller (2000). However, the current study uses simple stimuli and concentrates on the responses of thalamic cell populations, which allows the use of a feed-forward mechanism for cortical RF formation.

Reid & Alonso (1995) also showed that a given cortical cell's RF subregion (ON and OFF, centre and flanking) is constructed by receiving inputs from TC cells whose RF centres are at the same retinotopic location and have the same ON/OFF phase (Reid & Alonso, 1995). This is schematised in figure 4.8, which also shows the connectivity adopted in the model in order to create the cortical receptive field structure. Here a horizontal ON cell population receives input from three aligned ON-centre TC cell populations to form the central region of the RF. The cell population also receives input from three aligned TC OFF-centre cell populations at either side of its central RF region, to form flanking subregions of the opposite polarity.

Other than the spatial receptive field structure, no other response properties are imposed on the cell populations. Hence, all observed temporal responses can be assumed to arise from the nonlinear dynamics of the network activity.

4.2.5 The phase relationship

As described in section 4.2.1, results based on three alternative corticothalamic feedback arrangements will be presented. One involves phase reversed (or anti-phase) corticothalamic feedback, where a TC cell population of a given phase, receives feedback from a cortical cell population whose central subregion is of the opposite ON/OFF polarity. Anti-phase feedback was shown to exist in the cat visual thalamocortical

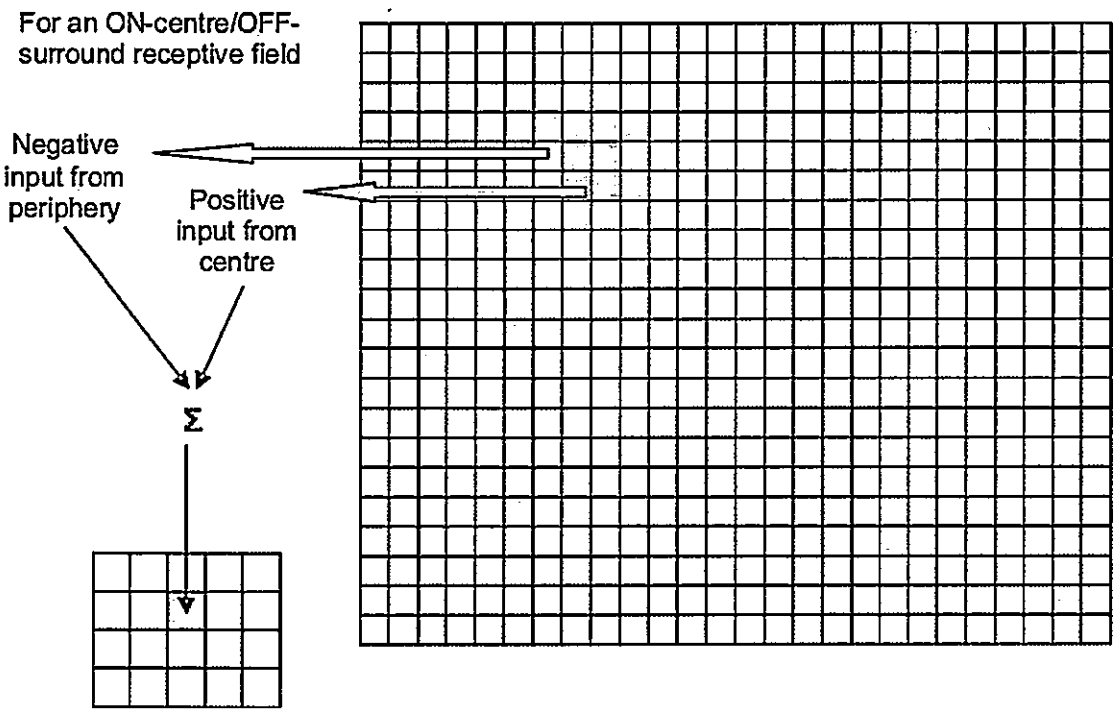

Figure 4.7: The setting up of an ON-centre, OFF-surround TC cell population's receptive field. The cell population receives input from 16 (4x4) pixels in the 10x12 array that represents the visual field. The central four give a positive input and the outer 12 a negative input. This situation would be reversed for the construction of an OFF-centre RF.

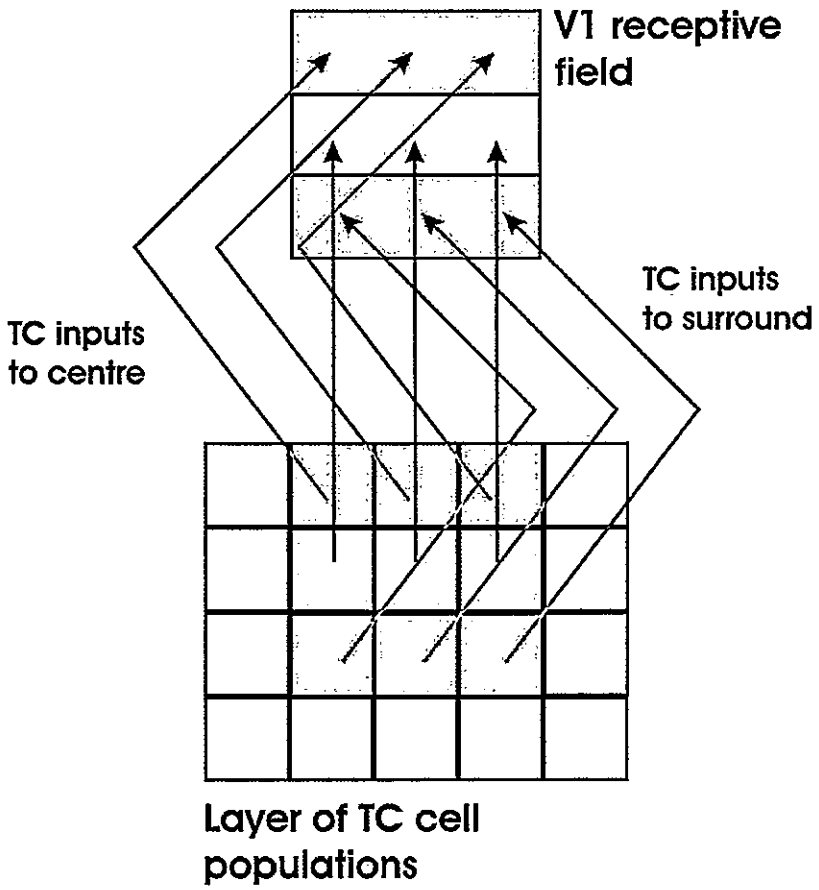

Figure 4.8: The setting up of a cortical, horizontal, ON receptive field. The figure shows the arrangements of TC cell populations, which are represented by their RF centres, which form the cortical RF. The PY population receives input from three TC populations, whose centres are at the same retinotopic location as the PY6 cell population's central subregion. It also receives input from 6 TC populations of the opposite polarity (3 either side) to form antagonistic, flanking subregions.

circuitry by Wang *et al.* (2004). The second contains no feedback connections. The third involves phase matched (or in-phase) corticothalamic feedback, where a TC cell population of a given ON/OFF phase receives feedback from a cortical cell population whose central subregion is of the same ON/OFF polarity.

The network is represented by the coupled differential equations (equations 4.1 to 4.5 in section 4.2.2). The parameters representing the time constant of each cell population, and the weight of each connection between the populations, were set such that the constraints outlined in sections 3.2.4 and 4.2.3 were adhered to. These parameters were then explored within the ranges permitted by these constraints and set at the values shown in table 4.1, which were used for the anti-phase case, the case without feedback, and the in-phase case.

4.2.6 Mapping spatiotemporal receptive fields

The process of reverse correlation was first described by DeBoer & Kuyper (1968), and has been used a great deal to map receptive fields in the visual (reviewed by DeAngelis *et al.* (1995)), auditory (reviewed by King & Schnupp (1998)) and somatosensory modalities (reviewed by Ghazanfar & Nicolelis (2001)). Reverse correlation involves stimulating a neuron with a continuous random sequence of brief stimuli, whilst recording the ongoing response of that neuron. Two fundamental assumptions are that, (1) the cell responds linearly, and (2) the stimulation approximates white-noise. If these assumptions are satisfied, then calculating the cross-correlation of the response with the stimulus at various time delays yields the spatiotemporal filter of the recorded neuron.

Prior to the development of the reverse correlation technique, the prevalent method used for mapping the STRF properties of neurons was the "response-plane" technique,

Parameter name	Value
τPY6	20ms
τIN6	20ms
τRE	20ms
τTC	20ms
τTIN	20ms
wPY6IN6	5
wPY6RE	15
wPY6TC	15
wPY6TIN	15
wIN6PY6	10
wRETC	15
wRETIN	5
wTCPY6	40
wTCIN6	5
wTCRE	10
wTCTIN	10
wTINTC	15
wPY6PY6	0.5
wIN6IN6	1
wRERE	1
wTINTIN	1

Table 4.1: Table of parameters used in the model. The weights are labelled by wPrePost, where "Pre" refers to the presynaptic population and "Post" refers to the postsynaptic population. For example, the connection from TC cell populations to PY6 cell populations is weighted by a parameter labelled wTCPY6.

which was described by Stevens & Gerstein (1976). This process involves presenting a brief stimulus at sequential positions in a cell's receptive field, and recording the cell's response in the form of a peri-stimulus time histogram (PSTH) to each stimulus for a give period of time. The PSTH at each position then represents the response profile at that point. The main benefit of using reverse correlation rather than the response-plane method is time. Reverse correlation involves presenting a continuous stream of stimuli and recording the response of the neuron continuously, and therefore it is much faster than the response-plane method. When mapping the response-plane, there must be a delay after the presentation of each stimulus and before a subsequent stimulus can be presented, while the response is recorded.

There are two major reasons why it is not necessary to record STRFs in the model using reverse correlation: (1) time is not a constraint, as the computational simulations performed here are faster than the equivalent experimental recordings; (2) the spatial structure of the receptive field is already known, as these are "hard wired" into the model (as described in section 4.2.4). Therefore, in the current work, a technique analogous to plotting the response-plane was used. Stimuli were briefly presented (for 30ms) at sequential positions in the receptive field of the cell population. The firing rate was recorded for a period of 300ms post-stimulus. This was done for both positive contrast stimuli (relative to a zero background) and negative contrast stimuli, and responses at each position for each stimulus type were recorded. Finally, in order to compare the results with those of Cai *et al.*, the dark response was subtracted from the light response for each stimulus presentation, and the "composite" STRF was constructed.

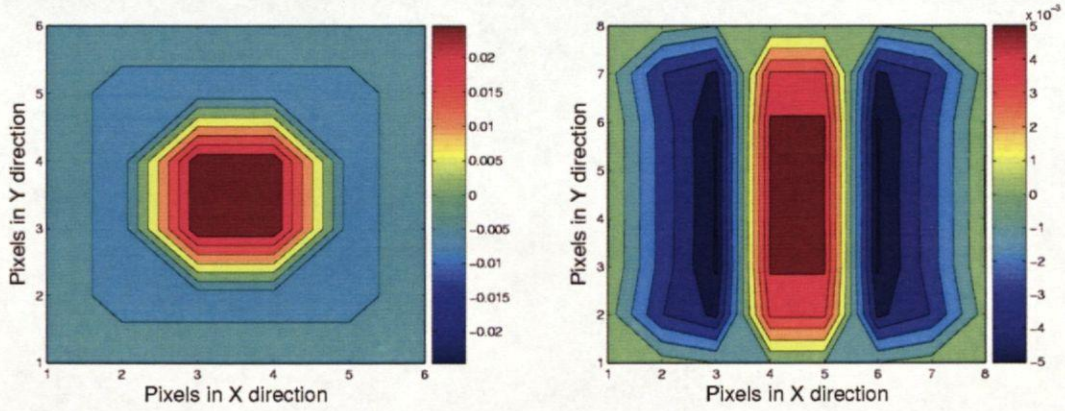

(a) (b)

Figure 4.9: The static receptive field of a TC (a) and a PY6 (b) population. In (a) the response clearly has an ON-centre/OFF-surround structure in space, as expected from the input connectivity. In (b) the cell population has an elongated three subregion receptive field, which is also expected from the wiring of the model and consistent with experimental results.

4.3 Results

4.3.1 Feed-forward visual responses

As discussed above, TC cells have been shown to have static centre/surround RFs which spatially resemble those of their retinal inputs. To ensure that the model agreed with this, responses to feed-forward information from the visual field were examined when corticothalamic feedback was not present. At this point there was no need to consider the three versions of the model separately, as without feedback these versions are identical. Initially, the static RFs were mapped using a similar technique to that described above (section 4.2.6).

To reiterate, single spots of light and then dark stimuli (positive and negative contrast) were flashed for 30ms at all points within a TC cell population's receptive field, while the response of that population to each stimulus was observed. The peak

amplitude of the cell population's response was recorded. The final step was to calculate the composite response as a light minus dark profile (as in Cai *et al.* (1997)). An ON response is a response to a positive stimulus, and an OFF response is a response to a negative stimulus, therefore it is reasonable to calculate a light-minus-dark RF which can be directly compared to the results of Cai *et al.*. Figure 4.9 shows examples of typical TC and PY6 cell population static RFs. The TC cell population in figure 4.9(a) is expected to have (from its input connections), and is shown to have, an ON-centre/OFF-surround receptive field. Similarly, the PY6 cell population in figure 4.9(b) should have and is shown to have three elongated subregions, vertically aligned, and with a central ON subregion.

Having ascertained that the shape of the spatial RFs matches those shown in previous experimental studies and the expectations from the wiring of the model, responses to more complex stimuli were examined, also in the absence of feedback. In the first of these simulations the stimuli used were spots of varying diameter and annuli. The four stimuli are shown schematically in figure 4.10. The TC cell populations responded as expected due to their centre/surround RFs. As shown in figure 4.11(a), this ON centre cell population responds preferentially to a spot of light covering the entire RF centre, but with a slightly suppressed firing rate to the dark central spot. It also responds vigorously to a dark annulus covering the surround of the RF, but with slightly suppressed firing to a light annulus. Hence, the model produces the responses expected from thalamocortical cells with centre/surround RFs.

The responses shown in figure 4.11(b) are from a cortical cell population, which is a target of the TC cell population shown in figure 4.11(a). The PY6 cell population has very similar responses as the TC cell population to the same four stimuli. The main deviation is in the response to the spot extending beyond the TC RF. In this

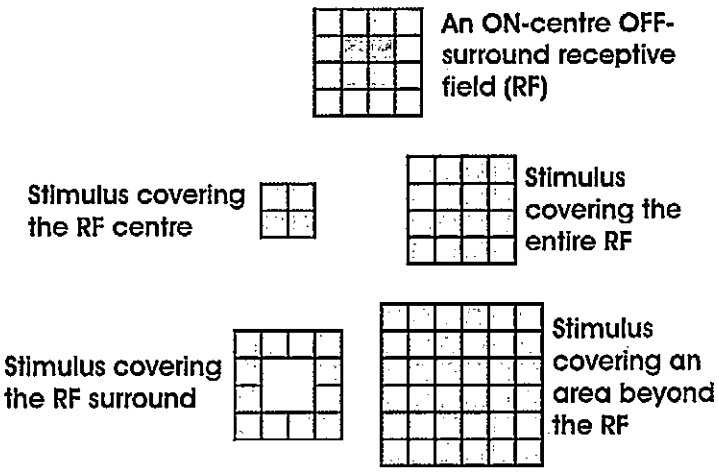

Figure 4.10: The figure shows the set of stimuli used to test the static responses of the cell populations. At the top is a depiction of a concentric antagonistic receptive field. Below are the four stimuli used, which are described in the figure.

case the PY6 cell population responds vigorously to the dark stimulus, though the TC cell population did not. This stimulus covers a substantial proportion of the PY6 population's flanking OFF subregions, which are larger than the surround of the TC RF. Hence, the wiring of the model explains why the PY6 population responds more vigorously than the TC population in this case.

It is widely known that when stimulated with oriented bars, cortical responses differ from those of their thalamic inputs, as cortical cells respond preferentially to bars at a particular angle (Gardner *et al.*, 1999; Hirsch, 2003; Hubel & Wiesel, 1961, 1962). Therefore, light and dark bars of different orientations were presented to the model, and the responses of the cortical cell populations were recorded. In this way tuning curves were produced, and an example is shown in figure 4.12. This figure shows that the cortical cell population has a distinct preference for vertically oriented bars. From the connectivity of the model, this preference is expected.

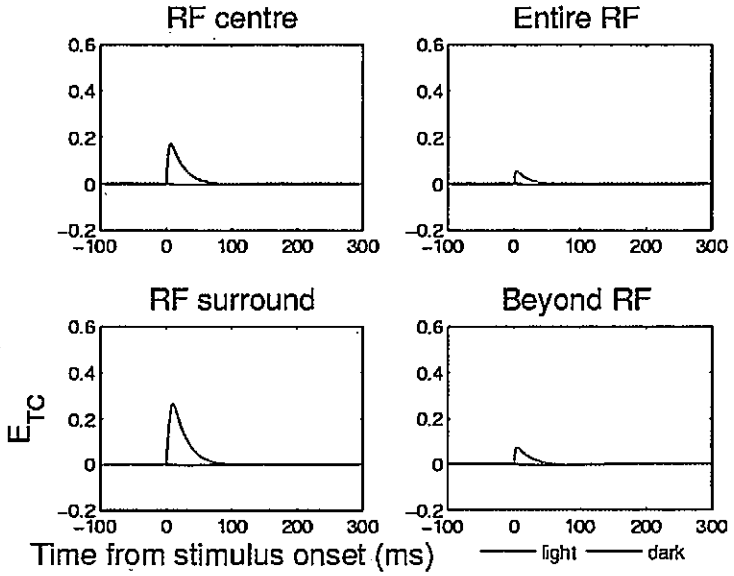

(a)

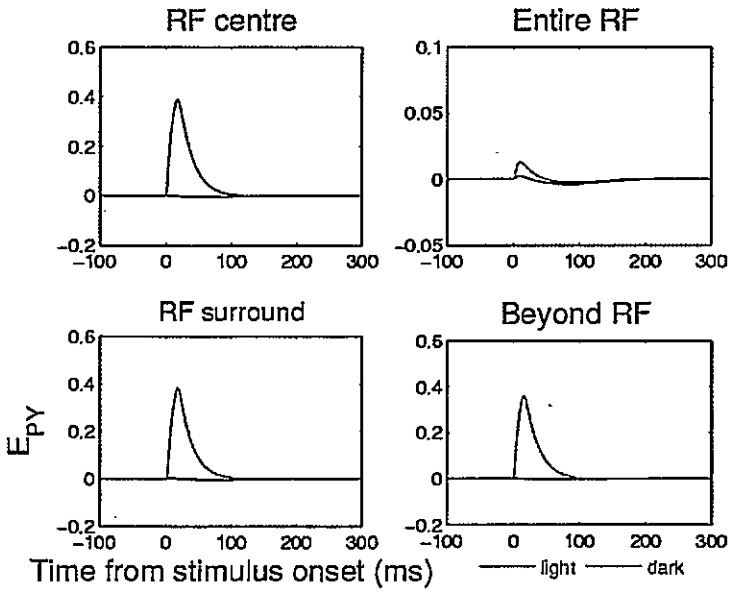

(b)

Figure 4.11: The responses of a typical TC (a) and a PY6 (b) cell population to flashed stimuli of varying diameters. In (a) the ON-centre TC cell population responds most strongly when stimulated by a bright spot covering just the centre of its RF, or a dark stimulus covering the surround. These responses are consistent with the expectations of the RF structure. The responses in (b) correspond well with the TC responses in (a), apart from the response to the stimulus that extends beyond the RF. This is discussed in the main text.

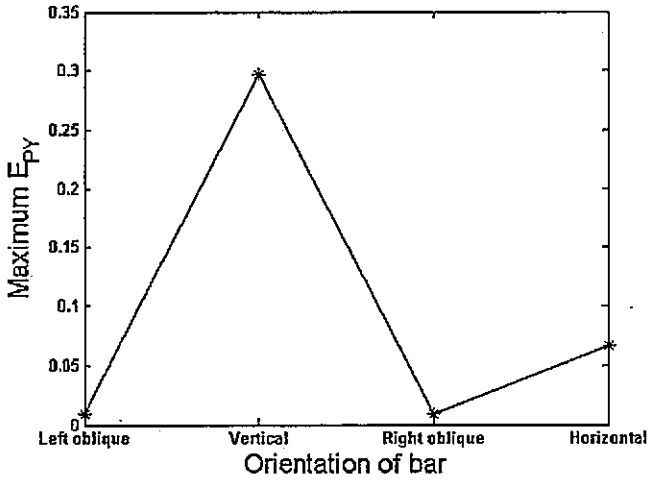

Figure 4.12: Response of a typical PY6 cell population to flashed bars at four different orientations. The plot shows that the PY6 cell population has a distinct preference for vertically oriented bars.

4.3.2 Thalamic spatiotemporal receptive fields

The effect of introducing corticothalamic feedback and completing the network was explored next. A protocol similar to the response-plane technique was used once more. However the evolution of the response over time was now considered. This means that a given population's response is recorded for a given amount of time, and these responses (light minus dark) are plotted against one spatial dimension to obtain the spatiotemporal receptive field of that cell population. These can then be directly compared to those shown by Cai *et al.* (1997). To reiterate, Cai *et al.* showed that reverse-correlation of TC cell responses produced STRFs that were centre-surround in space and biphasic in time. The latency between the peaks of the two phases was found to be approximately 35ms.

Typical responses of a TC cell population in the anti-phase model are shown in figure 4.13, which shows a TC cell population with ON-centre/OFF-surround input

wiring. Note that the results in this section are shown for both bar stimuli, as used by Cai *et al.*, and for single pixel stimuli. In agreement with the findings of Cai *et al.*, a biphasic response pattern is displayed by the thalamocortical cell population, such that during the first phase the cell population responds as expected in an ON-centre manner (that is light-excitatory). After a latency of approximately 20ms this response changes polarity and the cell populations respond in an OFF-centre manner (that is dark-excitatory). Note that this biphasic response can be seen if the stimuli used are either bars or single pixels. However, the surround response only shows this biphasic property when bars are used. This is consistent with the results of Cai *et al.*, who also used stimulating bars. In the model, this difference is due to the fact that bars excite the cortical cell populations more strongly, as PY6 cell populations are selective for oriented stimuli, and therefore cortical feedback to the TC cell populations is stronger when bars are used. This indicates that feedback plays a role in the formation of the second phase of the response.

In both the bar case and the single pixel case, the surround response merges with the centre response in time, which is consistent with the results of Cai *et al.* (1997). This is related to the idea that the surround response is delayed relative to the centre response, and therefore they appear to merge into one another. It is interesting to see that this model, with no imposed temporal response properties, also replicates this feature of thalamic receptive fields. When using single pixels, the latency between the bright-excitatory and dark-excitatory phases increases. This is because single pixels induce less excitation, hence the network is not driven as strongly or rapidly as it is with bars, and therefore the latency between the two phases is longer.

Cortical feedback to all thalamic cell populations was disconnected, by setting the weight of the connections to zero, and this is the second of the feedback arrangements

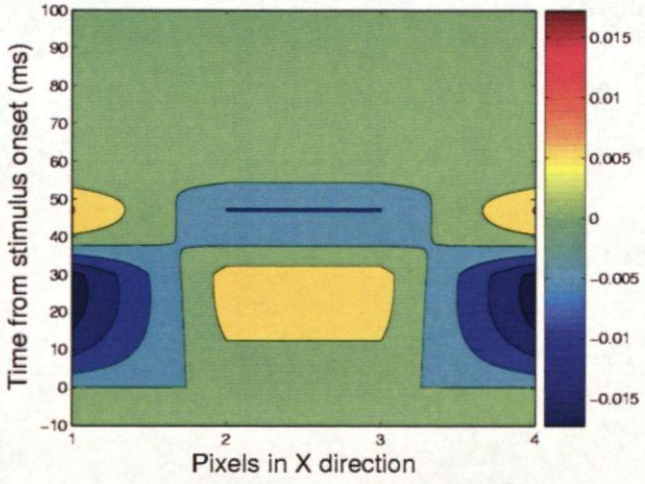

(a)

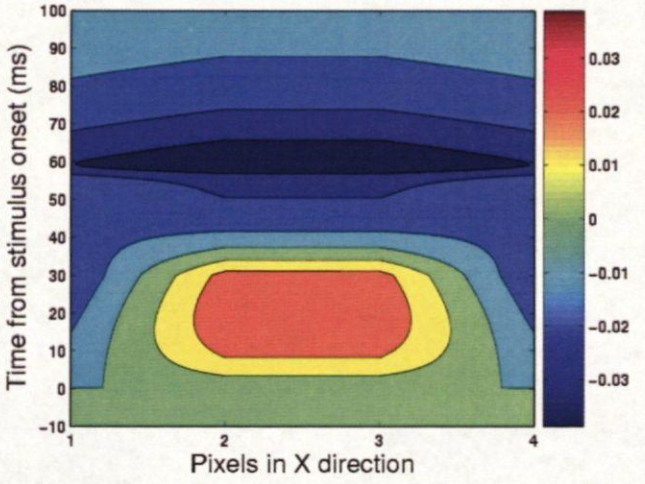

(b)

Figure 4.13: Temporal evolution of the response of a TC cell population stimulated with bars (a) and single pixels (b) along a row of its RF, in the intact network with anti-phase feedback. The biphasic response is clearly seen, such that during the first 30ms post-stimulus onset, the cell population displays a light-excitatory response in the RF centre. In the following 30ms of time the cell population shows a dark-excitatory response in the RF centre. The initial surround response merges into the secondary centre response, which is also consistent with the data of Cai *et al.* (1997). The latency between the peaks of these two response phases is approximately 20ms in the bars case and approximately 30ms in the single pixel case, which are both of the same order of magnitude as in the Cai *et al.* study.

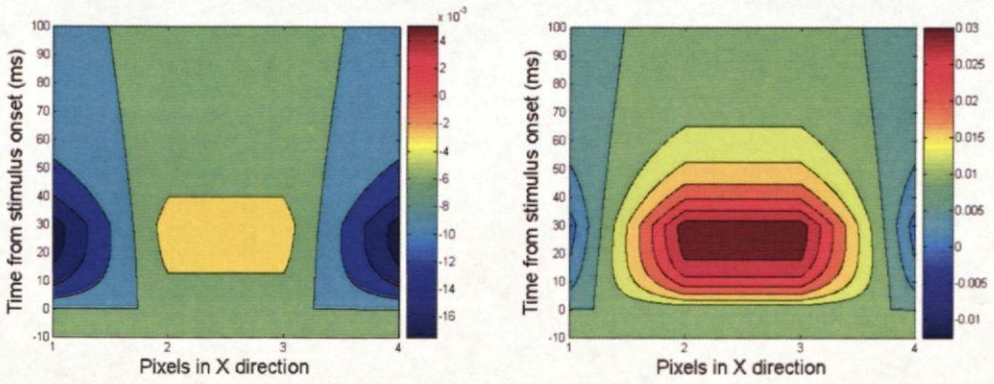

(a) (b)

Figure 4.14: Temporal evolution of the response of a TC cell population stimulated with bars (a), and single pixels (b) in the network with no corticothalamic feedback. In this case no biphasic response is seen, even at long latencies.

which was examined in this model. For simplicity no attempt was made to model retinal ganglion cells with biphasic temporal responses. Therefore the current reuslts show that when cortical feedback is not present the recorded TC cell population loses the second phase of its STRF, as shown in figure 4.14, regardless of whether bars or single pixels were used. These results indicate that in the model corticothalamic feedback plays a major role in generating this dynamic response property, and this is explored in more detail in section 4.3.3 below.

Finally the network was arranged to contain in-phase feedback connectivity, as described in section 4.2.5. In this case, simulations of the TC cell populations response to either bars or single pixels show that there is no appearance of a biphasic response, as shown in figure 4.15. Therefore, the simulations of the model in the three different feedback configurations clearly indicate that corticothalamic feedback is vital for the emergence of a biphasic response, and furthermore that anti-phase feedback is specifi-

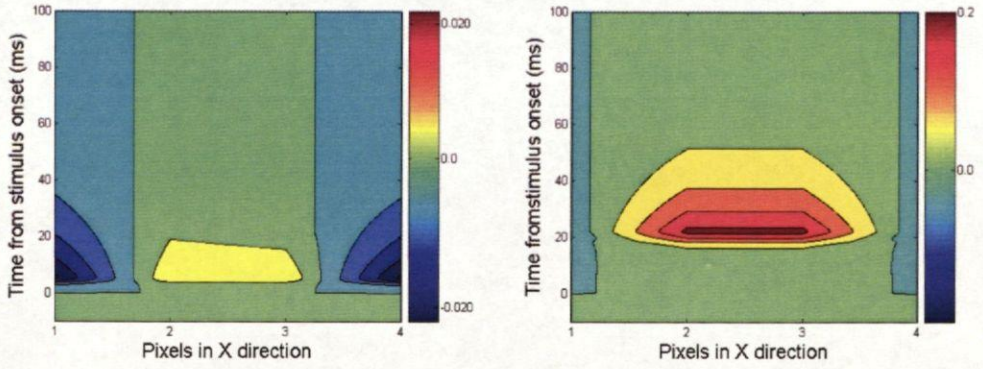

(a) (b)

Figure 4.15: Temporal evolution of the response of a TC cell population stimulated with bars (a), and single pixels (b) in the intact network with in-phase feedback. Once more, no biphasic response is seen.

cally required.

4.3.3 Parameter manipulations

When using a theoretical model to investigate neuronal systems, it is crucial that the robustness of a result with respect to parameter variations is considered. Unlike in the previous model, it was not possible to use bifurcation analysis, as there are too many equations and therefore parameters for the software (LOCBIF) to handle. Instead, the parameters of the anti-phase network were manually manipulated and the effects on the activity were observed, to assess the robustness of the behaviour. Initially all parameters were varied between $\pm 20\%$, and assuming that $\pm 5\%$ is the minimum acceptable variability, it was found that all parameters exceeded this minimum, which indicates that the response is robust to such parameter changes around the control values.

The next step was to specifically change (put to zero, halve and double) the con-

nection weights of the inputs to the TC population being observed. Note that for these experiments, single pixels and not bars were flashed in the centre of the TC cell receptive field. By using single pixels, less network activity is elicited, and this allows a clearer discrimination of the mechanisms which underly the observed behaviour. The results show that the second phase was absent during the manipulation of only two of the connection weights. This occurred when varying the PY6 to TC connection weight, as shown in figure 4.16, and when varying the TC to PY6 connection weight, as shown in figure 4.17. These plots show that without either part of this thalamocortical feedback loop, the biphasic response is not present. Looking at the light and dark responses individually (also shown in figures 4.16 and 4.17), it is apparent that the TC population cannot respond positively to a dark stimulus as it does in the control case, but instead responds with a small suppression of firing rate. Therefore, the composite response is dominated by a mainly light response.

Another interesting feature of this response property, which emerged from this set of experiments, relates to the timing of the second phase. The parameter manipulations revealed that the strength of the feed-forward thalamocortical connection, and the strength of the corticothalamic feedback connection can change the relative timing of the two phases. This is shown in figure 4.18, where the weights of these connections are varied around their control values. The figure shows that as either of these connections increases, the latency between the first (bright-excitatory) phase and the second (dark-excitatory) phase decreases. Therefore, it seems that in the model the effect of feedback on the temporal response properties of the TC cell populations is not static, but a dynamic effect. Note that it was also found that the RE to TC, and TIN to TC connections can have a similar controlling effect on the latencies of the response phases, which is demonstrated in figure 4.19. However, as the second phase is not present

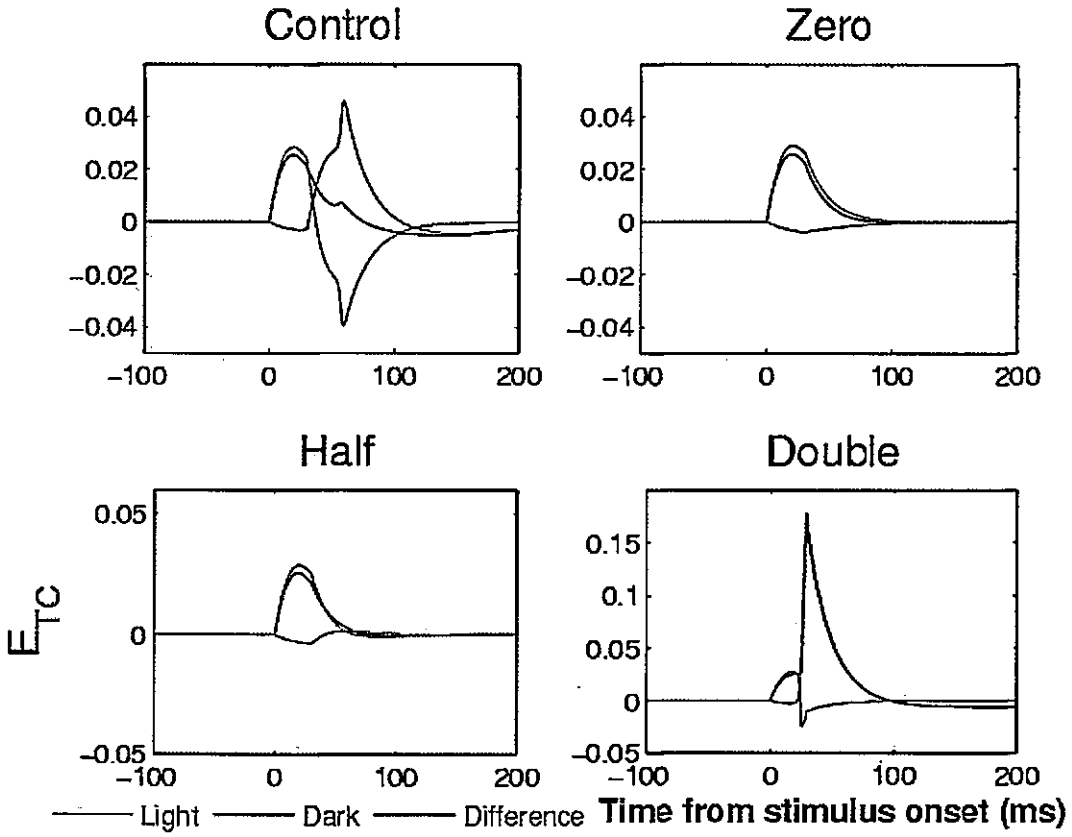

Figure 4.16: Manipulations of the PY6 to TC connection weight. When this weight is set to zero, the TC cell population no longer has a positive response to dark stimuli as it does in the control case. Hence, the composite light-minus-dark response is no longer biphasic.

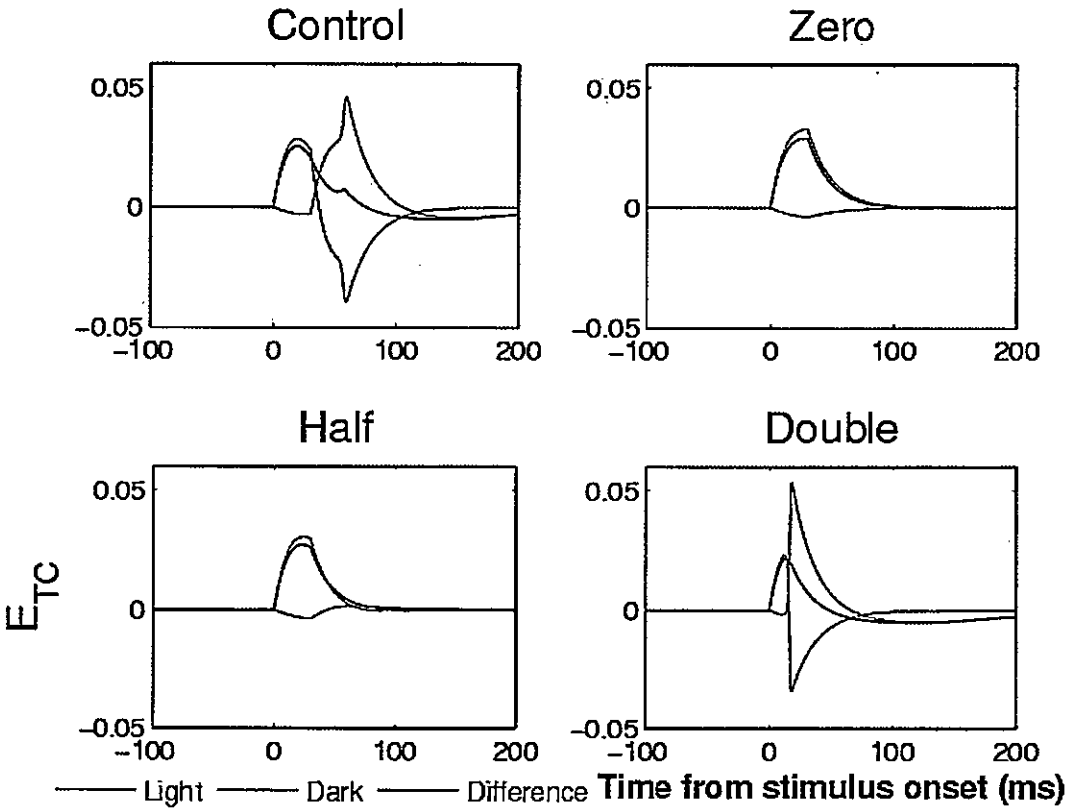

Figure 4.17: Manipulations of the TC to PY6 connection weight. When this connection weight is set to zero, the TC cell population does not show a positive dark response. Hence the light-minus-dark response is no longer biphasic.

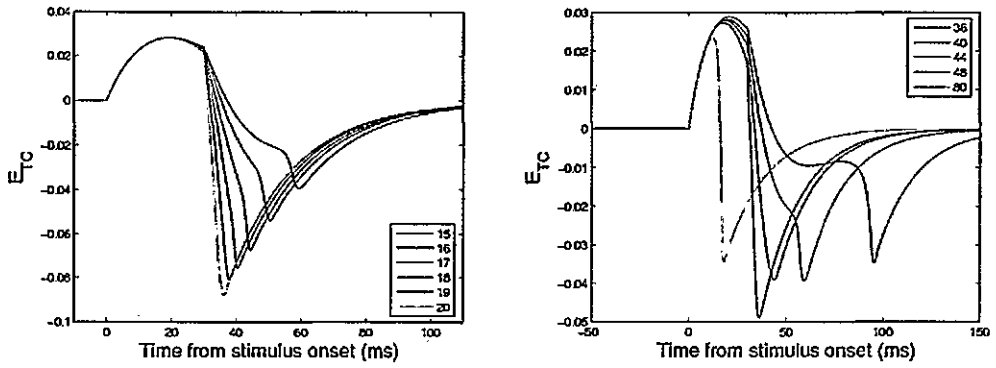

(a) (b)

Figure 4.18: These plots show that PY6 to TC (a) and TC to PY6 (b) connection weights can control the timing of the second phase in the TC cell population response. In (a) wPY6TC is varied at the values shown in the legend, and in (b) wTCPY6 is set at the values shown in the legend. In both cases the latency decreases as the weights increase.

without the TC to PY6 feedback loop, the former case is of more significance.

The results presented thus far strongly suggest that in the model the second phase of the TC STRF occurs due to the following pathway: the OFF cell population at the same retinotopic position as the ON cell population being recorded, responds positively to the dark stimulus. This is relayed to cortical OFF cell populations at and around that retinotopic position, which feedback to the ON cell population in that retinotopic position, thereby feeding back a positive response to a dark stimulus. As well as fitting the data presented thus far, this is intuitively the simplest manner that this response profile could be generated in the model via anti-phase feedback.

To test if this postulated pathway was responsible for this effect, focal lesions were made along this pathway in the following ways (which refers to the labelling in figure 4.20):

- The control situation (A).

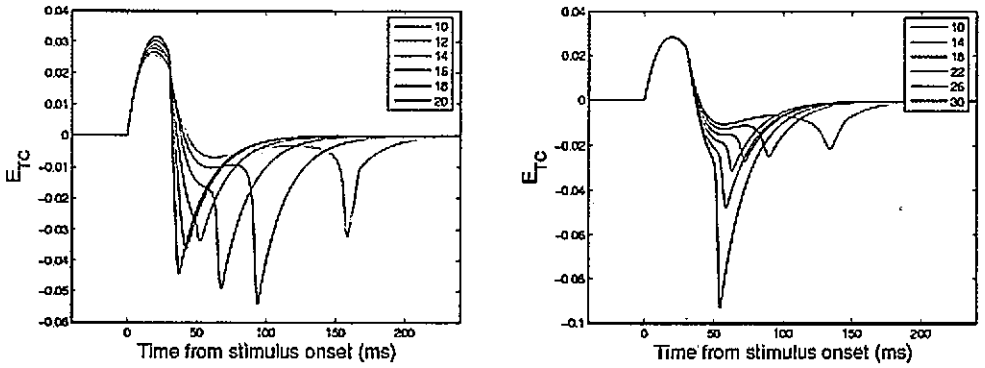

(a) (b)

Figure 4.19: These plots show that TIN to TC (a) and RE to TC (b) connection weights can control the timing of the second phase in the TC cell population response. In (a) wTINTC, and in (b) wREPY6 are set at the values shown in the legend. In both cases the latency increases as the weights increase.

- The retinal input to the OFF TC cell population was removed (B).
- Disconnection of the OFF TC cell population input to the horizontal OFF PY6 cell populations (C).
- Disconnection of the OFF TC cell population input to the vertical OFF PY6 cell populations (D).
- Disconnection of the OFF TC cell population input to both the horizontal and vertical OFF PY6 cell populations (E).
- Disconnection of the horizontal OFF PY6 cell population inputs to the ON TC cell population (F).
- Disconnection of the vertical OFF PY6 cell population inputs to the ON TC cell population (G).

- Disconnection of inputs from both OFF PY6 cell populations to the ON TC cell population (H).

The results of these lesions are shown in figure 4.20, and they clearly show that losing any part of this pathway inhibits or eradicates the dark response. In particular when there is no input to the OFF TC population at the same retinotopic position as the ON TC population, the dark response is absent. In the remainder of the plots there remains some dark excitation, though it is significantly reduced compared to the control case. The remaining dark excitation is due to the OFF cell population providing input to form the flanking subregions of surrounding cortical populations. Therefore there are divergent connections, which allow some dark-excitation to spread. In order to observe the emergence of the biphasic response more clearly, the next step of this investigation involved reducing the circuitry of this STRF model, to find the minimal required architecture.

4.4 Reducing the model

The results from the previous section have shown that the model thalamocortical network has the dynamics intrinsic to its circuitry to contribute to the generation of biphasic STRFs as measured by Cai *et al.* (1997); Reid *et al.* (1997); Usrey *et al.* (1999). These results also show that in the model, this response is mainly reliant on the corticothalamic feedback loop, and in particular on anti-phase feedback. Therefore, the model was reduced in order to capture the minimal description of the thalamocortical network that can produce these responses, as was done for the spindles model in chapter 3.

There were two routes by which this was achieved. The first involved eliminating

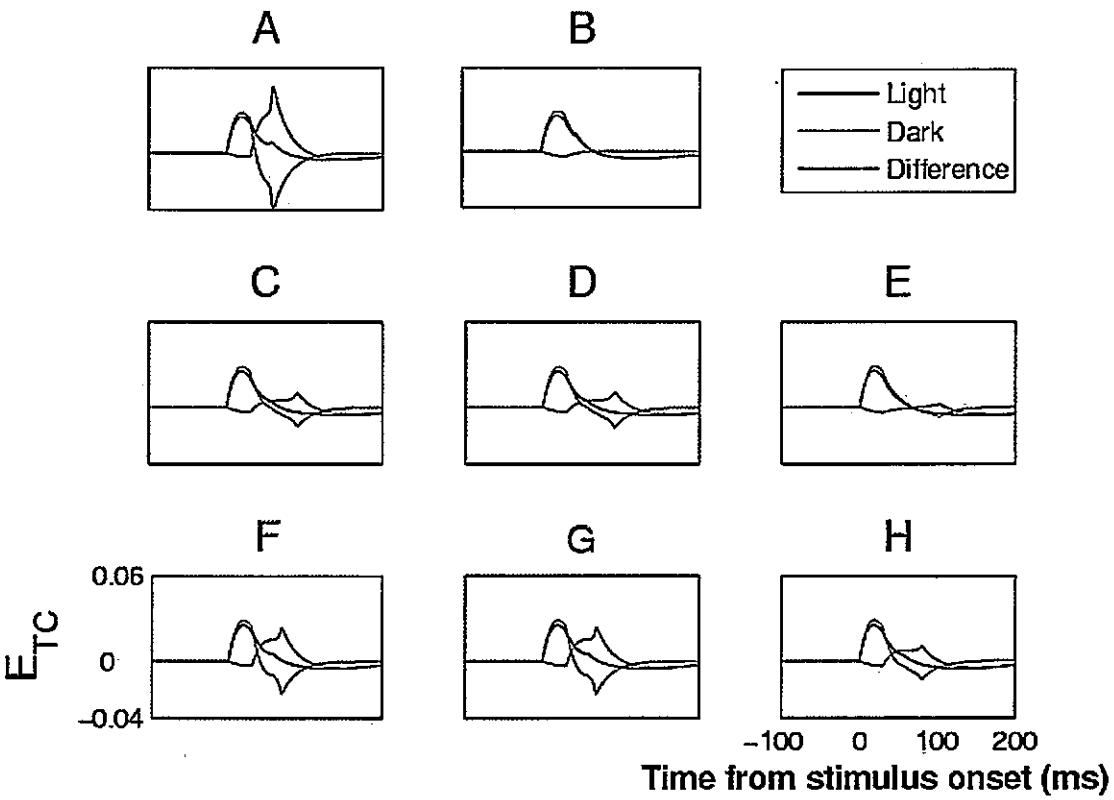

Figure 4.20: Focal lesions along the pathway proposed to mediate the biphasic response in the TC cell populations: (A) The control situation; (B) The retinal input to the OFF TC cell population was removed; (C) Disconnection of the OFF TC cell population input to the horizontal OFF PY6 cell populations; (D) Disconnection of the OFF TC cell population input to the vertical OFF PY6 cell populations; (E) Disconnection of the OFF TC cell population input to both the horizontal and vertical OFF PY6 cell populations; (F) Disconnection of the horizontal OFF PY6 cell population inputs to the ON TC cell population; (G) Disconnection of the vertical OFF PY6 cell population inputs to the ON TC cell population; (H) Disconnection of inputs from both OFF PY6 cell populations to the ON TC cell population. The results show that a lesion at any point in this pathway causes a loss of the biphasic response.

cell populations that did not contribute to the generation of the STRFs. Therefore the interneuron populations at the level of the thalamus and of the cortex were removed. The reticular population also did not play a significant role in the generation of this biphasic response property, however the inclusion of these cell populations was considered to be essential to the definition of the thalamocortical circuit.

The second method was to consider the minimum number of populations that were needed to represent a thalamocortical network. To produce a single cortical receptive field, with three antagonistic subregions, as described in section 4.2.4, a minimum of three TC populations of one polarity and six of the opposite polarity are needed. To produce two cortical receptive fields of opposite polarities, nine TC ON populations and nine TC OFF populations are needed. If there are 18 such populations in a model, 4 different classes of cortical receptive fields can be formed: ON horizontal, OFF horizontal, ON vertical, and OFF vertical. In addition nine RE populations would be needed to provide topographic inhibition of the TC cells. As a result of these considerations a reduced model was built, and the architecture of this model is described in detail in the following sections, followed by presentation and discussion of the results of the simulations of this network.

4.4.1 Architecture of the reduced model

As in both of the previous models, the basic component of the circuitry is the feedback loop between layer 6 excitatory cells in primary visual cortex, and the thalamocortical relay cells in the LGN. Anti-phase feedback connectivity (Wang *et al.*, 2004) is utilised in the description of this model, as the results from the previous sections suggest that this architecture is crucial for the formation of thalamocortical STRFs (as described by Cai *et al.* (1997) and Reid *et al.* (1997)). Populations of reticular cells are also

included, as the participation of this nucleus to thalamic activity was deemed essential. Therefore, the model architecture is as shown schematically in figure 4.21.

As in the previous STRF model, each cortical cell population receives input from 9 TC cell populations, three to form an elongated central subregion, and a scaled input from six others to form the flanking subregions of the opposite phase. Each of these cortical cell populations feeds back to the cental TC cell population of the opposite phase preference. The surrounding TC cell populations are included for the formation of the cortical RFs and not for functionality, therefore they do not receive cortical feedback. This was in order to keep the model as simple as possible. The TC cell populations receive inputs from the visual field, which are structured in order to form centre/surround RFs as described before in section 4.2.4. Finally, the populations in the RE layer make reciprocal point-to-point connections with the topographically matching TC cell populations (ON and OFF), and the central RE cell population receives input from all four cortical cell populations.

In summary, the following cell types are included in the model:

1. PY6 horizontal ON dominant population.
2. PY6 horizontal OFF dominant population.
3. PY6 vertical ON dominant population.
4. PY6 vertical OFF dominant population.
5. Nine TC ON-centre populations.
6. Nine TC OFF-centre populations.
7. Nine RE populations.

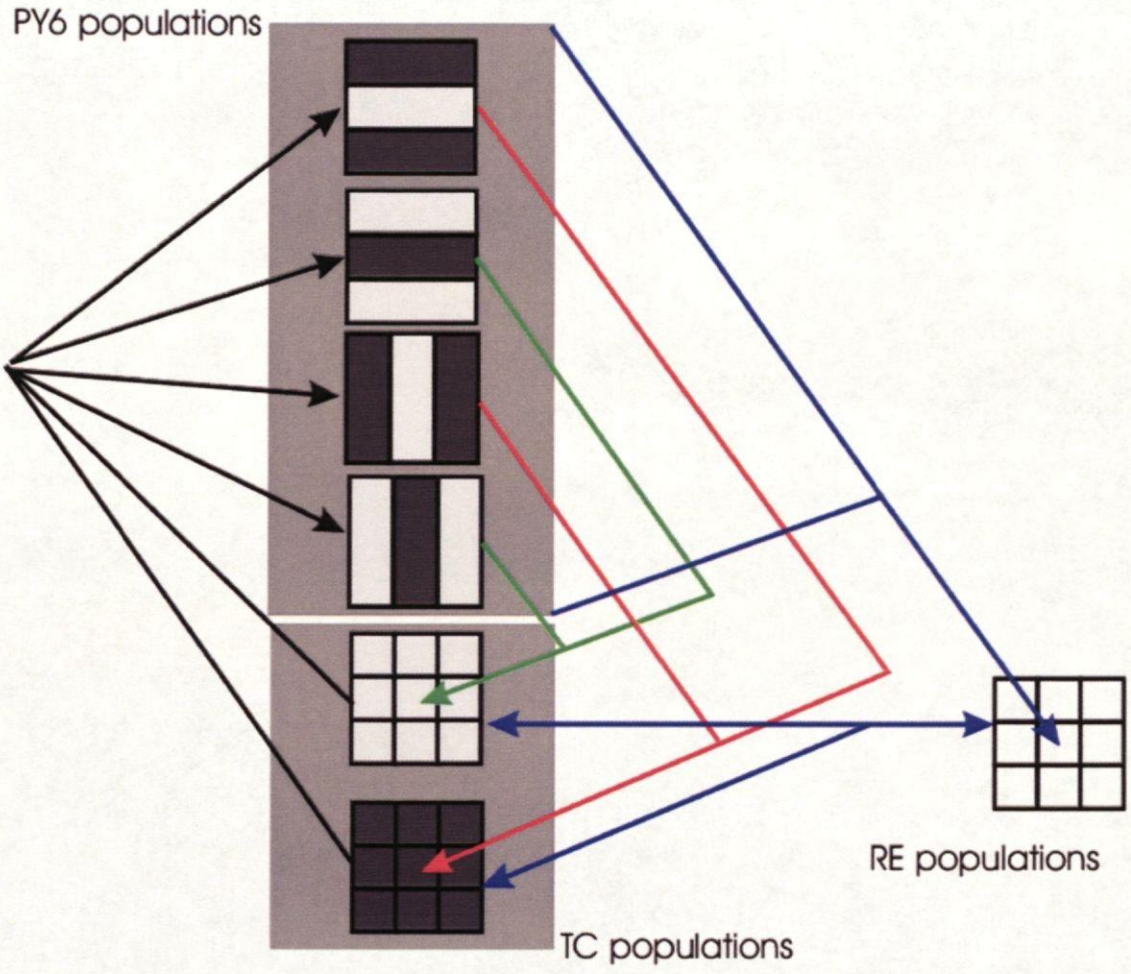

Figure 4.21: This figure shows the connectivity between the populations in the final model. In each of the TC and RE layers, there are 9 cell populations of each cell sub-type. There are four cortical cell populations, which have four different orientation and phase preferences. Red connections originate from ON-dominant cortical cells, and green from OFF-dominant cortical cells. Details of the connectivity can be found in the main text.

4.4.2 The Wilson-Cowan equations

Once more, the Wilson & Cowan equations for the nonlinear dynamics of populations of neurons were used for this study. Both the motivation and the short-comings of this approach are described elsewhere (sections 3.2.2 and 3.2.3), and will not be repeated here. The equations for this model are given in equations 4.6 to 4.8. These appear to be identical to those for the first model, because every connection is not specifically shown, only the connections between cell types. Therefore, while there are only three equations shown here, the model actually consists of 31 equations, one for each cell population. Similarly, only one of each connection type is shown here, but there may be up to nine of each type.

$$\tau PY6\frac{dE_{PY6}}{dt} = -E_{PY}(t) + (k_e - E_{PY}(t)) \cdot Z_e(w1 \cdot E_{TC}(t)) \tag{4.6}$$

$$\tau RE\frac{dI_{RE}}{dt} = -I_{RE}(t) + (k_i - I_{RE}(t)) \cdot Z_i(w2 \cdot E_{TC}(t) + w3 \cdot E_{PY}(t)) \tag{4.7}$$

$$\begin{aligned}\tau TC\frac{dE_{TC}}{dt} &= -E_{TC}(t) + (k_e - E_{TC}(t)) \cdot Z_e(-w4 \cdot I_{RE}(t) \\ &\quad +w5 \cdot E_{PY6}(t) + Retinal)\end{aligned} \tag{4.8}$$

In summary, this model takes into account the minimal architecture which has been shown to be necessary for the initiation and maintenance of the spindle oscillation. It also incorporates the feed-forward connectivity that is required for the formation of spatial thalamic and cortical receptive fields. The model includes feedback projections which connect cortical cell populations with TC cell populations of the opposite phase

preference. Therefore, this model investigated whether these few distinctive features constitute a sufficient representation of the thalamocortical feedback loop, such that the visual STRF properties of TC cells could be replicated.

4.4.3 The choice of parameters

Once again, the parameters for this model were set using data from physiological experiments. The specific pieces of data used are those outlined previously (see sections 3.2.4 and 4.2.3). To reiterate: the strength and reliability of TC to RE projections (Contreras *et al.*, 1993; Gentet & Ulrich, 2003); the relative strength of the thalamocortical projections (TC to PY6 cells) compared to the feedback corticothalamic projections (Castro-Alamancos & Calcagnotto, 2001); van Horn *et al.* (2000) show that the greatest number of inputs into TC cells are cortical; the greater strength of thalamocortical innervation compared to intra-cortical innervation of a cortical cell (Amitai, 2001; Beierlein & Connors, 2002); but the larger number of intra-cortical connections compared with thalamocortical connections (Usrey, 2002); the fact that RE cells send most of their outputs to innervate TC cells (Wang *et al.*, 2001).

The parameter space was explored within these constraints, and set at the values shown in table 4.2, which will be referred to as the control set of parameters. Compared to the situation in the large-scale model, these parameter relationships show less need for a large weight on the feed-forward projection from thalamus to cortex, but a need for a larger weight on the feedback from cortex. Therefore, the overall gain of the feedback loop is adjusted slightly. This is likely to be due to the re-scaling of the size of the network. Furthermore, the excitatory projections to the RE populations are slightly weaker than in the large-scale model, which reflects the smaller gain of the feedback loop.

Parameter name	Value
τPY6	20ms
τRE	20ms
τTC	20ms
w1	20
w2	5
w3	5
w4	10
w5	15
Input	3

Table 4.2: The table shows the parameters used into obtain STRFs in the third model. As in chapter 3, w1 is the TC to PY6 connection, w2 is the TC to RE connection, w3 is the PY6 to RE connection, w4 is the RE to TC connection, and w5 is the PY6 to TC connection.

4.4.4 Results

The model, as described in the previous sections, was investigated by running the same simulations as for the full STRF model. The reduced model displays static feed-forward responses which are consistent with those seen in the large-scale model, as shown in figure 4.22. The TC cell population has a centre-surround RF in space, as expected from the wiring of the model. The cortical cell population has an elongated oriented receptive field, as expected from the inputs it receives from the TC cell populations. Both of these populations respond as anticipated due to their receptive fields, to either the spots of various diameters, or to the bars of changing orientation (also shown in figure 4.22). This shows that the loss of the inhibitory interneurons at the level of the thalamus and the cortex, has no significant effect on the replication of visual responses within the model.

Figure 4.23 shows this biphasic response of the central TC ON cell population. The population's response to a light stimulus (single pixel in RF centre), to a dark stimulus, and the composite light minus dark response, are all shown. The composite response is clearly biphasic, which occurs due to a light-excitatory phase in the initial part of the response, followed by a delayed dark-excitatory phase. This is the same mechanism as in the larger-scale model. The STRF of the same ON-centre cell population is shown in figure 4.24(a) as a surface plot. The biphasic nature of the response is clearly seen in the centre of the RF, but is not so obvious in the surround. However, using a bar stimulus as in figure 4.24(b), yields an STRF which is unmistakeably biphasic in both the centre and the surround of the RF. Once more, the use of bar stimuli is more effective than single pixels as cortical cell populations are selective for bars and send stronger feedback to the TC cell populations.

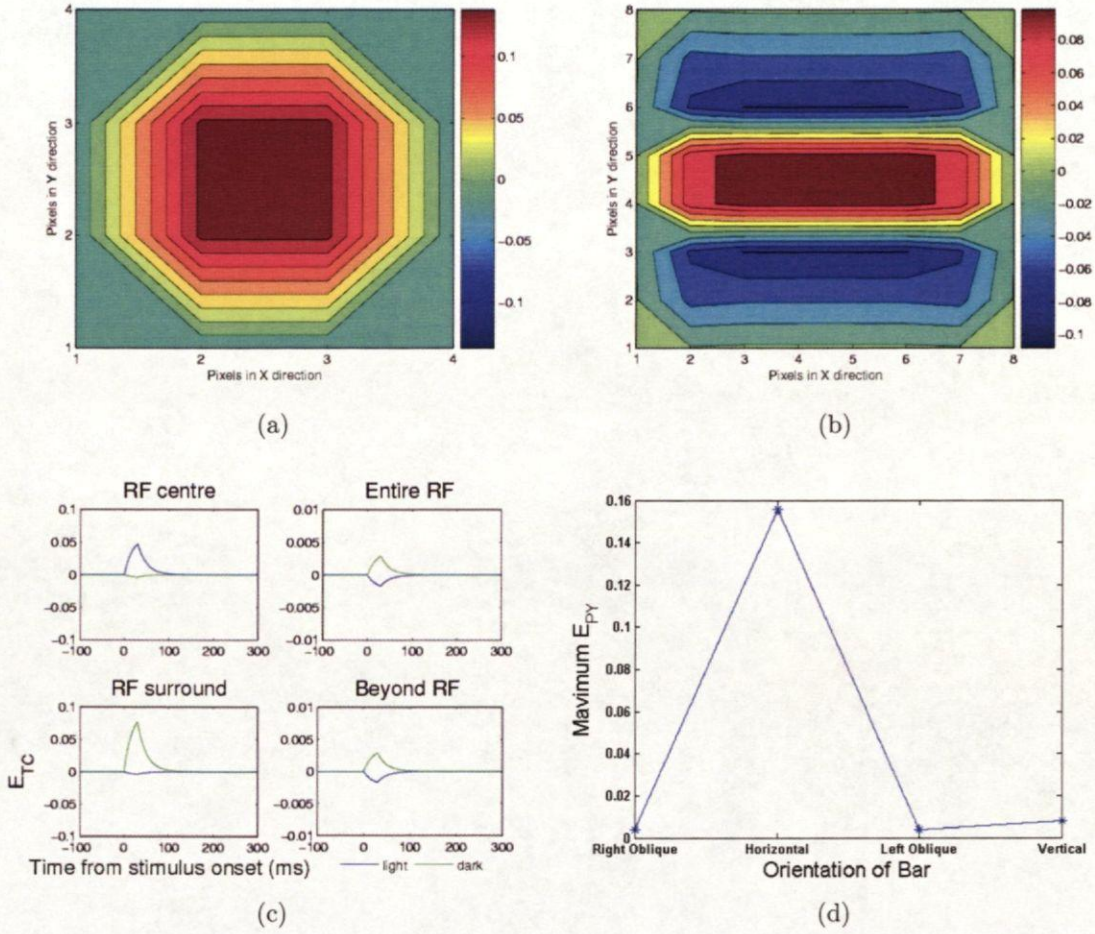

Figure 4.22: This figure shows the static feed-forward responses of a TC ON-centre cell population (a) and (c), and an ON-dominant horizontal PY6 cell population (b) and (d). In (a) and (b) the static receptive fields are plotted, and these are as expected from the connectivity of the model. The figure in (c) shows the response of the TC population to spots of varying diameters. As predicted from the RF, the population responds maximally to light in the RF centre and to dark in the surround. Finally, (d) shows the orientation tuning curve of the PY6 cell population, and consistent with its RF, the population is optimally tuned to horizontal stimuli.

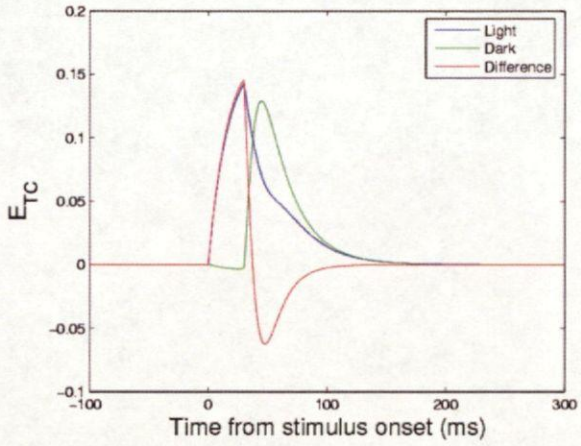

Figure 4.23: The responses of the central TC ON-centre population to a single pixel in the centre of its RF. The response to a light pixel, a dark pixel, and the composite light-minus-dark response are all shown. The formation of the biphasic composite response occurs due to the early light-excitatory phase followed by a late dark-excitatory phase. This is consistent with the dynamics of the large-scale model.

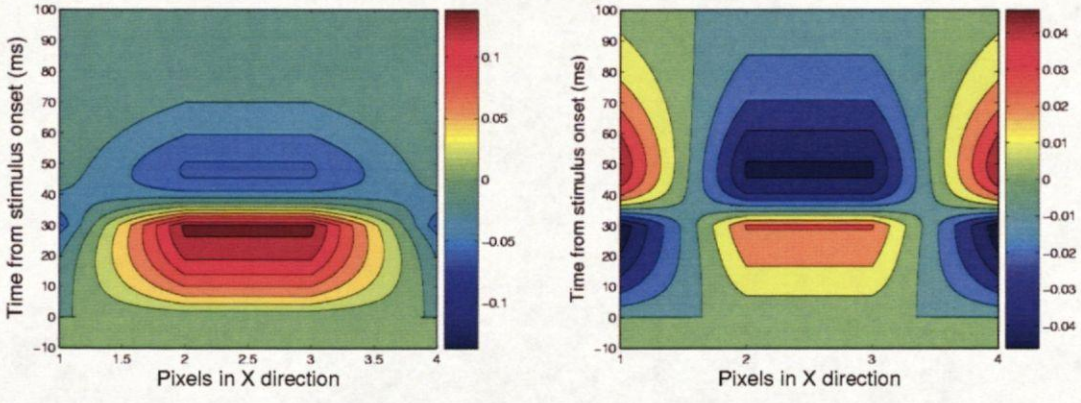

(a) (b)

Figure 4.24: The STRF of the central TC ON-centre population was measured with single pixels (a), and with bars (b), in the intact network with anti-phase feedback. Though a biphasic response can be seen in both cases, the surround is only clearly biphasic when bar stimuli are used.

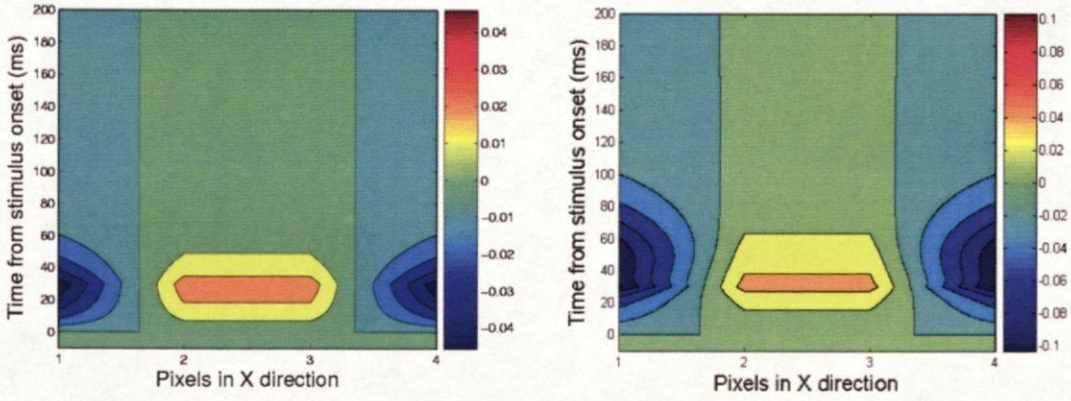

(a) (b)

Figure 4.25: The STRF of the central TC ON-centre population was measured with bars, in the network without corticothalamic feedback in place (a), and with in-phase cortical feedback connectivity (b). Note that in the in-phase case all weights were set to 80% of their control values, in order to avoid saturation of the network activity.

TC cell population STRFs were also measured when the network had no feedback, and in-phase feedback. The case when there is no feedback is shown in figure 4.25(a), and this result clearly shows that there is no appearance of a second phase. In the in-phase case, responses of all populations saturate due to the positive feedback circuitry. However, if the weights are scaled by 80% to lower the overall level of activity in the network, the result in figure 4.25(b) shows that there is no observation of a second phase. These results agree with those of the detailed model, by suggesting that in this model network, anti-phase cortical feedback is required for the generation of the biphasic thalamocortical STRF.

Investigation of the parameter ranges which maintain the TC cell population's biphasic response, shows that this response is robust with respect to parameter variations. Each parameter was investigated individually between -20% and +20% of its

Parameter name	Upper range	Lower range
w1	10%	5%
w2	20%	20%
w3	20%	20%
w4	20%	20%
w5	20%	20%
Input	20%	5%

Table 4.3: Table showing the range (relative to the control values given in table 4.2) that each parameter can take, while the biphasic response persists.

value in table 4.2, and the ranges that allow the biphasic response to persist are shown in table 4.3. Assuming a 5% range as a minimum requirement for robustness, it is clear that all the weight parameters can vary within this amount while the biphasic response is maintained. Therefore, the model's behaviour seems to be robust with respect to such parameter fluctuations. Note that the TC to PY6 connection weight, and the input value (to the TC cell populations) cannot decrease below 5%. Therefore the gain of the feed-forward route to the cortex cannot be compromised.

Each parameter was also set to zero, half and double its value in table 4.2. From these manipulations, it became clear that the reticular cell populations contribute very little to the biphasic response, as setting any of the weights of the connections with the RE populations to zero did not eradicate the second phase. However the TC to PY6, and PY6 to TC connections are essential for the existence of the phase of excitation to the non-preferred stimulus. That is if they are set to zero or halved, the response is no longer observed.

Specifically, and as in the earlier model, the pathway for the occurrence of a bipha-

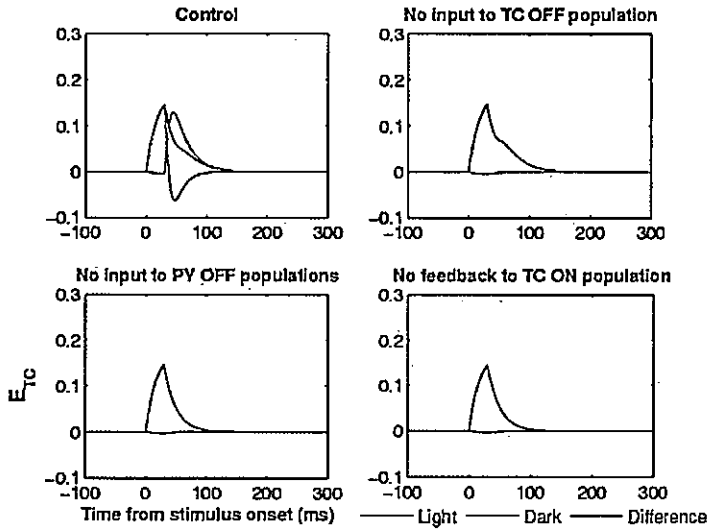

Figure 4.26: Focal lesions along the proposed pathway which mediates the occurrence of the biphasic response. In each of the three lesioned cases, the dark-excitation, and consequently the second phase disappears.

sic response in an ON TC cell population was predicted to consist of the following connections: 1) Input to OFF TC cell population at the same retinotopic position as the TC ON cell population; 2) TC OFF to cortical OFF populations; 3) Cortical OFF populations to the TC ON population. In order to test this prediction, focal lesions were made along this pathway. As can be seen in figure 4.26, eliminating any of these sections of the pathway eliminates the dark-excitatory response, and therefore the second phase of the composite response. Therefore, it is clear that the same dynamics are at play in this model as in the large-scale STRF model.

The biphasic response observed in this model, displayed a latency of approximately 20ms. As in the previous model, this latency could be manipulated by varying the connection weights of the thalamocortical feedback loop. Figure 4.27 shows this effect, in the two plots of the latency between the two phases (measured as the time between

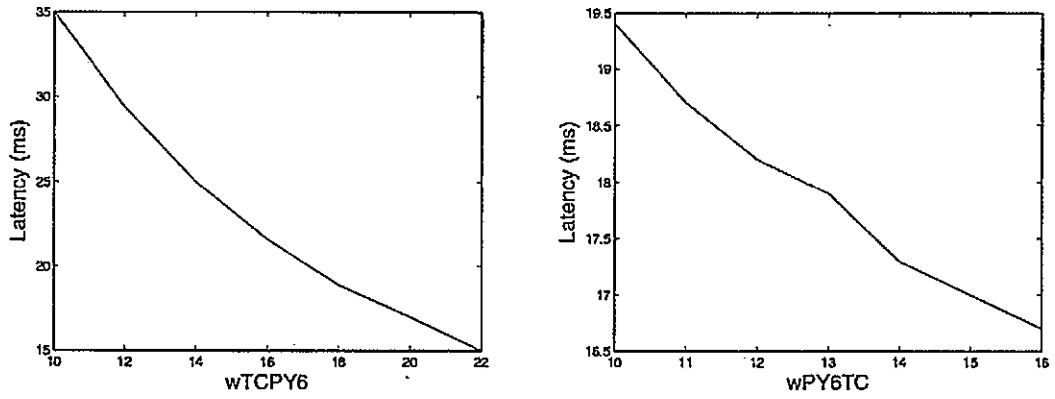

(a) (b)

Figure 4.27: These plots show that TC to PY6 (a), and the PY6 to TC (b) connection weights can control the latency between the STRF phases in the TC cell population response.

the peak of light excitation and the peak of dark excitation). Both plots clearly show that as the weight of either of the connections increases, the latency between phases decreases.

Finally, in order to ensure that the model continues to respond as expected when feedback is present, the static experiments were repeated. The results are shown in figure 4.28 and demonstrate that feedback does not have a significant effect on the static structure of the responses.

4.5 Discussion

The main finding presented in the current chapter, is that a population model of the visual thalamocortical system can replicate experimentally derived (Cai *et al.*, 1997) spatiotemporal responses of LGN thalamocortical cells. In particular, the model goes on to show that only when the thalamocortical feedback loop is completed the TC

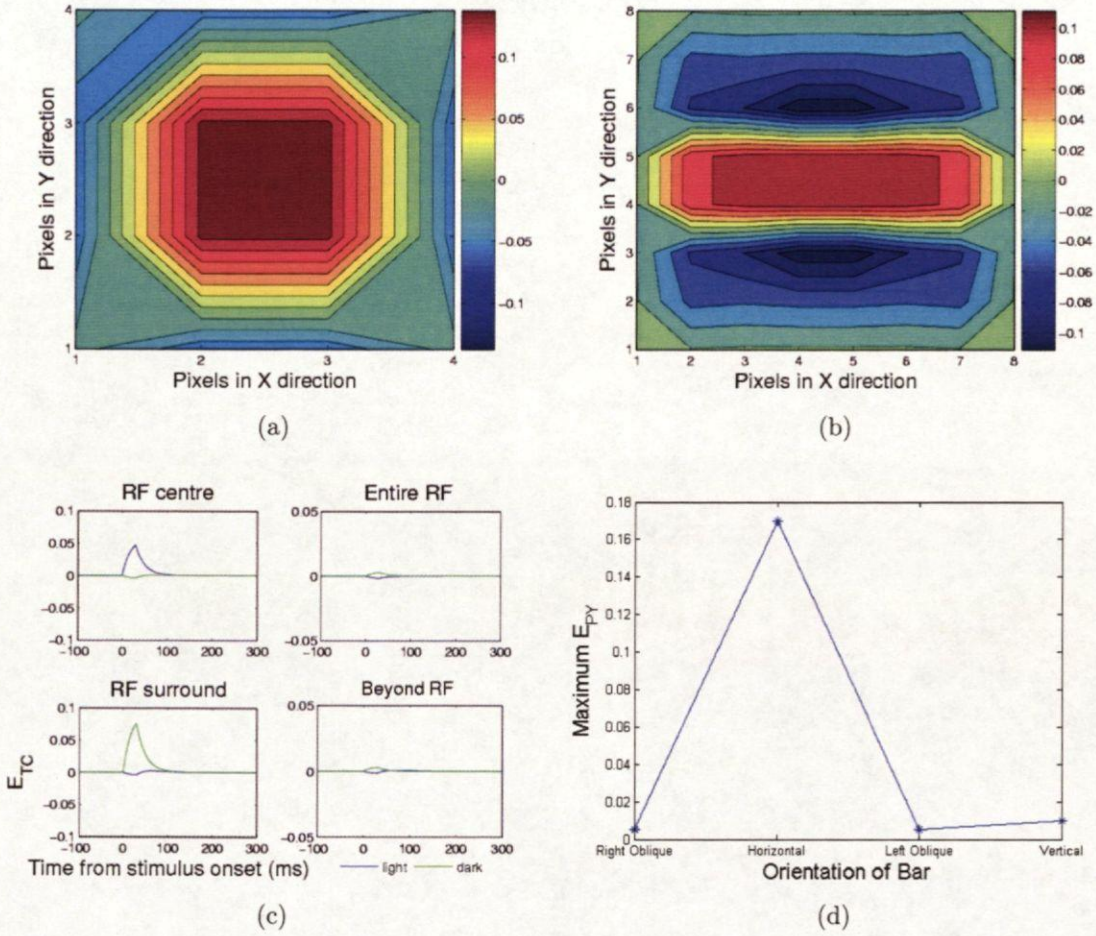

Figure 4.28: This figure shows the static responses when feedback is in place, of a TC ON-centre cell population (a) and (c), and an ON-dominant horizontal PY6 cell population (b) and (d). In (a) and (b) the static receptive fields are plotted, and these are as expected from the connectivity of the model. The figure in (c) shows the response of the TC population to spots of varying diameters. Finally, (d) shows the orientation tuning curve of the PY6 cell population, which is consistent with its RF.

cell populations develop a second phase in their visual responses. This second phase is a delayed response (relative to the initial phase) of the opposite ON/OFF polarity. As biphasic RGCs were not present in the model, these modelling results show that the dynamics of corticothalamic feedback is able to contribute to the formation of the thalamic biphasic temporal response. This pathway can therefore account for the amplitude difference between the magnitude of the second phase in TC cells and RGCs as measured by Usrey *et al.* (1999). This property arises only if corticothalamic feedback to TC cells is arranged in anti-phase, as reported by Wang *et al.* (2004). This means that a cortical cell population with a given ON/OFF preference, feed back to thalamocortical cell populations with the opposite ON/OFF preference.

This result could be inaccurate for a number of reasons. A main concern when using a population-level description of neuronal dynamics, is that it is difficult to relate the variables used in the description of the model to measurable quantities. Though the weight parameters and the time constant parameters are derived from physiologically observable values, in practice the user is more free to choose parameter values than when using conductance based models. This issue was discussed in detail in section 3.2.3, and it was explained that the dependence on parameters could be tested through various experiments. In the current chapter, the results of parameter manipulations were shown, and these indicate that the biphasic property of the thalamic receptive fields is a robust response within reasonable parameter ranges.

A further short-coming is that the model may be too simple, in that it does not explicitly contain the detailed physiological neuronal properties of the thalamocortical network. However, the use of a population model is a step towards understanding the sensory thalamocortical network, which should be considered in partnership with other models and further experimental work. This is also an important way to validate

results.

An alternative explanation for the generation of an increased second phase in TC cells is via feedforward inhibition. TC cells receive inhibition from local inhibitory interneurons, which in turn receive direct visual input from the retina. As these interneurons have membrane time constants of up to 94ms (Zhu *et al.*, 1999), it is possible that the TC cell second phase is augmented via this pathway of feedforward inhibition. Another criticism is that there is no experimental evidence to support the involvement of cortical feedback in the manipulation of biphasic responses in thalamocortical cells. Furthermore, the data from Wang *et al.* (2004) does not show that corticothalamic feedback only occurs between cells of the opposite polarity, but indicates that there is a high correlation between cells connected in this way and their results. Despite these concerns, the models presented in this chapter show that the dynamics of the thalamocortical feedback circuit allows anti-phase cortical feedback to have such a role. This is the main experimentally testable hypothesis to emerge from the work presented in this chapter. Therefore although alternative explanations exist, and corticothalamic feedback is not necessarily exclusively arranged in anti-phase, the results from the current work necessitates experimental verification.

The parameter manipulations also allowed the exploration of the genesis of biphasic STRFs. These experiments showed that in the model, cortical feedback onto the TC cell populations is crucial for the presence of the response, and this innervation changes an ON-centre TC cell population's response to a dark stimulus (presented in its RF centre) from being small and negative, to being delayed and positive. The most obvious pathway that could generate such a dark response is through anti-phase feedback. The involvement of this pathway was tested with "focal lesions" of connections, and as shown in figure 4.20 this proposed disynaptic feedback loop appears to be mediating

the emergence of this response.

This effect on the temporal structure of the thalamic receptive field properties, is a novel suggestion for the purpose of corticothalamic feedback. Previous suggestions for the role of corticothalamic feedback in the visual system, have centred around feedback imposing higher level processing capabilities on thalamic cells. For example, Bickle *et al.* (1999) proposed that the thalamocortical feedback circuit directs selective attention to various points of a stimulus. Hayot & Tranchina (2001) suggested that feedback causes geniculate cells to be sensitive to orientation discontinuity. A model presented by Sastry *et al.* (1999) offered the possibility that corticothalamic feedback allows the uncluttering of a visual stimulus with respect to line detection. A study by Hillenbrand & van Hemmen (2001) also investigated the possibility that cortical feedback modulates the temporal response properties of TC cells in order to control cortical velocity tuning. Bressloff & Cowan (2003b) recently suggested that cortical feedback manipulates thalamic responses in order to improve thalamic relay and facilitate cortical responses. Here however, feedback is shown to affect the fundamental temporal structure of geniculate RFs.

The modulation of TC cell temporal response properties, also has the ability to be a dynamic property. This comes to light in the plots showing that the latency between phases can be varied, by changing the weights which mediate the feed-forward and feedback connections between the TC cell and the PY6 cell populations. This means that it is possible for the thalamocortical network to continuously modulate thalamic response properties via these weights. This could be determined by top-down information to the primary visual cortex from higher cortical areas. Such ideas for a dynamic role of the cortical feedback projection have been previously proposed (for example in the discussion by Sillito & Jones (2002)), and the current results provide evidence that

the thalamocortical feedback network has the intrinsic dynamical properties to support such a role.

The purpose of this strengthened biphasic STRF is an interesting question. Natural images tend to vary slowly in time, such that there is significant redundancy in natural stimuli. If we assume that the goal of the visual system is to rid the input signal of these correlations and therefore maximise information transfer, we can predict the optimal form of the visual receptive field. An early study by Atick & Redlich proposed that spatial decorrelation occurs through retinal ganglion cells, and derived the form of retinal spatial responses based on this hypothesis. Dong & Atick (1995) performed a similar theoretical study of temporal decorrelation, and found that the optimal form for a temporal receptive field which achieves temporal decorrelation of a natural image is biphasic. Therefore a possible role for a strengthened second phase is to allow the thalamocortical cells to temporally decorrelate natural images.

Subsequent studies have examined LGN responses both experimentally (Dan *et al.*, 1996; Lesica & Stanley, 2004) and theoretically (Truccolo & Dong, 2001) to test to what extent this theory can be proven to be true. These studies have shown that the impulse response function of cells in the LGN is well suited, both theoretically and experimentally, to temporally decorrelating an incoming visual signal. Therefore the input into the cortex should in this sense be optimal, with the retina removing spatial correlations, and the LGN removing temporal correlations. This will consequently allow the visual system to respond more efficiently.

A stronger biphasic temporal RF in thalamus conpared to retina also allows TC cells to respond more transiently to stimuli, which is consistent with more band-pass temporal tuning in TC cells compared to the retina (Usrey *et al.*, 1999). In addition, Mukherjee & Kaplan (1995) suggest that the temporal tuning of LGN cells is modu-

lated by cortical feedback and neuromodulation from the brainstem. Sillito & Jones (2002) proposed that feedback to the LGN from as high up as MT cortex can influence thalamic responses to moving stimuli. The possibility of such top down modulation of thalamic temporal responses is the possible reason why this effect is achieved in the thalamus and not the retina. Cortical feedback reaches thalamic cells, but not retinal ganglion cells. Therefore if feedback from higher cortical areas aims to manipulate the temporal responses in the visual pathway, the first subcortical relay at which this can happen is in the LGN. The idea of a top-down influence on responses to moving stimuli may also be involved in eye movements. When the eyes move, the afferent sensory information will be similar to that from a moving stimulus. For the differentiation to be made between moving eyes and moving stimuli, top-down and bottom-up information must be combined. The thalamus is an ideal site for this processing to occur. However, these ideas require more theoretical and experimental work in order to understand how these observations fit together.

The model was reduced in order to find the minimal architecture which could produce the correct structure for the STRFs. The results of simulations of this reduced model show that the same dynamics are at work as in the original model. That is, the dynamics of the thalamocortical feedback circuitry described by this model support the relay of visual information, such that experimentally recorded visual responses are accurately replicated in the model's responses. This architecture simply contains three cell types, which are interconnected as found experimentally, and these results therefore suggest that this could be considered as a fundamental thalamocortical unit. This has implications for future investigations of early sensory pathways, as this thalamocortical unit displays the dynamic visual behaviour expected from the network. Such an active role in neuronal activity for the thalamus has been previously overlooked, particularly

when considering the thalamic contribution to sensory processing.

The structure and physiology of the thalamocortical system in the visual, auditory and somatosensory modalities is very similar (Alitto & Usrey, 2003). Using the Wilson-Cowan equations to represent a system, means that the detail of the model is contained in the connectivity. Therefore, if the main components of the circuitry are similar then we can extrapolate the results between systems. The current findings lead to the prediction that the same effect will be seen in the auditory and somatosensory thalamocortical circuits. Although there are fewer studies in these other two sensory modalities, there is experimental evidence for changes in the RF structure of TC cells as a result of changes in corticothalamic feedback, in both the auditory (Suga *et al.*, 2000; Yan & Suga, 1996; Zhang & Suga, 2000), and somatosensory (Ghazanfar *et al.*, 2001; Krupa *et al.*, 1999) systems. Therefore this may be a common effect across modalities, and a general principle for the role of cortical feedback in the sensory thalamocortical network.

4.5.1 Summary and contributions

Once more the thalamocortical feedback circuit was represented by a set of Wilson-Cowan equations. However, this time an extended architecture was used in order to replicate RF properties. The dynamics arising in the system were examined to see if the network is able to display transient responses that are consistent with those seen experimentally. This is the first time that a population-level model of the visual thalamocortical network with biologically accurate architecture has been constructed. It is also the first time that anyone has attempted to discover the full neural mechanism underlying the thalamocortical cell STRF, as measured by Cai *et al.* (1997) and Reid *et al.* (1997), and explain the amplitude difference between TC cells and RGCs

measured by Usrey *et al.* (1999).

The network involves TC cell populations, cortical (excitatory and inhibitory) cell populations, reticular cell populations, and inhibitory thalamic interneuron populations. The connections between these populations are only included if they have been observed experimentally. The parameters for the network are also derived from experimental data. Three feedback patterns were investigated in the modelling work, an anti-phase arrangement, a network with no feedback present, and an in-phase arrangement. A reduced version of the model highlights the fact that the main component of the architecture required to produce these responses is the feedback loop between cortex and thalamus.

The current results show that cortical feedback contributes to the formation of the thalamic receptive field structure, and in particular that anti-phase feedback strengthens the change in polarity (with respect to ON/OFF phase preference) of the responses in the temporal domain. Therefore, the feedback generated response can account for the discrepancy between retinal and thalamic responses, as measured in simultaneous reverse correlation experiments by Usrey *et al.* (1999), where the authors showed that the thalamic second phase has a consistently larger amplitude than the retinal second phase. This indicates that feedback is not just a modulator of thalamic responses as suggested previously, but could also be what Sherman & Guillery (1998) called a driving input; their definition being that a driver is involved in the formation of receptive field properties. The effect of feedback on the temporal properties of thalamic cells has been proposed previously, for example in spindle oscillations (Bal *et al.*, 2000) and in the spike timing of visual responses (Worgotter *et al.*, 1998). However, this is the first report of feedback playing a part in the temporal properties of geniculate receptive fields, and it has implications for the processing of even the simplest visual stimuli.

Chapter 5

Spindle oscillations and receptive fields

5.1 Introduction

It is well established that the responses of the thalamus (along with other brain areas) change dramatically throughout the sleep/wake cycle (Hobson & Pace-Schott, 2002; McCormick & Bal, 1994). Looking at the membrane potential of individual thalamocortical cells, this change can be seen as a hyperpolarisation during sleep states (relative to awake states), or a depolarisation during awake states (relative to sleep states) (Hirsch *et al.*, 1983). Looking at this in terms of firing mode, this variation manifests itself as burst-firing during sleep and tonic firing during wakefulness (McCarley *et al.*, 1983), which is due to the activation kinetics of the T-type calcium current (Jahnsen & Llinas, 1984a,b). The latter is a traditional view that has been challenged in recent years, by reports of bursting during awake activity (Sherman, 2001; Swadlow & Gusev, 2001). At the functional level this activity translates into oscillations during sleep, and the relay of afferent information during wakefulness.

The models that have been presented thus far in this thesis, have examined the circuitry which is required to produce these two temporally separated phenomena,

through the nonlinear dynamics of the thalamocortical network. A logical question to emerge from this work, is whether these two isolated depictions of the thalamocortical feedback circuit can be united into one. Attempting to answer this question would help to understand not only the dynamics involved in producing each behaviour individually, but also the re-organisation that the circuitry must undergo, if any, in order to make the transition between them.

There have been numerous previous attempts to experimentally investigate the behaviour of the thalamocortical feedback loop during transitions from sleep to wake (for a review see McCormick & Bal (1994)). These have mainly been interested in studying the membrane potential, firing rate, and oscillatory behaviour in these two states. A modelling study by Bazhenov *et al.* (2002), presented a large-scale conductance-based model of the thalamocortical circuit to look specifically at the behaviour of this network during slow-wave-sleep, and activated states (awake states and REM) with respect to sleep oscillations and information transfer. The model was compared to simultaneous in vivo experiments performed in anaesthetised cats.

The authors investigated the switch between the two states, and modelled the transition from sleep to activated states by blocking the resting potassium conductance in the PY and TC cells, which is known to be caused by an increase in the levels of the neuromodulator acetylcholine (McCormick, 1992). There is also a change from low-frequency synchronised activity to tonic firing at 30-40Hz. Relating these neuromodulatory changes to the configuration of the model circuitry based on previous experimental evidence (Gil *et al.*, 1997), the authors note that the change from sleep to activation is associated with a weakening of PY to PY connections, which in turn causes a reduction in the strength of RE to TC to RE connections. Hence, this study considers the transition between sleep and awake states, and provides clues about the

functional re-organisation of the network during this process.

A very recent study by Hill & Tononi (2005), presented a large-scale model of the thalamocortical network. Again the neurons in this model were conductance-based, and the authors include a number of intrinsic and synaptic currents. The aim of this study was also to investigate the transition between awake states and slow sleep oscillations. Their work shows that the change from wakefulness to sleep requires an increase in a leak potassium current, which explains the hyperpolarisation observed during this transition. They also model the transition by an increase in the strength of cortico-cortical connections, which they find synchronises the slow sleep oscillations. Though this model replicates the data at a very detailed level, it provides limited information regarding the functional reorganisation at the level of the connectivity.

In this chapter, the third population-level model of the thalamocortical network which was presented in the previous chapter, is used to look at the steady-state dynamics associated with spindle-range oscillatory behaviour, in addition to the transient generation of thalamocortical STRFs. This is the first time that a model has investigated the switch from awake sensory processing to early sleep spindling states. In particular, the use of a population-level description allows the analysis to be based upon the dynamics of the connectivity, which Bazhenov *et al.*; Hill & Tononi suggested are involved in the switch in activity. The results from this model predict that this transformation between early sleep oscillations and awake visual processing, are reliant upon a relative change in gain of the thalamocortical loop and the thalamo-reticular loop, and specifically due to a relative change in the feedback weights.

5.2 Method

The reduced model which was presented in chapter 4, section 4.4, contains TC cell populations, RE cell populations and cortical cell populations, as in the simple spindles model. However, unlike that first model this version now involves more than a single population for each cell type, which allows for the definition of receptive fields. The model has 9 TC ON populations and 9 TC OFF populations, which are arranged in two 3x3 topographic arrays. These TC cell populations project to the cortex, in such a way that the receptive fields of 4 cortical cell populations are formed. These RFs, which are spatially superimposed, have four different preferences with respect to phase and orientation: 1) horizontal ON, 2) horizontal OFF, 3) vertical ON, 4) vertical OFF. These cortical cell populations are considered to topographically match the central TC cell populations. There are also 9 RE cell populations which have reciprocal projections (also arranged topographically) with all nine TC cell populations in each of the ON- and the OFF-centre layers. The central RE population also receives innervation from all four of the cortical cell populations. The cortical cell populations project to the TC cell populations topographically (that is to the central TC populations only), and these feedback connections are arranged in anti-phase (Wang *et al.*, 2004), as in the earlier STRF model. The model architecture is duplicated from chapter 4 in figure 5.1.

5.3 Results

The model was investigated by running the same simulations that were described in the previous chapters. Active visual processing, early sleep activity, and the transition from the former state to the latter is of interest here. Hence the next section will summarise the results of the transient behaviour first presented in chapter 4, and the

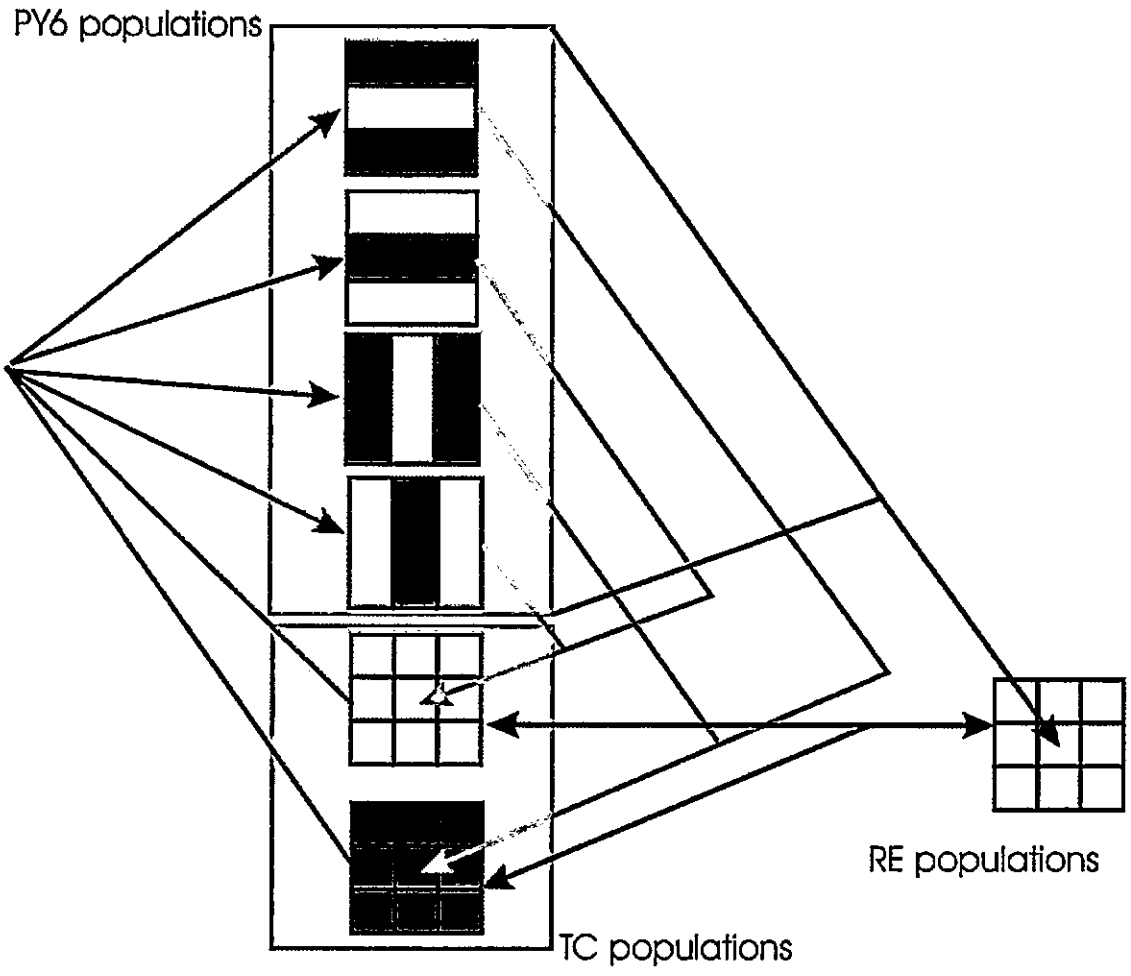

Figure 5.1: This figure shows the connectivity between the populations in the final model. In each of the TC and RE layers, there are 9 cell populations of each cell sub-type. There are four cortical cell populations, which have four different orientation and phase preferences. Red connections originate from ON-dominant cortical cells, and green from OFF-dominant cortical cells. Details of the connectivity can be found in the main text.

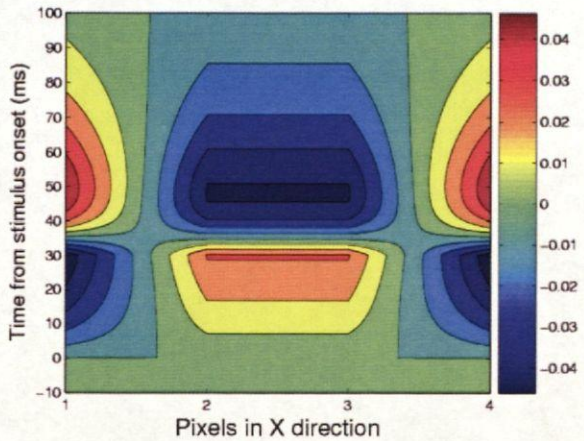

Figure 5.2: The STRF of the central TC ON-centre population was measured with bars. A biphasic response can be clearly seen in both the centre and the surround of the receptive field.

subsequent section will present the results of the steady state oscillatory activity.

5.3.1 Visual responses

To reiterate, when the reduced model's parameters were set at the values in table 5.1, the model produces the biphasic response seen in figure 5.2, and this response only arises when the PY6 to TC feedback connections are arranged in anti-phase. The precise pathway was hypothesised to be as follows: Visual input to OFF TC cell population at the same retinotopic position as the TC ON cell population; This TC OFF population transmits to cortical OFF populations; These cortical OFF populations feedback to the TC ON population being recorded. This pathway was tested with focal lesions, and the results in figure 5.3 show that losing any part of this pathway eradicates the second phase. Therefore, this model exhibited the same responses as the more detailed receptive field model.

Parameter name	Value
τPY6	20ms
τRE	20ms
τTC	20ms
w1	20
w2	5
w3	5
w4	10
w5	15
Input	3

Table 5.1: The table shows the parameters used into obtain STRFs in the unified model. As in chapter 3, w1 is the TC to PY6 connection, w2 is the TC to RE connection, w3 is the PY6 to RE connection, w4 is the RE to TC connection, and w5 is the PY6 to TC connection.

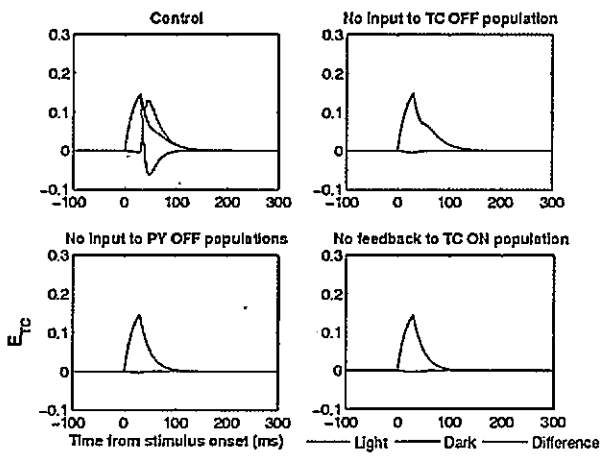

Figure 5.3: Focal lesions along the proposed pathway which mediates the occurrence of the biphasic response. In each of the three lesioned cases, the dark-excitation, and consequently the second phase disappears.

5.3.2 Spindle range oscillations

In order to observe oscillations in this same model, the parameters were changed to the values shown in table 5.2. These will be referred to as the control set of parameters for the oscillatory simulations. A specific aim was to keep as many of the parameters consistent between the two regimes, so that only the crucial changes are made. Comparing these control parameters to the control set for the STRF responses in the previous section, the only differences are in the feedback connection weights from the cortical cell populations to the two types of thalamic populations. Feedback to the TC cell populations is decreased (compared to its value in the STRF simulations), and assuming that the role of the feedback loop during awake states is to transmit information, then this weight decrease is appropriate as this role becomes negligible during sleep (Bazhenov *et al.*, 2002).

There is an associated need for the cortical feedback to the reticular population to be increased, which agrees with the idea that the reticular nucleus is central to the generation of spindles (Steriade *et al.*, 1987). The relative switch in the weights of the feedback connections also fits with the idea that dominant inhibition is required for oscillations in this system (Destexhe *et al.*, 1998), and with the prediction that dominant excitation is required for relay of information (le Masson *et al.*, 2002).

Compared to the values used in the simpler spindles model of chapter 3, these parameters have not changed a great deal in relative terms. However, in that first model, the largest connection weight was assigned to the PY6 to RE connection, and in the current model it is assigned to the TC to PY6 connection. This is mainly due to the fact that it was intended to keep as many of the parameters as possible the same between the two regimes, and in the STRF regime a large feed-forward weight is

Parameter name	Value
τPY6	20ms
τRE	20ms
τTC	20ms
w1	20
w2	5
w3	10*
w4	10
w5	6*
Input	3

Table 5.2: The table shows the parameters used in order to obtain oscillations in the third model. These parameters will be referred to as the control set for oscillations in this model. Those marked with an asterisk are different to the control STRF set shown in table 5.1.

necessary for obtaining the appropriate visual responses.

The oscillatory behaviour from all 31 populations is shown in figure 5.4(a), and it is clear to see that all populations oscillate. The frequency of oscillations is 12Hz, which is within the 7-14Hz spindle range. Figure 5.4(b) shows a close up of the activity recorded from a PY6 population, an RE population, and a TC population. The TC cells lead the oscillation, which is consistent with both the simpler model and with previous studies (Destexhe *et al.*, 1998, 1999). The RE cells have the highest amplitude of activity, which indicates that there is the most synchrony within the RE population. The amplitude of the activity in the PY6 populations is the next largest, and the TC cells display the smallest amplitude activity. This follows from the idea that in a population of spindling TC cells not every cell will fire at each cycle, and therefore TC

Parameter name	Upper range	Lower range
w1	10%	20%
w2	20%	20%
w3	20%	20%
w4	20%	5%
w5	5%	20%
Input	20%	20%

Table 5.3: Table showing the range (relative to the control value given in table 5.2) that each parameter can take and still allow oscillatory activity to persist.

activity will not show high synchrony compared to the RE cell population (Destexhe & Sejnowski, 2002).

Due to the large number of equations, it was not possible to plot the oscillatory regions of parameter space using the bifurcation analysis software (LOCBIF) which was used previously. However, the parameter values were examined within -20% and +20% of their control values. As shown in table 5.3, in no case was the upper or the lower limit less than 5%, and so all the parameters exceeded the threshold of acceptable variability. Therefore, the oscillatory activity in this model (in addition to the visual responses) is also robust to parameter fluctuations within reasonable ranges. If the PY6 to TC weight exceeds 5% of its control value, or the RE to TC connection weight drops below 5% of its control value, the activity in the network saturates. Therefore it seems that there is a requirement for a minimum amount of inhibition (and not too much excitation) of TC responses.

Parameters were also set to zero, half, and double their control values, as before in the earlier spindles model. The network continues to oscillate when the TC to RE

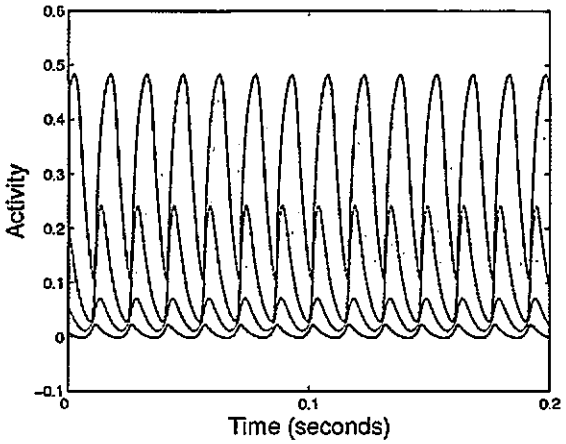

(a)

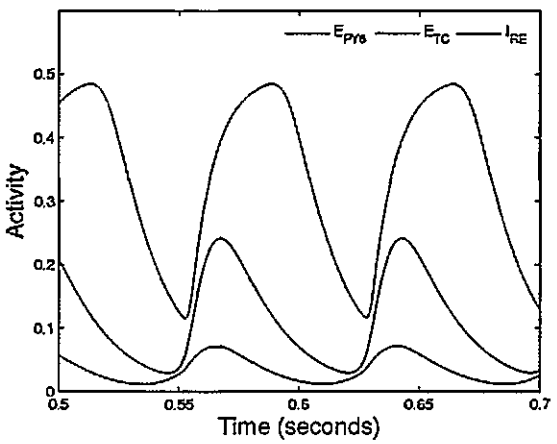

(b)

Figure 5.4: This figure shows the oscillatory activity displayed by the final model. All cell types and populations participate in the oscillation as shown in (a). Looking at the activity close up in (b), we can see that the frequency of the oscillations is 12Hz, that the TC population leads the activity, and that the relative pattern of amplitudes (and therefore synchrony) are consistent with experimental findings (see main text).

connection is severed. Once again, it is proposed that this case exists because the RE populations receive an excitatory input from the PY6 cells, and therefore do not rely on input from the TC cells. This is consistent with the idea of dominant inhibition, as the feedback route to the RE nucleus is strong compared to the feed-forward innervation of the RE nucleus. These manipulations also show that when either of the excitatory connections of the TC-PY6-TC feedback loop are doubled, the activity saturates and therefore oscillations are no longer observed. This is expected if we consider that the oscillatory state requires a balance of excitation and inhibition, and increasing excitation destroys this balance.

The main result from the spindles model in chapter 3, showed a switch in the oscillation frequency following an increase in the time constant of the reticular cell population. This was also replicated in the current model as shown in figures 5.5(a) and 5.5(b). Therefore, this model also supports the hypothesis that the transition in oscillation frequency is due to the effect of slower $GABA_B$ inhibition on the nonlinear dynamics of the thalamocortical network. There is also an increase in synchrony which manifests itself as an increase in the amplitude of the activity, and arises from an increase in the RE time constant. This situation is shown in figure 5.5(c), and is consistent with experimental results. Once again, the dynamics of the thalamocortical network appear to be the same in this model as in the simpler model, and are able to explain experimentally observed phenomena.

Finally, it was not possible to compare the regions of oscillatory parameter space in the (w_3, w_5) plane in order to consider dominant inhibition. However, the model's behaviour is consistent with such a relationship, as discussed above. Furthermore, increasing cortical feedback (onto the TC cell population while keeping feedback to the RE population constant) increased the synchrony of the activity, as shown in

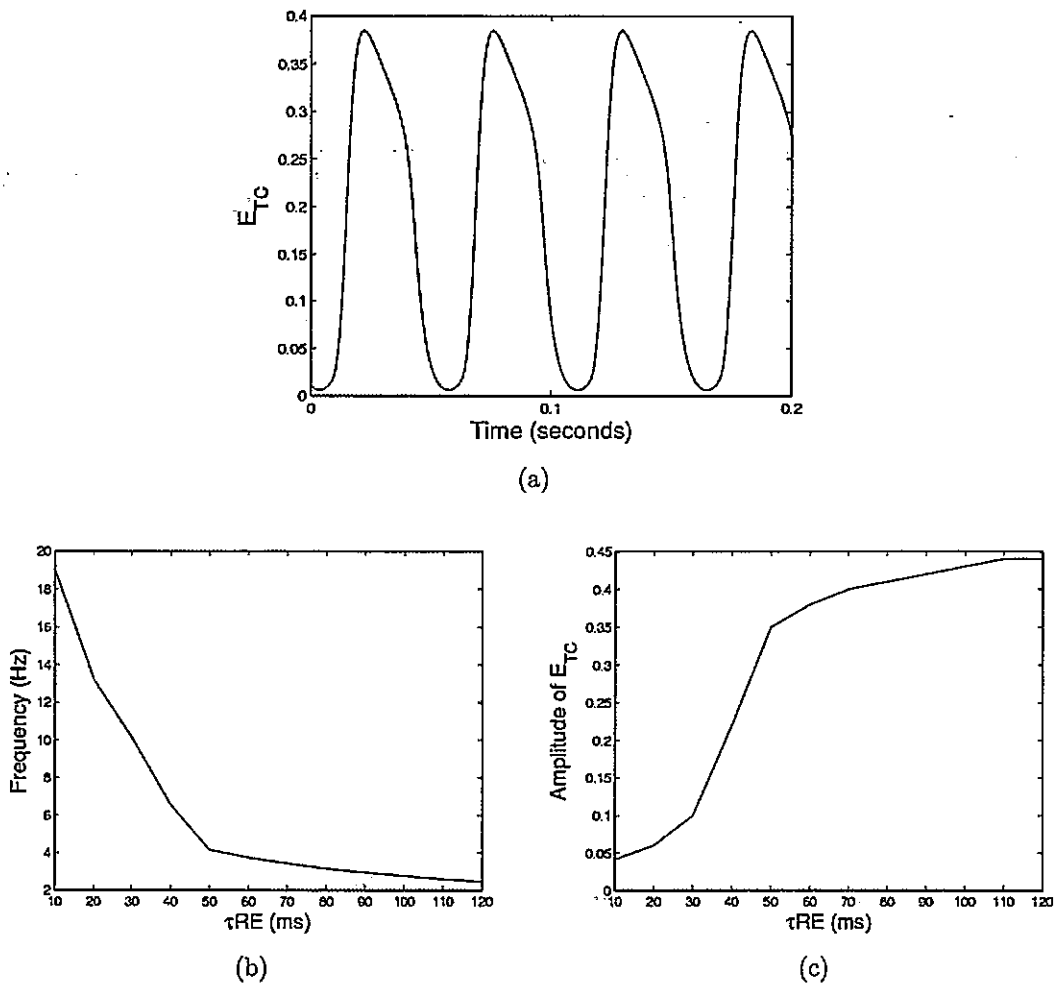

Figure 5.5: The plot in (a) shows the occurrence of slow oscillations in the model, when the RE time constant is increased. In (b) the frequency of oscillations is plotted against the value of the reticular time constant, and (c) shows the relationship with the amplitude of the oscillations.

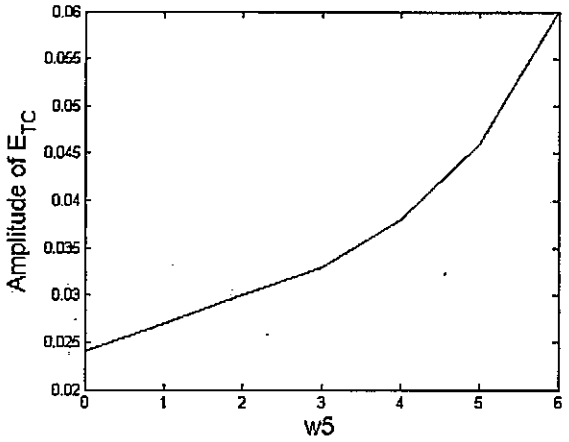

Figure 5.6: This plot shows the relationship between the value of the feedback connection weight onto the TC cell populations, and the synchrony of the oscillatory activity. It is clear that as the feedback increases, the amplitude and therefore the synchrony of the oscillation increases.

figure 5.6. This is in line with previous studies showing that increases in the strength of corticothalamic feedback synchronises spindles (Bal *et al.*, 2000). Therefore these results show that once more the thalamocortical network has an intrinsic resonant frequency in the spindle range, which is capable of explaining activity observed in previous experimental and theoretical studies based only on the nonlinear dynamics of the network.

5.4 Discussion

In the previous chapter a third population-level model of the thalamocortical network was built, as a simplification of the detailed STRF model. In this chapter it was intended that this model would bring together the behaviour replicated by the two previous models into a single model of the thalamocortical network. The main benefit of doing so is that it makes it possible to consider a generic form of the thalamocortical

circuitry, whose dynamics support two types of activity which are considered integral to the role of the thalamus. Furthermore, the changes that this circuitry needs to undergo to make the transition from sleep to wakefulness in the healthy brain, could also be considered via connectivity strengths between the included populations.

The results show that the same dynamics are at work in the sleep/wake parameter regimes of this unified model, as in the separate sleep/wake models that were presented previously. This indicates that the dynamics described in the earlier models are universal to the thalamocortical network. That is, the dynamics of the thalamocortical feedback circuitry described by this model support the relay of visual information, such that experimentally recorded visual responses are accurately replicated in the model's responses. Specifically, the response pattern is such that a TC cell of a given ON/OFF phase preference, responds with excitation to a light/dark stimulus early on, but responds with excitation to dark/light stimuli after a delay. In the model this reversal in phase is driven by cortical feedback, and may serve as a dynamic control of thalamic responses.

The model is also capable of supporting oscillations in the 7-14Hz spindle frequency range, which are oscillations measured during early sleep throughout the thalamocortical network. This shows that the intrinsic nonlinear dynamics of the thalamocortical feedback circuit are sufficient to support oscillations. Furthermore, manipulations of these dynamics replicate experimental manipulations which lead to switches in the oscillation frequency. Hence these activities, which are inseparable from the description of the thalamus, are embedded in the dynamics of the circuitry, and not in separate accounts of the circuitry, but in a single representation of it.

This architecture simply contains three cell types, which are interconnected as found experimentally, and these results therefore suggest that this should be considered as

a fundamental thalamocortical unit. This has implications for future investigations of early sensory pathways, as this thalamocortical unit displays a range of dynamic behaviour expected from the thalamus. Such an active role in neuronal activity for the thalamus has been previously overlooked, particularly when considering the thalamic contribution to sensory processing. However, this study shows that this simple three cell architecture can produce oscillations, as well as perform the relay of visual information which is dependent on an anti-phase arrangement of feedback (Wang *et al.*, 2004).

When an animal passes from being awake into sleep, the brain undergos a variety of changes, particularly with respect to neuromodulatory innervation (for two recent reviews see Hobson & Pace-Schott (2002); Pace-Schott & Hobson (2002)). In the thalamocortical circuitry in particular, it is known that the activity changes from unsynchronised high-frequency activity which is crucial for the relay of visual information, into a variety of slower frequency synchronised oscillations (McCormick & Bal, 1994). These changes occur due to changes in intra-cellular properties, but can also be seen in the strength of connections as shown by Bazhenov *et al.* (2002); Hill & Tononi (2005). Here the parameter changes that were required to make the transition from the awake behaviour to the early sleep state, are consistent with previous ideas about this network. In particular with an idea that there is a need for dominant inhibition during sleep oscillations (Destexhe *et al.*, 1998), and with the prediction that dominant excitation for the relay of information during awake states (le Masson *et al.*, 2002). This is the major hypothesis to emerge from this model, and this needs to be fully investigated in future experimental work.

The results from the current model could be inaccurate due to errors in assignment of parameter values, or oversimplifications. However, the model was scrutinised

alongside previous experimental work and more detailed models, hence it ought to be considered as an additional tool for understanding the thalamocortical network, and not a full description in isolation of all other work. The parameter manipulations show that this activity is robust to parameter variations within acceptable ranges, and therefore does not depend critically on the parameter choices. Furthermore, the results of this model are consistent with those of the previous two models of the thalamocortical network, and exhibit observed patterns of activity.

The main hypothesis of the current model is that in order to make a transition between early sleep and awake states, there needs to be an accompanying change in the relative strength of cortical feedback to TC and RE cells. Although this agrees with previous theoretical hypotheses, there is no experimental evidence to support this idea. Furthermore, this idea conflicts with a study which measured the quantal amplitudes (that is the size of the EPSC elicited due to the release of a single quanta of neurotransmitter) in corticothalamic and cortico-reticular synapses (Golshani *et al.*, 2001). This study was performed in slices of mouse ventrobasal nucleus and TRN, and the authors made estimations of quantal size based upon the measurement of EPSCs elicited in RE cells and TC cells after minimal stimulation of the corticothalamic fibers. They find that EPSC size and consequently quantal amplitude is larger in RE cells compared with TC cells, which they take to indicate that cortico-reticular synapses are more effective than corticothalamic synapses. Therefore, these experimental results do not agree with the hypothesis of the current model. However, in order to obtain a clear view of synaptic strength, other factors need to be addressed, such as the number of synapses, the number of synaptic contact sites, and the locations of the synaptic contacts throughout the dendritic tree. Furthermore, the assessment of synaptic efficacy needs to be performed in vivo, both in awake animals, and in the same animals during

sleep states, in order to test the current hypothesis accurately.

Finally, as in the previous two models, there are a number of assumptions made during the formulation of this model. The first is that in the process of simplifying the second model into this third form, the cortical and the thalamic interneurons were left out, while the reticular neurons were kept. From previous models of spindle oscillations, it is known that the presence of the reticular nucleus is crucial for the observation of this activity, and it was felt that a model neglecting this population would not have be valid. This model also dramatically reduces the number of cortical populations, and while there are nine TC cell populations of each ON/OFF types, there are only four cortical cells populations in total. Although this does not represent the true ratio of TC to PY cells, the aim of this model was to find a minimal representation of the thalamocortical network which could account for spindling and STRFs. Nine ON centre and nine OFF centre TC cell populations were required to generate cortical populations of opposite ON/OFF preference, therefore the minimum number of TC cell populations had to be 18, with four cortical populations to represent vertical and horizontal receptive fields.

As before, the current model uses the population approach, which assumes homogeneity in a large group of neurons, and as discussed previously, such assumptions limit the scope of the work. However, for understanding the change in dynamics which occurs as this system passes from transient awake activity to steady state sleep activity, the use of population level modelling has proved useful, allowing testable hypotheses to be made about the thalamocortical network during this transition.

5.4.1 Summary and contributions

This is the first time that a model representing the transition from awake visual processing to early sleep activity in the thalamocortical network has been attempted. It is also the first population-level model that has attempted to bridge the gap between steady state oscillatory activity and transient sensory responses in the early visual system. The results from the model are successful at representing the two types of behaviour that was shown in the previous models of the two isolated descriptions of the network. This unified model shows that it is possible to represent both aspects of thalamic functionality through the dynamics intrinsic to a single architecture. This has implications for the way the thalamus is considered as a unit within both sensory processing and sleep states. The model also uncovers the relationships required between populations in order to make the transition between the two states, predicting that it is heavily reliant on a shift in the relative weights of the feedback connections to the TC and RE cell populations.

Chapter 6

General Discussion

The aim of this thesis was to investigate the dynamics intrinsic to the activity of the thalamocortical network, through the use of population-level, computational models. The contribution of the thalamus to neural activity has been overlooked in the past, with the role of the thalamus often relegated to a passive relay. However, due to the observation that there is a large cortical innervation of the thalamus, recent studies have started to investigate a more substantial role for the thalamocortical network. The three hypotheses of this thesis were as follows: (i) The intrinsic dynamics of a simple thalamocortical network are able to support oscillatory activity in the spindle frequency range; (ii) The dynamics of corticothalamic feedback contributes to the formation of temporal thalamic receptive field properties; (iii) A single description of the thalamocortical feedback loop can account for both the sustained spindle range oscillatory activity, and the transient relay of visual information. By producing three biologically-defined models, which represent this network during an early sleep state and an awake state, both individually and together, these hypotheses have been addressed in detail. In the present chapter the results that have arisen from the work presented in chapters 3, 4, and 5 are summarised and discussed in the context of the

original hypotheses.

6.1 Computational modelling

As a starting point, it is useful to refer back to the discussion in the introduction, and to consider whether the approach of computational modelling was fruitful in this case. When studying a system with the approach of computational modelling, it is important to clearly state and consider the aims of the work. As discussed in chapter 1, the aims of a study are vital to determine whether a chosen paradigm is appropriate. For example in this thesis the hypotheses all relate to investigating the dynamics of the thalamocortical network, therefore the choice of population models is fitting. If instead the aim with the spindling model, for example, was to investigate the waxing-and-waning phenomenon, then this approach would be unsuitable.

The assumptions intrinsic to the chosen modelling paradigm must also be considered alongside the results from such work. In this thesis the assumptions of the particular Wilson & Cowan population approach used are discussed with the results in each discussion section, and are discussed again in section 6.4.1 below. The discussion of assumptions allows one to specify the limitations of the modelling approach and relate this to the results presented. Consequently, it is less tempting to infer too much from the results and draw unsubstantiated conclusions. Thus, the models in this thesis have made conclusions about the thalamocortical network, which are testable hypotheses, and while alternative explanations may be plausible, this study calls for further work in order to verify or disprove these hypotheses.

6.2 The use of population models

Population models were initially developed in order to investigate neuronal activity from a global perspective rather than at the detailed biophysical level. There are a number of different approaches that have been taken in order to derive various population descriptions of neurons, ranging from the approach used in this thesis (Wilson & Cowan, 1972) and similar paradigms (Gerstner, 1995), to mean-field approaches which consider the average activity of populations of spiking neurons (Nykamp & Tranchina, 2000; Treves, 1993). Such population descriptions have been used extensively to examine a large variety of systems with a vast range of functional specificity. These models do not explicitly represent the distinguishing cell to cell attributes found in the nervous system, such as conductances, dendritic structure, etc. However, the link to biological reality lies in the connectivity between the included cell populations. Therefore, these models consider that the behaviour to arise from a network occurs as a consequence of the dynamical interaction between populations.

This allows such models to be applied to a range of neuronal systems. In fact, a single population can encompass an entire brain area rather than a specific cell type, which allows for large-scale representations. As discussed in chapter 1, many studies have shown that these models can successfully be used to study a system of interest, such that experimental findings are replicated by the behaviour of the model, and hypotheses can be made, which can be tested by further or simultaneous experimental work. The replication of observations, and subsequent ability to propose plausible roles for the thalamocortical network are the main requirements of any modelling paradigm, and it is clear that population-level models are able to fulfil this need. However, as discussed throughout the thesis, it is extremely important to remember that inherent

to this approach are a number of assumptions and simplifications which limit the conclusions that can be drawn from such studies. These are discussed in section 6.4.1 below.

In the current thesis, the aim was to investigate the dynamics intrinsic to the circuitry of the thalamocortical feedback network. By doing the emerging activity could be related to the behaviour previously observed and described, in order to make plausible hypotheses about the nature and purpose of this feedback loop. This was done through the specific use of the Wilson & Cowan equations, which constitute a simple representation of neuronal dynamics. The form of these equations was described both in general and with specific reference to the models produced in this thesis, in chapters 3, 4, and 5. The three models display behaviour that has been reported in previous electrophysiological work, and consequently hypotheses have been made (reviewed in section 6.5) about the thalamocortical network in early sleep, in vision, and during the transition between the two states. In the next section, the results of this thesis are re-iterated in more detail, and discussed both sequentially, and in unison with reference to the specific insights gained from this work.

6.3 The dynamics of the thalamocortical network

6.3.1 The spindle oscillation

The first model presented in this thesis (chapter 3) consisted of a minimal three-population network, which includes only the fundamental cell types that are considered to be essential for generating spindle oscillations (Steriade *et al.*, 1993). The hypothesis that was to be addressed by creating this model, was that the nonlinear dynamics of the thalamocortical circuitry is able to display oscillatory activity in the spindle

frequency range (7-14Hz). A further goal was to determine if this three population representation is sufficient to describe this oscillation as an intrinsic, resonant activity of the thalamocortical network. The connectivity of the model network was strictly defined by information about the thalamocortical feedback circuit, which exists in the literature. The behaviour of this first model shows that this simple description of the thalamocortical network can oscillate with a frequency in the 7-14Hz range (section 3.3.1).

A major implication of this result is that the dynamics intrinsic to the activity of the thalamocortical network can be used to understand the network behaviour. The circuit displays robust oscillations in the correct frequency range, and previous experimental results can be understood in terms of the underlying nonlinear dynamics. Previous theoretical studies of the spindling thalamocortical network have been largely restricted to conductance-based paradigms (such models are reviewed by Destexhe & Sejnowski (2001, 2002), and are discussed in detail in section 2.2). Therefore, oscillatory activity in these previous models arises from the interplay of a number of currents, which have been found to be present in thalamic neurons (Huguenard & McCormick, 1992; McCormick & Huguenard, 1992). The present work shows that the thalamocortical network has an intrinsic ability, due to its connectivity, to oscillate at this 7-14Hz frequency range. This does not imply that studies at the ionic level are unnecessary, but does indicate that simplifying the level of complexity can be a useful way to understand the processes at play within neuronal systems. Furthermore the population-level model does not propose a new mechanism for the generation of spindle oscillations, but implies that the dynamics of the circuitry supports the oscillatory activity.

However, there are a number of limitations in the spindling model which need to be discussed. Initially, it ought to be noted that the existence of spindling is dependent

upon the presence of the cortical population. This is not correct with respect to the known mechanism underlying the spindle oscillation, as spindling is observed in thalamic slices, therefore in isolation from the cortex (von Krosigk *et al.*, 1993). However, the aim of the current model is to investigate whether the nonlinear dynamics of the thalamocortical network allows it to sustain the oscillatory behaviour. Therefore, the reliance on the cortical population shows that the cortex is involved in such a process. In addition, the Wilson & Cowan approach models homogenous populations of cells with no spatial dimension. As discussed in section 6.4.1, homogeneity is not perfect, but within a localised region one can assume that cells are similar. The lack of a spatial dimension also limits the phenomena which can be investigated. Identifying such short comings are a vital part of the understanding of a computational model, but using this model as one approach to tackling questions about thalamocortical oscillations, to be used with other theoretical and experimental studies allows useful observations to be made.

Hence, the work presented in this thesis looks at the involvement of the dynamics of the minimal and healthy thalamocortical network in producing normal oscillatory brain activity, which occurs in early sleep and periods of drowsiness. The results from this research show that this simple dynamical representation is adequate to observe activity which has previously been replicated through ionic descriptions.

6.3.2 Spatiotemporal receptive fields

The aim of the second model was to study the thalamocortical network in the awake state, and specifically the role of this network in visual processing. The definition of visual responses which was considered is the spatiotemporal receptive field (STRF). The hypothesis was that corticothalamic feedback drives TC cell visual responses, and

in particular contributes to the formation of the temporal receptive field, which has been shown to have a greater amplitude second phase than that of afferent RGCs (Usrey *et al.*, 1999). The main result arising from this model suggests that only phase-reversed feedback allows thalamocortical relay cells to develop a second stage to their temporal receptive fields, which matches experimentally observed STRFs (Cai *et al.*, 1997; Reid *et al.*, 1997). These previous results showed that a TC cell's STRF reverses in ON/OFF polarity (or light/dark preference) over time (see section 4.3.2).

The model also produces responses that have previously been measured in the visual system, such as transient responses to spots of light, and cortical orientation tuning curves (section 4.3.1), which all indicate that the model's replication of visual activity is reliable. Hence, the main hypothesis to emerge from the second part of the thesis, is that anti-phase feedback connectivity allows cortical cells to dynamically drive thalamocortical cells, such that their temporal response properties are shaped by this input. The implications of this result are far reaching. They support the idea that the feedback projection from cortex to thalamus modulates neuronal response properties, which is an idea that has started to emerge in the literature (Alitto & Usrey, 2003; Ghazanfar *et al.*, 2001). However, there is a need for future experimental work to verify this main hypothesis, and this is discussed in section 6.5 below.

Again, it is important to recognise the limitations of this part of the current work. In particular, another pathway which could cause an increased second phase in TC cells is via feed-forward inhibition. If this pathway did account for the change it would be much simpler for the nervous system to achieve. Secondly, no previous experimental work has shown that cortical feedback is linked to the biphasic responses of thalamocortical relay cells. Thirdly, although Wang *et al.* (2004) show a correlation between their results and anti-phase feedback connectivity, there is no evidence to suggest that this

is the only way that cortical cells are connected to TC cells. However, considering that the top-down control of thalamic temporal responses has the potential to modulate temporal decorrelation (Dong & Atick, 1995), responses to moving stimuli (Sillito & Jones, 2002), and possibly eye movement related information (sections 1.1.1 and 4.5), the added expense of a top-down control of thalamic RFs is conceivable. Furthermore, some involvement of corticothalamic feedback in controlling a variety of aspects of thalamic RFs has been shown experimentally in different modalities (see section 1.2.2.2 for a review). Therefore, this work proposes that the dynamics of the thalamocortical feedback circuit allows anti-phase cortical feedback to augment the second phase of the temporal RF. This proposed hypothesis can be verified experimentally, and hence future work could address these doubts experimentally.

This result implies that the previously overlooked role of the thalamus is central to sensory processing. Due to the stereotypical structure of the thalamocortical network within sensory systems, this result can be extrapolated to apply to the MGN and VPN. The latter point is particularly true as the current work utilises a population description, and therefore the details of the connectivity are the most important characteristic of the network. As described in chapter 1 the thalamocortical network in the visual, auditory, and somatosensory systems is very similar, hence the results of the current work can be assumed to be universal to the three first-order sensory nuclei of the thalamus.

The STRF model was reduced to form the third model presented in this thesis, which preserved the three population architecture of the first model, but extended this representation to allow the formation of receptive fields. This model was produced in order to clearly identify the pathway underlying the STRF formation, and to find the minimal architecture which can produce the biphasic STRF properties. This

model showed clearly that it is the anti-phase feedback arrangement, via a disynaptic thalamocortical pathway that produces the biphasic STRF, and that the minimum thalamocortical model requires only enough thalamic populations to create one each of four different cortical receptive fields. This minimal model can therefore account for the properties of the STRF generation well, and via the same mechanism as in the full STRF model.

6.3.3 Transition from receptive fields to spindles

This third model was used to address the final hypothesis which predicted that both the steady state oscillatory behaviour, and the transient receptive field behaviour could exist in a single description of the thalamocortical network. If so, the requirements that the transition between these states puts onto the network configuration could also be investigated.The results from this model showed that the representation of the thalamocortical network adopted in this part of the thesis can account for both types of behaviour. The main hypothesis of this model is that the transition between these two regimes requires a switch from cortical feedback to TC cell populations being dominant, in the receptive field case, to cortical feedback to the RE cell populations being dominant, in the spindles case. The model produced the expected responses when the experiments performed in the previous two models were repeated, which validates the responses of this third model.

Once more, a number of assumptions were made when defining this model. Cortical and thalamic interneurons were neglected, and the numbers of populations, particularly cortical, were dramatically reduced. However, one of the aims was to find the minimal representation of the thalamocortical network which displays the activity in the preceding two networks. The population approach also introduces simplifications,

with respect to homogeneity, and the lack of explicit representation of ionic behaviour. As an initial step in investigating changes in neuronal population dynamics which occur as an animal passes from a awake activity to a early sleep activity, this approach has proved useful, allowing suggestions about the system to be made. Finally, there is no experimental verification for the idea of dominant excitation in awake states, and the current knowledge shows that quantal amplitude of cortical synapses is larger in RE cells compared with TC cells (Golshani *et al.*, 2001), which indicates that corticoreticular synapses are stronger than corticothalamic synapses. Therefore further experimental work is necessary to measure the relative strengths of these synaptic contacts, which would involve considering a number of different factors in vivo, which can effect efficacy.

Hence, the hypothesis from the third model is supported by the evidence currently available in the literature, but requires further experimental verification as described in section 6.5 below.

6.3.4 Dynamics reflect functionality

Taken together these results show that the functionality of the thalamocortical network can be understood through an appreciation of the dynamics of the circuit. In the case of oscillatory activity, this statement is intuitive. Such that if there exists ionic properties to generate oscillatory activity, it would be beneficial for the circuitry which underlies this behaviour to have a resonant frequency in the same range, in order to sustain the oscillations and not damp the activity. In the model of visual processing it is also clear that the circuitry, and specifically the fact that there exists a precise wiring of feedback connections with respect to the phase preference of cells, is arranged to suit the facilitation of top-down control of temporal thalamocortical cell responses. The

unified model shows that a switch in the relative strength of the weights of the two cortical feedback connections, facilitates the switch in wake/sleep regimes. In the brain, this switch is initiated by the actions of various neuromodulators.

Population-level models could be used as the first stage of a theoretical investigation of a system, to see if the dynamics of the circuitry yield the behaviour that is of interest. As in this thesis, it is also possible to go on and look specifically at which components of the circuitry are particularly important for the observation of the given activity, either through bifurcation analysis, or via parameter manipulations. This type of research has been done in the past, but possesses a number of limitations as discussed in the next section. However, the current results show that such models can be used alongside electrophysiological data and ionic models, to produce biologically defined networks, replicate previously observed data, and make plausible hypotheses about the networks under scrutiny.

6.4 Limitations of the paradigm

When considering the results from the current work, there are a number of limiting issues that must be taken into account. The population-level approach is a simplified representation of neuronal dynamics, and the derivation of the Wilson & Cowan equations requires a number of assumptions to be made, which were outlined in section 3.2.2. Here, the areas where these assumptions may not hold are discussed in detail. In the second part of this section, parameter choices are discussed as another shortfall of this modelling paradigm.

6.4.1 Assumptions

As in the derivation of any mathematical model, assumptions are made to simplify the model sufficiently to make it usable. In the equations of Wilson & Cowan, which were adopted for the models in the current work, the main assumption is that populations consist of a homogenous set of neurons. While this is clearly never the case, as no two neurons are entirely identical, we can assume that this is approximately the case in the populations represented here, particularly as a population of cells in this thesis refers to a particular cell type and not an entire brain area, which may contain many different cell types.

Wilson & Cowan state that the cells within a population are assumed to be fully connected either directly or via interneurons. Again this is an assumption that is likely not to be true, with cells being connected only to cells that are in close topographical proximity. This assumption can be overlooked given that here each population represents a localised topographic region of cells, which is particularly true in the visual models. A linked assumption, imposed not by the modelling paradigm but by the architecture, is that in the visual models each population has a single receptive field. Therefore a number of cells are assumed to have receptive fields that are entirely overlapping in space. This is not precisely the case, though receptive fields of nearby cells do overlap in early sensory areas (Reid & Alonso, 1995), and so this assumption is not without physiological basis.

An issue which has been discussed by other modelling studies, is that of transient responses. Due to the structure of the Wilson & Cowan equations, and in particular the time coarse graining performed at the end of the derivation, the activity exhibited by the equations cannot vary over extremely short time scales (Gerstner, 2000; Nykamp &

Tranchina, 2000). However, as the models presented in this thesis deal with interacting populations in different brain regions, the delays introduced can be accounted for by delays in axonal propagation. Furthermore, in both of the regimes it is interactions that occur over time scales which are longer than those unaccounted for, which are of primary interest. Finally, all three models display responses that fit the experimental data well, particularly temporally, and therefore this issue does not appear to have a significant effect on the activity here.

6.4.2 Parameters

Another issue that was discussed in an earlier chapter (see section 3.2.3), and is reiterated here, is that of parameters. The parameters that are required for the definition of the models, the population time constants and connection weight parameters, have no directly physiologically measurable counterparts. As discussed before, the choice of parameters can be justified by the use of physiological data, and therefore there will be some correlation with the cellular properties in the brain. However, the assignment of parameter values remains arbitrary, and therefore the range of parameters for which a given result is observed should be found, either by bifurcation analysis or manual manipulation of each of the parameters. These processes are by no means conclusive, as they are performed in one, two, or at most three dimensions of parameter space at a time. Hence they yield no appreciation of the effect of manipulating more than three parameters at a time. This shortfall can only be overcome by being aware that it exists, and by taking it into account when considering the results of the work.

6.4.3 Conclusions about limitations

Despite the shortcomings, population models are a good first step towards understanding the functionality of neuronal networks, and particularly for looking at the dynamics without the complication of ionic properties. A major reason for believing this assertion is that the models presented here do not only hypothesise about what could be happening in the thalamocortical network, but also display activity that is consistent with the expectations from previous experimental results. Furthermore, it is inevitable that the modelling paradigm does not precisely represent the neuronal circuitry in every aspect, because any model makes assumptions and simplifications, which is why it is merely a model. If the limitations are fully understood, and discussed with respect to the particular model under scrutiny, as has been done here, then the precise scope of the work can be appreciated.

6.5 Future work

This section considers the questions that have arisen from this current work, in terms of how they could be addressed in the future, through both experimental work and extensions of the modelling work.

6.5.1 Experiments to test hypotheses

An essential consequence of such a theoretical study is that it fuels a need for experimental work to test the hypotheses which arise from it. The main hypotheses that have emerged from this work are summarised below, along with ideas for experiments to investigate these questions:

1. The spindles model suggests that the slowing of the intrinsic oscillatory activity in the TC circuitry, occurs due to $GABA_B$ affecting the nonlinear dynamics of the network. Experiments to investigate this idea further are also required, as this frequency change has not been investigated to a great extent previously, particularly not in terms of the network dynamics.

2. The main hypothesis of the STRF model, is that corticothalamic feedback strengthens the second phase of the temporal response of TC cells, which allows an ON centre TC cell to respond like an OFF centre cell after a certain latency. Experiments could manipulate the gain of the corticothalamic feedback whilst light/dark responses are measured. The expectation is that the reduction of feedback would reduce the late phase-reversed component of the TC cell receptive field, so that it has the same magnitude as an RGC's second phase.

3. The unified model investigated the transition from sleep to wakefulness, and in the model there is a requirement for cortical feedback to TC populations to outweigh feedback to RE populations in the transient visual regime. Whilst the opposite relationship is necessary for the sustained oscillatory regime. This hypothesis needs experimental verification by the measurement of the synaptic properties, such as conductances, efficacy etc, of the PY6 to TC and PY6 to RE connections during sleep states and active behaving awake states.

6.5.2 Extension to the spindles model

The spindles model is an intentionally simplified version of the thalamocortical network. However, the work in this thesis has attempted to explain processes which depend on the ionic properties of the cells by the nonlinear dynamics of the circuitry

alone. In particular, the switch to slower frequencies is explained by a rearrangement of the dynamics of the circuitry due to a slowing of the inhibitory population's time constant. In order to investigate this further, an extended model could be built, which would include ionic components. To maintain the simplicity of the model, the conductances could be limited to the TC cell, while the Wilson & Cowan equations for the reticular and cortical cell populations are preserved. That is, the new model would be a population/conductance-based hybrid. This extended model for the TC cell is shown in figure 6.1.

The synaptic currents would allow the investigation of the frequency switch phenomenon, while the interface between population dynamics and conductances would be an interesting approach to investigate. Furthermore, the cell shown in figure 6.1 includes intrinsic currents. This factor would allow the investigation of another intriguing and unresolved issue with respect to spindles, that is the basis of the waxing-and-waning. As described in chapter 2, spindle oscillations wax-and-wane over 3-5 second periods, and the basis for this property is thought to be the up-regulation of the I_h current via calcium. A hybrid model, which maintains the dynamics that allow 7-14Hz oscillations, but includes the ionic properties of thalamic cells, could yield extremely interesting results on a number of issues related to spindling.

6.5.3 The receptive field model

The major feed-forward cortical targets of TC cells are cells in layer four. The simple cells in this layer are considered to be the first stage of cortical processing, and a great deal of experimental work has been done to investigate their properties. In fact most of the information in the literature about simple cells is based upon experiments performed on layer 4 cells. Furthermore, the cells in layer 4 have interconnections with

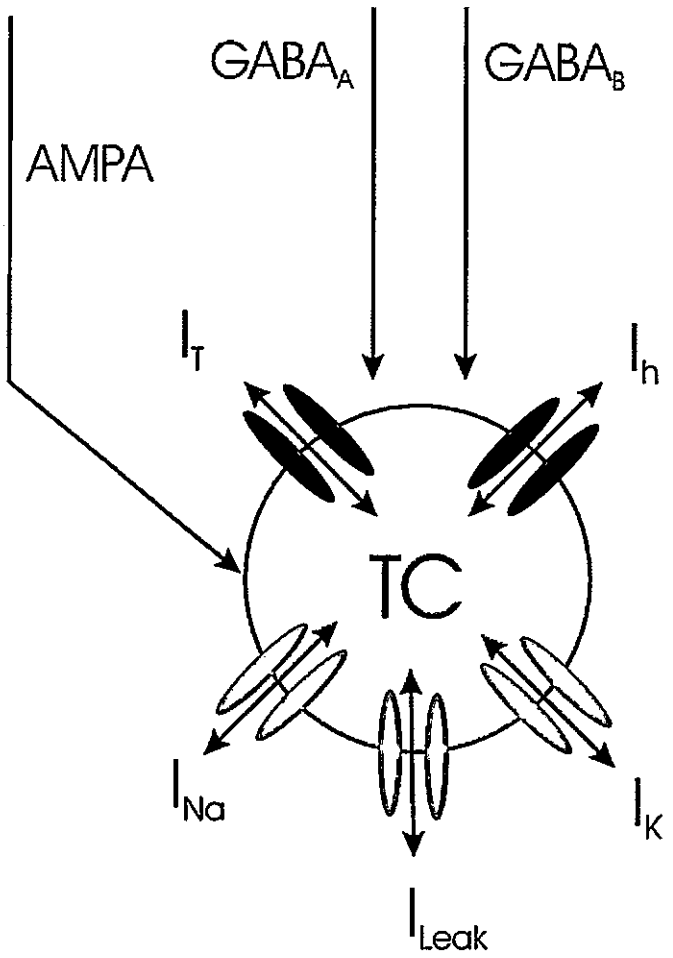

Figure 6.1: A schematic representation of a proposed extension to the TC cell component of the spindles model. The cell has five intrinsic currents, a T-type calcium current I_T, a hyperpolarisation-activated cation current I_h, in addition to sodium, potassium, and leak currents I_{Na}, I_K, and I_{Leak}. There are also three synaptic currents, $GABA_A$ and $GABA_B$ for reticular inputs, and AMPA for cortical inputs.

the corticothalamic cells of layer 6 (Thomson *et al.*, 2002), forming an additional loop between the main thalamocortical input layer and the main thalamocortical output layer. Therefore, a useful extension of the STRF model, would involve the inclusion of this cortical layer.

A schematic depiction of what such an extended model would look like is given in figure 6.2. This extra level of cortical processing may have interesting effects on the emergence of visual responses in thalamic cells. Furthermore, it would also be possible to look at how cortical responses are in turn affected by the changing thalamic responses, given that this is essentially a recurrent circuit which may be dynamically updating its own inputs. This latter point is an extremely interesting suggestion, which has been discussed in the literature (Alitto & Usrey, 2003), but has not been investigated a great deal experimentally or theoretically.

6.5.4 The unified model

The main neural mechanism involved in changing the dynamics during sleep/wake cycle is neuromodulation. Acetylcholine (ACh) is particularly important in controlling this transition, and the thalamus receives dense innervation by cholinergic fibres (McCormick, 1992). Application of ACh into the thalamus has opposite effects on TC and RE cells, such that TC cells are excited, but RE cells are inhibited (McCormick, 1992). When the brain switches from wake to sleep states, the level of ACh in the thalamus decreases. Therefore, TC cells will be more excited during wakefulness when there are higher levels of ACh, and RE cells will be more excited during sleep states when there is lower concentrations of ACh.

This is consistent with the model's prediction of dominant excitation during visual activity, and dominant inhibition during sleep oscillations, and leads to the question of

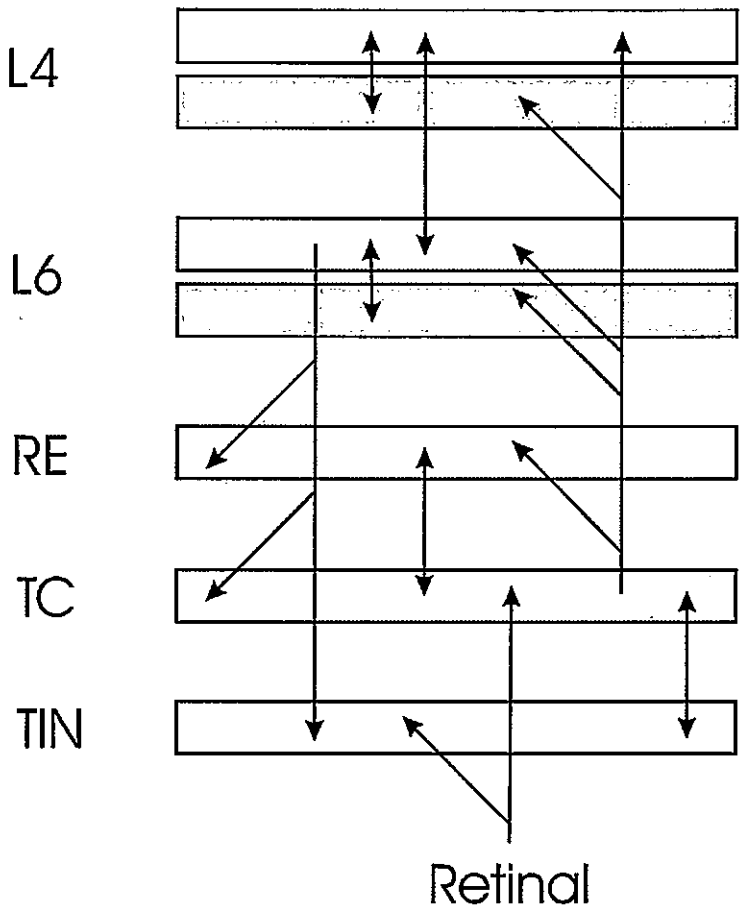

Figure 6.2: A schematic representation of the proposed extension to the STRF model. This model would include more of the cortical circuitry, by including layer 4 (L4) as well as layer 6 (L6) cells. Both cortical layers have excitatory (white) as well as inhibitory (grey) cells. The layers of cells shown here may include sub-types of cells, such as ON and OFF cells in the TC and TIN layers, and horizontal/vertical and ON/OFF cells in the excitatory cortical layers.

what would happen if the modulation of the thalamic activity by ACh were explicitly incorporated into the model. The interaction of this neuromodulator with the network dynamics could then be explored. The action of ACh could be modelled via a leak potassium current, as has been done previously (Bazhenov *et al.*, 2002; Hill & Tononi, 2005), which would therefore transform the population model into a hybrid model (as in section 6.5.2), with a single extra conductance. As the role of neuromodulation is central to the sleep/wake cycle, this extension should yield interesting and useful results for understanding the wake to sleep transition.

6.6 Conclusions and contributions to knowledge

In this section the main findings of the research are re-iterated, with the specific aim of highlighting the significance, novelty, and contribution to knowledge.

6.6.1 Population models

There have been previous attempts at describing the thalamocortical network at a population-level (Bressloff & Cowan, 2003b; Hoppensteadt & Izhikevich, 1998; Robinson *et al.*, 2002). However, these previous cases have not taken into account the accurate connectivity of the thalamocortical network (Hoppensteadt & Izhikevich, 1998), have considered the existence of pathological activity in the thalamocortical activity (Robinson *et al.*, 2002), or have focussed on cortical response properties (Bressloff & Cowan, 2003b). Thus, the models in this thesis are novel; the first because it represents spindle-frequency oscillations in the thalamocortical network of a healthy, normal brain, and retains only the circuitry that has been previously proposed to be essential for the generation and maintenance of these spindle oscillations. The second model is

an extended thalamocortical architecture within the visual system, and looks at the temporal responses arising from the dynamics of the circuitry. Finally the third model is novel as it represents both spindling and receptive field properties in the same model.

The results suggest that the functions of the thalamocortical network are reflected in the nonlinear dynamics of the inter-connected cell populations. Previous studies have not considered this feature of the circuitry before, and yet the current results suggest that this is an extremely fruitful level of investigation. However, it is important to recall that this approach contains a number of assumptions and simplifications, as explained throughout the thesis. Hence, if these limitations are discussed in context of the observed results, then the conclusions drawn will be tempered by these issues, allowing for realistic hypotheses to be made. Therefore, the models presented here are indicative of the benefits of using population-level descriptions as a methodology in neuroscience research.

6.6.2 Spindles are a resonant intrinsic activity

The first model investigated the existence of spindles as an activity arising from the simple representation of the thalamocortical network. In this model spindles exist as a resonant property of the dynamics of the thalamocortical circuitry. Bifurcation analysis of the equations of the network show that this activity is robust with respect to parameter variations, and that relationships between connections, which have been either shown to exist in experimental work or hypothesised based on previous modelling studies, also exist in the present model. Therefore, this approach is consistent with the dynamics of previous models which have involved increased levels of complexity, and with the dynamics of the network in real tissue.

This spindle frequency-range oscillation can be converted into other oscillatory

states through the transformation of the intrinsic dynamics. In particular, as in manipulations carried out in thalamic slices, the oscillation was changed into a slow 4Hz oscillation by varying the temporal properties of the inhibitory dynamics within the network. Hence, the main hypothesis of the model is that changes in oscillation frequency occur as a re-arrangement of the dynamics in the thalamocortical circuitry, which is caused by the slower $GABA_B$ inhibition. This calls for future work to address this question (as described in section 6.5). The model also supports previous findings which showed that corticothalamic feedback is involved in the synchronisation of spindle oscillations, and therefore that cortical feedback acts on the spatiotemporal properties of thalamocortical activity.

6.6.3 Spatiotemporal responses due to the dynamics of feedback

The receptive field model had spatial response properties hard-wired into the system through input connections to the various cell populations, and temporal responses arose from the dynamics of the circuitry. It is known that retinal inputs alone do not sufficiently account for the second phase of thalamic temporal responses (Usrey *et al.*, 1999), therefore this model was used to examine the STRFs of TC cells as described previously (Cai *et al.*, 1997; Reid *et al.*, 1997), and the dependence of those responses on the arrangement of cortical feedback. Consistent with the experimental studies these TC cell STRFs were shown to be biphasic in time, such that TC cells have response properties that reverse in ON/OFF phase preference over time. The basis of such responses should be of great interest to the understanding of the early visual system, yet no previous attempt has been made to investigate this feature.

Very recent work has shown that corticothalamic feedback is specific with respect to the phase preference of a cortical cell and its target TC cells (Wang *et al.*, 2004).

The STRF model shows that the emergence of biphasic responses can be explained based on the nonlinear dynamics of the anti-phase feedback network. Hence the main hypothesis of the second model is that anti-phase feedback augments the feed-forward biphasic response property that TC cells receive from their retinal inputs. It may be that this control is dynamically applied during active vision to alter the thalamocortical cell responses dynamically in time. The latter point is particularly plausible, as the model shows that changes in the weights of the TC to PY6 and PY6 to TC connections can change the latency between the phases of the STRF. This may have implications for the thalamic involvement in the processing of information about moving stimuli, and possibly also eye movements. However, more work needs to address such ideas in detail. This model was reduced in order to find the minimal architecture required to generate this response property. In this way, the reduced model clearly showed that a disynaptic pathway, via anti-phase feedback, mediates the emergence of the second phase in the model TC cell populations.

6.6.4 The transition from receptive fields to spindles

This reduced model contained the three cell type architecture of the simple spindle oscillation model, which was extended to allow for the formation of spatial receptive field structures. This model was used to examine both the transient STRFs of TC cells, and the steady state spindle frequency range oscillatory activity. As in the receptive field model, the TC cell STRFs were shown to be biphasic in time, such that the phase preference reverses over time. Furthermore, the model also produced oscillations in the spindle frequency range, which were robust to parameter variations within reasonable ranges. These oscillations underwent the same manipulation observed in the spindles model, such as changes in frequency, and control of synchrony via corticothalamic

feedback.

Hence, these results show that the sustained and transient responses that were observed individually in models of the thalamocortical network can be observed in a single description of the circuitry. Furthermore, the switch between the two involves a switch in the relative strength of cortical feedback to the TC and RE populations, such that dominant excitation is required for the STRF responses, and dominant inhibition for the oscillatory responses. This latter point is the main hypothesis of the unified model and is consistent with previous theoretical findings relating to the thalamocortical circuitry. However this hypothesis necessitates further verification through experimental studies of the thalamocortical circuitry, as there is no experimental evidence to support the switch in synaptic strength.

6.7 Summary

The results of this current work show that population-level, biologically defined descriptions of the thalamocortical feedback circuit can be used to look at the role of this network in the asleep and the awake state, both separately and simultaneously. The results show that the spindle oscillation occurs as a resonant activity of a simple thalamocortical circuit. A second model of the STRFs of TC cells agrees with experimental findings which showed that corticothalamic feedback ought to be arranged in anti-phase, as this arrangement is necessary for the thalamic temporal receptive fields to match those derived experimentally, and exceed the strength of the second phase of the temporal retinal response as measured by Usrey *et al.* (1999). The final model shows that a single description of the thalamocortical network can display both sleep and awake activity, and that the switch between the two relies upon a switch in the

relative cortical feedback strength, which is also consistent with previous theoretical hypotheses.

The specific implications of these results are as follows: The first model shows that the thalamocortical network has an intrinsic resonance within the spindle range, and that cortical feedback influences the synchrony of this oscillatory activity. The results from simulations of the second model show that anti-phase feedback shapes the temporal responses of TC cells, and therefore cortical cells may be able to dynamically control thalamic responses, and therefore their own inputs, via feedback. The third model shows that feedback also controls the responses of thalamic cells through the wake to sleep transition. In all cases corticothalamic feedback controls the temporal structure of thalamic activity: via synchrony of oscillations, STRFs, and the switch between transient and steady state activity. This has implications for the involvement of the thalamus and the thalamocortical network in dynamic activity in the brain. Hence these results suggest robust, theoretically derived roles for the thalamocortical feedback network, which was previously dismissed as a passive relay of afferent information.

List of References

ALITTO, H.J. & USREY, W.M. (2003). Corticothalamic feedback and sensory processing. *Curr Opin Neurobiol*, **13**, 440–5. 1.3, 1.2.2.2, 4.5, 6.3.2, 6.5.3

ALONSO, J., USREY, W. & REID, R. (2001). Rules of connectivity between geniculate cells and simple cells in cat primary visual cortex. *J Neurosci*, **21**, 4002–15. 4.2.1

ALONSO, J.M. (2002). Neural connections and receptive field properties in the primary visual cortex. *Neuroscientist*, **8**, 443–56. 4.2.1

AMITAI, Y. (2001). Thalamocortical synaptic connections: efficacy, modulation, inhibition and plasticity. *Rev Neurosci*, **12**, 159–73. 1.2.1, 4.2.1, 4.2.3, 4.4.3

ANDERSON, J., CARANDINI, M. & FERSTER, D. (2000). Orientation tuning of input conductance, excitation, and inhibition in cat primary visual cortex. *J Neurophysiol*, **84**, 909–26. 3.2.4, 4.2.3

ATICK, J.J. & REDLICH, A.N. (1990). Towards a theory of early visual processing. *Neural Computation*, **2**, 308–320. 4.5

AVANZINI, G., DE CURTIS, M., PANZICA, F. & SPREAFICO, R. (1989). Intrinsic properties of nucleus reticularis thalami neurones of the rat studied in vitro. *J Physiol*, **416**, 111–22. 2.2

BAIR, W., CAVANAUGH, J.R., SMITH, M.A. & MOVSHON, J.A. (2002). The timing of response onset and offset in macaque visual neurons. *J Neurosci*, **22**, 3189–205. 4.1

BAL, T., VON KROSIGK, M. & MCCORMICK, D. (1995a). Role of the ferret perigeniculate nucleus in the generation of synchronized oscillations in vitro. *J Physiol*, **483**, 665–85. 3.3.9.1

BAL, T., VON KROSIGK, M. & MCCORMICK, D. (1995b). Synaptic and membrane mechanisms underlying synchronized oscillations in the ferret lateral geniculate nucleus in vitro. *J Physiol*, **483**, 641–63. 2.1, 3.3.9.1, 3.4

BAL, T., DEBAY, D. & DESTEXHE, A. (2000). Cortical feedback controls the frequency and synchrony of oscillations in the visual thalamus. *J Neurosci*, **20**, 7478–88. 1.2.2.1, 2.1, 2.2, 3.4, 4.2.1, 4.5.1, 5.3.2

BANNISTER, N., NELSON, J. & JACK, J.J.B. (2002). Excitatory inputs to spiny cells in layers 4 and 6 of cat striate cortex. *Philos Trans R Soc Lond B Biol Sci*, **357**, 1793–808. 3.2.1

BAZHENOV, M., TIMOFEEV, I., STERIADE, M. & SEJNOWSKI, T.J. (2002). Model of thalamocortical slow-wave sleep oscillations and transitions to activated States. *J Neurosci*, **22**, 8691–704. 1.2.2.3, 5.1, 5.3.2, 5.4, 6.5.4

BEIERLEIN, M. & CONNORS, B.W. (2002). Short-term dynamics of thalamocortical and intracortical synapses onto layer 6 neurons in neocortex. *J Neurophysiol*, **88**, 1924–32. 1.2.1, 4.2.3, 4.4.3

BELLEBAUM, C., DAUM, I., KOCH, B., SCHWARZ, M. & HOFFMANN, K.P. (2005). The role of the human thalamus in processing corollary discharge. *Brain*, **128**, 1139–1154. 1.1.1

BICKLE, J., BERNSTEIN, M., HEATLEY, M., WORLEY, C. & STIEHL, S. (1999). A functional hypothesis for LGN-V1-TRN connectivities suggested by computer simulation. *J Comput Neurosci*, **6**, 251–61. 1.2.2.2, 4.2.1, 4.5

BLUMENFELD, H. & MCCORMICK, D. (2000). Corticothalamic inputs control the pattern of activity generated in thalamocortical networks. *J Neurosci*, **20**, 5153–62. 3.4

BOLZ, J. & GILBERT, C. (1986). Generation of end-inhibition in the visual cortex via interlaminar connections. *Nature*, **320**, 362–5. 4.2.1

BRESSLOFF, P.C. & COWAN, J.D. (2003a). The functional geometry of local and horizontal connections in a model of V1. *J Physiol Paris*, **97**, 221–36. 1.3, 2.2.1

BRESSLOFF, P.C. & COWAN, J.D. (2003b). A spherical model for orientation and spatial-frequency tuning in a cortical hypercolumn. *Philos Trans R Soc Lond B Biol Sci*, **358**, 1643–67. 1.2.2.2, 4.5, 6.6.1

BULLIER, J. & NORTON, T. (1979). Comparison of receptive-field properties of X and Y ganglion cells with X and Y lateral geniculate cells in the cat. *J Neurophysiol*, **42**, 274–91. 4.1

CAI, D., DEANGELIS, G. & FREEMAN, R. (1997). Spatiotemporal receptive field organization in the lateral geniculate nucleus of cats and kittens. *J Neurophysiol*,

78, 1045–61. 4.1, 4.1, 4.1, 4.2, 4.2.6, 4.3.1, 4.3.2, 4.13, 4.4, 4.4.1, 4.5, 4.5.1, 6.3.2, 6.6.3

CASTI, A.R.R., OMURTAG, A., SORNBORGER, A., KAPLAN, E., KNIGHT, B., VICTOR, J. & SIROVICH, L. (2002). A population study of integrate-and-fire-or-burst neurons. *Neural Comput*, **14**, 957–86. 4.1

CASTRO-ALAMANCOS, M. & CALCAGNOTTO, M. (2001). High-pass filtering of corticothalamic activity by neuromodulators released in the thalamus during arousal: in vitro and in vivo. *J Neurophysiol*, **85**, 1489–97. 3.2.4, 1, 4.4.3

CASTRO-ALAMANCOS, M.A. (2002). Role of thalamocortical sensory suppression during arousal: focusing sensory inputs in neocortex. *J Neurosci*, **22**, 9651–5. 1.2.2.2

CASTRO-ALAMANCOS, M.A. (2004). Absence of rapid sensory adaptation in neocortex during information processing states. *Neuron*, **41**, 455–64. 1.2.2.2

CITRON, M., KROEKER, J. & MCCANN, G. (1981). Nonlinear interactions in ganglion cell receptive fields. *J Neurophysiol*, **46**, 1161–76. 4.1

CONTRERAS, D. & STERIADE, M. (1996). Spindle oscillation in cats: the role of corticothalamic feedback in a thalamically generated rhythm. *J Physiol*, **490**, 159–79. 3.3.10

CONTRERAS, D., DOSSI, R. & STERIADE, M. (1993). Electrophysiological properties of cat reticular thalamic neurones in vivo. *J Physiol*, **470**, 273–94. 3.2.4, 4.4.3

CONTRERAS, D., DESTEXHE, A., SEJNOWSKI, T. & STERIADE, M. (1996). Control of spatiotemporal coherence of a thalamic oscillation by corticothalamic feedback. *Science*, **274**, 771–4. 1.2.2.1, 2.3, 2.2, 3.3.1

CONTRERAS, D., DESTEXHE, A., SEJNOWSKI, T. & STERIADE, M. (1997a). Spatiotemporal patterns of spindle oscillations in cortex and thalamus. *J Neurosci*, **17**, 1179–96. 2.1, 3.3.1, 3.4

CONTRERAS, D., DESTEXHE, A. & STERIADE, M. (1997b). Spindle oscillations during cortical spreading depression in naturally sleeping cats. *Neuroscience*, **77**, 933–6. 2.1, 4.2.1

CRICK, F. (1984). Function of the thalamic reticular complex: the searchlight hypothesis. *Proc Natl Acad Sci USA*, **81**, 4586–90. 3.2.1

DAN, Y., ATICK, J. & REID, R. (1996). Efficient coding of natural scenes in the lateral geniculate nucleus: experimental test of a computational theory. *J Neurosci*, **16**, 3351–62. 4.5

DAYAN, P. & ABBOTT, L. (2001). *Theoretical Neuroscience: Computational and Mathematical Modeling of Neural Systems*. The MIT Press. 3.2.6, 3.2.6, 3.3.8

DEANGELIS, G., OHZAWA, I. & FREEMAN, R. (1995). Receptive-field dynamics in the central visual pathways. *Trends Neurosci*, **18**, 451–8. 4.1, 4.2.6

DEBOER, E. & KUYPER, P. (1968). Triggered correlation. *IEEE Trans Biomed Eng*, **15**, 169–179. 4.2.6

DECO, G. & ROLLS, E.T. (2004). A neurodynamical cortical model of visual attention and invariant object recognition. *Vision Res*, 44, 621–42. 1.3, 2.2.1

DENHAM, M. & BORISYUK, R. (2000). A model of theta rhythm production in the septal-hippocampal system and its modulation by ascending brain stem pathways. *Hippocampus*, **10**, 698–716. 1.3, 3.2.3

DESCHENES, M., PARADIS, M., ROY, J. & STERIADE, M. (1984). Electrophysiology of neurons of lateral thalamic nuclei in cat: resting properties and burst discharges. *J Neurophysiol*, **51**, 1196–219. 3.2.1, 3.4

DESTEXHE, A. (1999). Can $GABA_A$ conductances explain the fast oscillation frequency of absence seizures in rodents? *Eur J Neurosci*, **11**, 2175–81. 4.2.1

DESTEXHE, A. (2000). Modelling corticothalamic feedback and the gating of the thalamus by the cerebral cortex. *J Physiol Paris*, **94**, 391–410. 4.1

DESTEXHE, A. & SEJNOWSKI, T. (2001). *Thalamocortical Assemblies*. Oxford. 6.3.1

DESTEXHE, A. & SEJNOWSKI, T. (2002). *The Handbook of Brain Theory and Neural Networks*, 1049–1053. MIT Press. 5.3.2, 6.3.1

DESTEXHE, A., MCCORMICK, D. & SEJNOWSKI, T. (1993). A model for 8-10 Hz spindling in interconnected thalamic relay and reticularis neurons. *Biophys J*, **65**, 2473–7. 2.2, 2.1, 2.2, 3.4

DESTEXHE, A., CONTRERAS, D. & STERIADE, M. (1998). Mechanisms underlying the synchronizing action of corticothalamic feedback through inhibition of thalamic relay cells. *J Neurophysiol*, **79**, 999–1016. 1.2.2.1, 1.4, 2.1, 2.2, 3.3.1, 3.3.10, 3.3.10, 3.4, 4.2.1, 5.3.2, 5.3.2, 5.4

DESTEXHE, A., CONTRERAS, D. & STERIADE, M. (1999). Cortically-induced coherence of a thalamic-generated oscillation. *Neuroscience*, **92**, 427–43. 1.2.2.1, 2.2, 3.3.1, 3.4, 5.3.2

DONG, D. & ATICK, J. (1995). Temporal decorrelation: a theory of lagged and nonlagged responses in the lateral geniculate nucleus. *Network*, **6**, 159–178. 4.5, 6.3.2

DOSSI, R.C., PARE, D. & STERIADE, M. (1991). Short-lasting nicotinic and long-lasting muscarinic depolarizing responses of thalamocortical neurons to stimulation of mesopontine cholinergic nuclei. *J Neurophysiol*, **65**, 393–406. 3.3.2

DUBIN, M. & CLELAND, B. (1977). Organization of visual inputs to interneurons of lateral geniculate nucleus of the cat. *J Neurophysiol*, **40**, 410–27. 4.2.4

ERGENZINGER, E., GLASIER, M., HAHM, J. & PONS, T. (1998). Cortically induced thalamic plasticity in the primate somatosensory system. *Nat Neurosci*, **1**, 226–9. 1.2.2.2

ERISIR, A., HORN, S.V. & SHERMAN, S. (1997). Relative numbers of cortical and brainstem inputs to the lateral geniculate nucleus. *Proc Natl Acad Sci USA*, **94**, 1517–20. 1.2.1

EYDING, D., MACKLIS, J.D., NEUBACHER, U., FUNKE, K. & WORGOTTER, F. (2003). Selective elimination of corticogeniculate feedback abolishes the electroencephalogram dependence of primary visual cortical receptive fields and reduces their spatial specificity. *J Neurosci*, **23**, 7021–33. 1.2.2.2

FERSTER, D. & MILLER, K. (2000). Neural mechanisms of orientation selectivity in the visual cortex. *Annu Rev Neurosci*, **23**, 441–71. 4.2.4

GARDNER, J., ANZAI, A., OHZAWA, I. & FREEMAN, R. (1999). Linear and nonlinear contributions to orientation tuning of simple cells in the cat's striate cortex. *Vis Neurosci*, **16**, 1115–21. 4.3.1

GAYMARD, B., RIVAUD, S. & PIERROT-DESEILLIGNY, C. (1994). Impairment of extraretinal eye position signals after central thalamic lesions in humans. *Exp Brain Res*, **102**, 1–9. 1.1.1

GENTET, L.J. & ULRICH, D. (2003). Strong, reliable and precise synaptic connections between thalamic relay cells and neurones of the nucleus reticularis in juvenile rats. *J Physiol*, **546**, 801–11. 3.2.4, 4.4.3

GERSTNER (1995). Time structure of the activity in neural network models. *Phys Rev E*, **51**, 738–758. 6.2

GERSTNER, W. (2000). Population dynamics of spiking neurons: fast transients, asynchronous states, and locking. *Neural Comput*, **12**, 43–89. 6.4.1

GHAZANFAR, A. & NICOLELIS, M. (2001). Feature article: the structure and function of dynamic cortical and thalamic receptive fields. *Cereb Cortex*, **11**, 183–93. 4.2.6

GHAZANFAR, A., KRUPA, D. & NICOLELIS, M. (2001). Role of cortical feedback in the receptive field structure and nonlinear response properties of somatosensory thalamic neurons. *Exp Brain Res*, **141**, 88–100. 1.2.2.2, 4.1, 4.5, 6.3.2

GIL, Z., CONNORS, B. & AMITAI, Y. (1997). Differential regulation of neocortical synapses by neuromodulators and activity. *Neuron*, **19**, 679–86. 5.1

GOLSHANI, P., LIU, X. & JONES, E. (2001). Differences in quantal amplitude reflect GluR4- subunit number at corticothalamic synapses on two populations of thalamic neurons. *Proc Natl Acad Sci USA*, **98**, 4172–7. 1.2.1, 2.2, 3.2.4, 3, 5.4, 6.3.3

HAYOT, F. & TRANCHINA, D. (2001). Modeling corticofugal feedback and the sensitivity of lateral geniculate neurons to orientation discontinuity. *Vis Neurosci*, **18**, 865–77. 1.2.2.2, 4.2.1, 4.5

HILL, S. & TONONI, G. (2005). Modeling sleep and wakefulness in the thalamocortical system. *J Neurophysiol*, **93**, 1671–98. 1.2.2.3, 5.1, 5.4, 6.5.4

HILLENBRAND, U. & VAN HEMMEN, J. (2001). Does corticothalamic feedback control cortical velocity tuning? *Neural Comput*, **13**, 327–55. 4.5

HIRSCH, J., FOURMENT, A. & MARC, M. (1983). Sleep-related variations of membrane potential in the lateral geniculate body relay neurons of the cat. *Brain Res*, **259**, 308–12. 1.2.2.3, 5.1

HIRSCH, J., GALLAGHER, C., ALONSO, J. & MARTINEZ, L. (1998). Ascending projections of simple and complex cells in layer 6 of the cat striate cortex. *J Neurosci*, **18**, 8086–94. 3.2.4, 4.2.3

HIRSCH, J.A. (2003). Synaptic physiology and receptive field structure in the early visual pathway of the cat. *Cereb Cortex*, **13**, 63–9. 4.1, 4.3.1

HIRSCH, J.A., MARTINEZ, L.M., ALONSO, M., DESAI, K., PILLAI, C. & PIERRE, C. (2002). Synaptic physiology of the flow of information in the cat's visual cortex in vivo. *J Physiol*, **540**, 335–50. 3.2.4, 4.2.3

HOBSON, J.A. & PACE-SCHOTT, E.F. (2002). The cognitive neuroscience of sleep: neuronal systems, consciousness and learning. *Nat Rev Neurosci*, **3**, 679–93. 5.1, 5.4

HODGKIN, A.L. & HUXLEY, A.F. (1952). A quantitative description of membrane current and its application to conduction and excitation in nerve. *J Physiol*, **117**, 500–544. 1.3.1

HOPPENSTEADT, F. & IZHIKEVICH, E. (1998). Thalamo-cortical interactions modeled by weakly connected oscillators: could the brain use FM radio principles? *Biosystems*, **48**, 85–94. 6.6.1

HUBEL, D. & WIESEL, T. (1961). Integrative action in the cat's lateral geniculate body. *J Physiol*, **155**, 385–98. 4.1, 4.3.1

HUBEL, D. & WIESEL, T. (1962). Receptive fields, binocular interaction and functional architecture in the cat's visual cortex. *J Physiol*, **160**, 106–54. 4.2.1, 4.2.4, 4.3.1

HUGUENARD, J. & MCCORMICK, D. (1992). Simulation of the currents involved in rhythmic oscillations in thalamic relay neurons. *J Neurophysiol*, **68**, 1373–83. 6.3.1

HUSAIN, F., TAGAMETS, M.A., FROMM, S., BRAUN, A. & HORWITZ, B. (2004). Relating neuronal dynamics for auditory object processing to neuroimaging activity: a computational modeling and an fMRI study. *Neuroimage*, **21**, 1701–20. 1.3

JAHNSEN, H. & LLINAS, R. (1984a). Electrophysiological properties of guinea-pig thalamic neurones: an in vitro study. *J Physiol*, **349**, 205–26. 1.1.1, 2.2, 3.2.1, 5.1

JAHNSEN, H. & LLINAS, R. (1984b). Ionic basis for the electro-responsiveness and oscillatory properties of guinea-pig thalamic neurones in vitro. *J Physiol*, **349**, 227–47. 1.1.1, 2.2, 3.2.1, 5.1

JONES, E. (1985). *The Thalamus*. Plenum Press. 1.1, 3.2.1

JONES, J., STEPNOSKI, A. & PALMER, L. (1987). The two-dimensional spectral structure of simple receptive fields in cat striate cortex. *J Neurophysiol*, **58**, 1212–32. 4.1

KANDEL, E.R., SCWARTZ, J.H. & JESSELL, T.M. (2000). *Principles of Neural Science*. McGraw-Hill, 4th edn. 1.2

KAPLAN, E. (2004). *The Visual Neurosciences*, chap. 30 The M, P, and K pathways of the primate visual system, 481–493. The MIT Press. 4.2.1

KHIBNIK, A., KUZNETSOV, Y., LEVITIN, W. & NIKOLAEV, E. (1993). Continuation techniques and interactive software for bifucation-analysis of ODEs and iterated maps. *Physica D*, **62**, 360–371. 3.2.5, 3.3.2

KIM, U., SANCHEZ-VIVES, M. & MCCORMICK, D. (1997). Functional dynamics of GABAergic inhibition in the thalamus. *Science*, **278**, 130–4. 3.3.9.1

KING, A. & SCHNUPP, J. (1998). Sensory neuroscience: visualizing the auditory cortex. *Curr Biol*, **8**, R784–7. 4.2.6

KIRKLAND, K., SILLITO, A., JONES, H., WEST, D. & GERSTEIN, G. (2000). Oscillations and long-lasting correlations in a model of the lateral geniculate nucleus and visual cortex. *J Neurophysiol*, **84**, 1863–8. 4.2.1

KRUPA, D., GHAZANFAR, A. & NICOLELIS, M. (1999). Immediate thalamic sensory plasticity depends on corticothalamic feedback. *Proc Natl Acad Sci USA*, **96**, 8200–5. 4.5

KUFFLER, S. (1953). Discharge patterns and functional organization of mammalian retina. *J Neurophysiol*, **16**, 37–68. 4.1

KUZNETSOV, Y.A. (1998). *Elements of Applied Bifurcation Theory*. Springer-Verlag New York Inc., 2nd edn. 3.2.5, 3.3.3

LANDISMAN, C.E., LONG, M.A., BEIERLEIN, M., DEANS, M.R., PAUL, D.L. & CONNORS, B.W. (2002). Electrical synapses in the thalamic reticular nucleus. *J Neurosci*, **22**, 1002–9. 3.2.4, 4.2.3

LANYON, L.J. & DENHAM, S.L. (2004). A model of active visual search with object-based attention guiding scan paths. *Neural Networks*, **17**, 873–97. 1.3

LE MASSON, G., LE MASSON, S.R., DEBAY, D. & BAL, T. (2002). Feedback inhibition controls spike transfer in hybrid thalamic circuits. *Nature*, **417**, 854–8. 1.4, 2.2, 4.2.1, 5.3.2, 5.4

LESICA, N.A. & STANLEY, G.B. (2004). Encoding of natural scene movies by tonic and burst spikes in the lateral geniculate nucleus. *J Neurosci*, **24**, 10731–40. 4.5

LEVICK, W., CLELAND, B. & DUBIN, M. (1972). Lateral geniculate neurons of cat: retinal inputs and physiology. *Invest Ophthalmol*, **11**, 302–11. 4.1

LI, J., WANG, S. & BICKFORD, M.E. (2003). Comparison of the ultrastructure of cortical and retinal terminals in the rat dorsal lateral geniculate and lateral posterior nuclei. *J Comp Neurol*, **460**, 394–409. 1.2.1

LI, Z. & HOPFIELD, J.J. (1989). Modeling the olfactory bulb and its neural oscillatory processings. *Biol Cybern*, **61**, 379–392. 3.2.6

LIU, X. & JONES, E. (1999). Predominance of corticothalamic synaptic inputs to thalamic reticular nucleus neurons in the rat. *J Comp Neurol*, **414**, 67–79. 1.2.1, 1.4, 4.2.1

LUTHI, A. & MCCORMICK, D. (1998). Periodicity of thalamic synchronized oscillations: the role of Ca2+-mediated upregulation of Ih. *Neuron*, **20**, 553–63. 2.1

MARROCCO, R., MCCLURKIN, J. & ALKIRE, M. (1996). The influence of the visual cortex on the spatiotemporal response properties of lateral geniculate nucleus cells. *Brain Res*, **737**, 110–8. 1.2.2.2

MARTINEZ-CONDE, S., MACKNIK, S.L. & HUBEL, D.H. (2002). The function of bursts of spikes during visual fixation in the awake primate lateral geniculate nucleus and primary visual cortex. *Proc Natl Acad Sci USA*, **99**, 13920–5. 1.1.1

MASTRONARDE, D. (1987). Two classes of single-input X-cells in cat lateral geniculate nucleus. I. Receptive-field properties and classification of cells. *J Neurophysiol*, **57**, 357–80. 4.1

MCALONAN, K. & BROWN, V.J. (2002). The thalamic reticular nucleus: more than a sensory nucleus? *Neuroscientist*, **8**, 302–5. 3.2.1

MCCARLEY, R., BENOIT, O. & BARRIONUEVO, G. (1983). Lateral geniculate nucleus unitary discharge in sleep and waking: state- and rate-specific aspects. *J Neurophysiol*, **50**, 798–818. 1.2.2.3, 5.1

McCormick, D. (1992). Neurotransmitter actions in the thalamus and cerebral cortex and their role in neuromodulation of thalamocortical activity. *Prog Neurobiol*, **39**, 337–88. 5.1, 6.5.4

McCormick, D. & Bal, T. (1994). Sensory gating mechanisms of the thalamus. *Curr Opin Neurobiol*, 4, 550–6. 1.2.2.3, 5.1, 5.4

McCormick, D. & Huguenard, J. (1992). A model of the electrophysiological properties of thalamocortical relay neurons. *J Neurophysiol*, **68**, 1384–400. 6.3.1

Montero, V. (1991). A quantitative study of synaptic contacts on interneurons and relay cells of the cat lateral geniculate nucleus. *Exp Brain Res*, **86**, 257–70. 1.2.1, 1.3, 1.2.1, 4.1

Montero, V. (1997). c-fos induction in sensory pathways of rats exploring a novel complex environment: shifts of active thalamic reticular sectors by predominant sensory cues. *Neuroscience*, **76**, 1069–81. 4.1

Montero, V. (2000). Attentional activation of the visual thalamic reticular nucleus depends on 'top-down' inputs from the primary visual cortex via corticogeniculate pathways. *Brain Res*, **864**, 95–104. 3.2.1

Morison, R. & Bassett, D. (1945). Electrical activity of the thalamus and basal ganglia in decorticate cats. *Journal of Neurophysiology*, **8**, 309–314. 2.2

Mukherjee, P. & Kaplan, E. (1995). Dynamics of neurons in the cat lateral geniculate nucleus: in vivo electrophysiology and computational modeling. *J Neurophysiol*, **74**, 1222–43. 4.5

MURPHY, P. & SILLITO, A. (1987). Corticofugal feedback influences the generation of length tuning in the visual pathway. *Nature*, **329**, 727–9. 1.2.2.2

MURPHY, P., DUCKETT, S. & SILLITO, A. (1999). Feedback connections to the lateral geniculate nucleus and cortical response properties. *Science*, **286**, 1552–4. 1.2.1, 4.1, 4.5

NICOLELIS, M.A.L. & FANSELOW, E.E. (2002). Thalamocortical optimization of tactile processing according to behavioral state. *Nat Neurosci*, **5**, 517–23. 1.2.2.2

NYKAMP, D. & TRANCHINA, D. (2000). A population density approach that facilitates large-scale modeling of neural networks: analysis and an application to orientation tuning. *J Comput Neurosci*, **8**, 19–50. 6.2, 6.4.1

PACE-SCHOTT, E.F. & HOBSON, J.A. (2002). The neurobiology of sleep: genetics, cellular physiology and subcortical networks. *Nat Rev Neurosci*, **3**, 591–605. 5.4

REID, R. & ALONSO, J. (1995). Specificity of monosynaptic connections from thalamus to visual cortex. *Nature*, **378**, 281–4. 4.2.4, 6.4.1

REID, R., VICTOR, J. & SHAPLEY, R. (1997). The use of m-sequences in the analysis of visual neurons: linear receptive field properties. *Vis Neurosci*, **14**, 1015–27. 4.1, 4.1, 4.4, 4.4.1, 4.5.1, 6.3.2, 6.6.3.

REINAGEL, P., GODWIN, D., SHERMAN, S. & KOCH, C. (1999). Encoding of visual information by LGN bursts. *J Neurophysiol*, **81**, 2558–69. 2.1

RINGACH, D. & SHAPLEY, R. (2004). Reverse correlation in neurophysiology. *Cognitive Science*, **28**, 147–166. 4.1

RIVADULLA, C., MARTINEZ, L.M., VARELA, C. & CUDEIRO, J. (2002). Completing the corticofugal loop: a visual role for the corticogeniculate type 1 metabotropic glutamate receptor. *J Neurosci*, **22**, 2956–62. 4.1

ROBINSON, P., RENNIE, C. & ROWE, D. (2002). Dynamics of large-scale brain activity in normal arousal states and epileptic seizures. *Phys Rev E Stat Nonlin Soft Matter Phys*, **65**, 041924. 2.2.1, 6.6.1

RUCCI, M. & CASILE, A. (2004). Decorrelation of neural activity during fixational instability: possible implications for the refinement of V1 receptive fields. *Vis Neurosci*, **21**, 725–738. 1.1.1

SASTRY, P., SHAH, S., SINGH, S. & UNNIKRISHNAN, K. (1999). Role of feedback in mammalian vision: a new hypothesis and a computational model. *Vision Res*, **39**, 131–48. 1.2.2.2, 4.5

SEJNOWSKI, T. & DESTEXHE, A. (2000). Why do we sleep? *Brain Res*, **886**, 208–223. 1.2.2.1

SHERMAN, S. (2001). A wake-up call from the thalamus. *Nat Neurosci*, 4, 344–6. 2.1, 5.1

SHERMAN, S. & GUILLERY, R. (1998). On the actions that one nerve cell can have on another: distinguishing "drivers" from "modulators". *Proc Natl Acad Sci USA*, **95**, 7121–6. 1.2.2, 4.1, 4.5.1

SHERMAN, S. & GULLERY, R. (2001). *Exploring the thalamus*. Academic Press. 1.1, 1.1.1, 3.2.1, 4.2.1, 4.2.1, 4.2.2

SHERMAN, S.M. & GUILLERY, R. (2002). The role of the thalamus in the flow of information to the cortex. *Philos Trans R Soc Lond B Biol Sci*, **357**, 1695–708. 3.2.1

SILLITO, A., JONES, H., GERSTEIN, G. & WEST, D. (1994). Feature-linked synchronization of thalamic relay cell firing induced by feedback from the visual cortex. *Nature*, **369**, 479–82. 1.2.2.2

SILLITO, A.M. & JONES, H.E. (2002). Corticothalamic interactions in the transfer of visual information. *Philos Trans R Soc Lond B Biol Sci*, **357**, 1739–52. 1.2.2.2, 4.5, 6.3.2

SINGER, W. & CREUTZFELDT, O. (1970). Reciprocal lateral inhibition of on- and off-center neurones in the lateral geniculate body of the cat. *Exp Brain Res*, **10**, 311–30. 4.1

SOLOMON, S.G., WHITE, A.J.R. & MARTIN, P.R. (2002). Extraclassical receptive field properties of parvocellular, magnocellular, and koniocellular cells in the primate lateral geniculate nucleus. *J Neurosci*, **22**, 338–49. 4.1

SOLTESZ, I., LIGHTOWLER, S., LERESCHE, N., JASSIK-GERSCHENFELD, D., POLLARD, C. & CRUNELLI, V. (1991). Two inward currents and the transformation of low-frequency oscillations of rat and cat thalamocortical cells. *J Physiol*, **441**, 175–97. 2.2

SOMMER, M.A. & WURTZ, R.H. (2004). What the brain stem tells the frontal cortex. II. Role of the SC-MD-FEF pathway in corollary discharge. *J Neurophysiol*, **91**, 1403–1423. 1.1.1

STERIADE, M. (2000). Corticothalamic resonance, states of vigilance and mentation. *Neuroscience*, **101**, 243–76. 3.3.2

STERIADE, M. & DESCHENES, M. (1984). The thalamus as a neuronal oscillator. *Brain Res*, **320**, 1–63. 2.1

STERIADE, M. & TIMOFEEV, I. (2003). Neuronal plasticity in thalamocortical networks during sleep and waking oscillations. *Neuron*, **37**, 563–76. 2.1

STERIADE, M., DESCHENES, M., DOMICH, L. & MULLE, C. (1985). Abolition of spindle oscillations in thalamic neurons disconnected from nucleus reticularis thalami. *J Neurophysiol*, **54**, 1473–97. 1.2.2.1

STERIADE, M., DOMICH, L., OAKSON, G. & DESCHENES, M. (1987). The deafferented reticular thalamic nucleus generates spindle rhythmicity. *J Neurophysiol*, **57**, 260–73. 2.1, 5.3.2

STERIADE, M., MCCORMICK, D. & SEJNOWSKI, T. (1993). Thalamocortical oscillations in the sleeping and aroused brain. *Science*, **262**, 679–85. 1.2.2.1, 2.1, 2.1, 2.2, 2.4, 3.2.1, 3.3.6, 3.4, 6.3.1

STERIADE, M., JONES, E. & MCCORMICK, D. (1997). *Thalamus. Volume I. Organisation and Function.*. Elsevier. 3.3.2

STEVENS, J. & GERSTEIN, G. (1976). Spatiotemporal organization of cat lateral geniculate receptive fields. *J Neurophysiol*, **39**, 213–38. 4.1, 4.2.6

STROGATZ, S. (1994). *Nonlinear dynamics and chaos*. Westview Press. 3.2.5

SUFFCZYNSKI, P., KALITZIN, S., PFURTSCHELLER, G. & DA SILVA, F.L. (2001). Computational model of thalamo-cortical networks: dynamical control of alpha rhythms in relation to focal attention. *Int J Psychophysiol*, **43**, 25–40. 2.1, 4.2.1

SUGA, N., GAO, E., ZHANG, Y., MA, X. & OLSEN, J. (2000). The corticofugal system for hearing: recent progress. *Proc Natl Acad Sci USA*, **97**, 11807–14. 1.2.2.2, 4.5

SWADLOW, H. & GUSEV, A. (2001). The impact of 'bursting' thalamic impulses at a neocortical synapse. *Nat Neurosci*, **4**, 402–8. 2.1, 5.1

SYLVESTER, R., HAYNES, J.D. & REES, G. (2005). Saccades differentially modulate human LGN and V1 responses in the presence and absence of visual stimulation. *Curr Biol*, **15**, 37–41. 1.1.1

SZENTAGOTHAI, J., HAMORI, J. & TOMBOL, T. (1966). Degeneration and electron microscope analysis of the synaptic glomeruli in the lateral geniculate body. *Exp Brain Res*, **2**, 283–301. 1.2.1

TERMAN, D., BOSE, A. & KOPELL, N. (1996). Functional reorganization in thalamocortical networks: transition between spindling and delta sleep rhythms. *Proc Natl Acad Sci USA*, **93**, 15417–22. 2.2, 4.2.1

THOMSON, A.M. & BANNISTER, A.P. (2003). Interlaminar connections in the neocortex. *Cereb Cortex*, **13**, 5–14. 1.2, 1.2, 1.4, 3.2.1, 4.2.1

THOMSON, A.M., BANNISTER, A.P., MERCER, A. & MORRIS, O.T. (2002). Target and temporal pattern selection at neocortical synapses. *Philos Trans R Soc Lond B Biol Sci*, **357**, 1781–91. 6.5.3

TIMOFEEV, I. & STERIADE, M. (1997). Fast (mainly 30-100 Hz) oscillations in the cat cerebellothalamic pathway and their synchronization with cortical potentials. *J Physiol*, **504**, 153–68. 2.1

TREVES, A. (1993). Mean-field analysis of neuronal spike dynamics. *Network*, 4, 259–284. 6.2

TRUCCOLO, W. & DONG, D. (2001). Dynamic temporal decorrelation: An information-theoretic and biophysical model of the functional role of the lateral geniculate nucleus. *Neurocomputing*, **38-40**, 993–1001. 4.5

TSODYKS, M., SKAGGS, W., SEJNOWSKI, T. & MCNAUGHTON, B. (1997). Paradoxical effects of external modulation of inhibitory interneurons. *J Neurosci*, **17**, 4382–8. 3.2.3, 3.2.4

TURNER, J. & SALT, T. (1998). Characterization of sensory and corticothalamic excitatory inputs to rat thalamocortical neurones in vitro. *J Physiol*, **510**, 829–43. 1.2.1

TURNER, J., ANDERSON, C., WILLIAMS, S. & CRUNELLI, V. (1997). Morphology and membrane properties of neurones in the cat ventrobasal thalamus in vitro. *J Physiol*, **505**, 707–26. 3.2.4, 4.2.3

UHLRICH, D. & CUCCHIARO, J. (1992). GABAergic circuits in the lateral geniculate nucleus of the cat. *Prog Brain Res*, **90**, 171–92. 4.2.1

ULRICH, D. & HUGUENARD, J. (1996). Gamma-aminobutyric acid type B receptor-dependent burst-firing in thalamic neurons: a dynamic clamp study. *Proc Natl Acad Sci USA*, **93**, 13245–9. 3.2.4, 4.2.3

USREY, W.M. (2002). The role of spike timing for thalamocortical processing. *Curr Opin Neurobiol*, **12**, 411–7. 4.2.3, 4.4.3

USREY, W.M., REPPAS, J.B. & REID, R.C. (1999). Specificity and strength of retinogeniculate connections. *J Neurophysiol*, **82**, 3527–3540. 4.1, 4.1, 4.4, 4.5, 4.5.1, 6.3.2, 6.6.3, 6.7

VAN BREDERODE, J. & SNYDER, G. (1992). A comparison of the electrophysiological properties of morphologically identified cells in layers 5B and 6 of the rat neocortex. *Neuroscience*, **50**, 315–37. 4.2.1

VAN HORN, S., ERISIR, A. & SHERMAN, S. (2000). Relative distribution of synapses in the A-laminae of the lateral geniculate nucleus of the cat. *J Comp Neurol*, **416**, 509–20. 1.2.1, 1.3, 1.2.1, 3.2.4, 2, 4.1, 4.2.3, 4.4.3

VERZEANO, M. & NEGISHI, K. (1960). Neuronal activity in cortical and thalamic networks. *J Gen Physiol*, **43**, 177–95. 3.3.1

VON KROSIGK, M., BAL, T. & MCCORMICK, D. (1993). Cellular mechanisms of a synchronized oscillation in the thalamus. *Science*, **261**, 361–4. 2.1, 2.2, 2.2, 3.3.6, 3.3.9.1, 3.4, 6.3.1

WANG, S., BICKFORD, M., HORN, S.V., ERISIR, A., GODWIN, D. & SHERMAN, S. (2001). Synaptic targets of thalamic reticular nucleus terminals in the visual thalamus of the cat. *J Comp Neurol*, **440**, 321–41. 3.2.4, 4, 4.2.1, 4.2.3, 4.4.3

WANG, W., JONES, H., ANDOLINA, I., SALT, T. & SILLITO, A. (2004). Functional alignment of feedback effects from visual cortex to LGN. In *SfN abstracts*. 1.2.1, 1.4, 4.1, 4.2.1, 4.6, 4.2.5, 4.4.1, 4.5, 5.2, 5.4, 6.3.2, 6.6.3

WANG, X., GOLOMB, D. & RINZEL, J. (1995). Emergent spindle oscillations and intermittent burst firing in a thalamic model: specific neuronal mechanisms. *Proc Natl Acad Sci USA*, **92**, 5577–81. 2.2

WILSON, H. & COWAN, J. (1972). Excitatory and inhibitory interactions in localized populations of model neurons. *Biophys J*, **12**, 1–24. 1.3, 2.2.1, 3.2.2, 3, 3.2.2, 3.2.2, 3.2.6, 3.4, 4.1, 4.2.2, 4.2.2, 4.4.2, 6.1, 6.2, 6.3.1, 6.4, 6.4.1, 6.5.2

WOLFE, J. & PALMER, L. (1998). Temporal diversity in the lateral geniculate nucleus of cat. *Vis Neurosci*, **15**, 653–75. 4.1

WORGOTTER, F., NELLE, E., LI, B. & FUNKE, K. (1998). The influence of corticofugal feedback on the temporal structure of visual responses of cat thalamic relay cells. *J Physiol*, **509**, 797–815. 4.5.1

YAN, J. & SUGA, N. (1996). Corticofugal modulation of time-domain processing of biosonar information in bats. *Science*, **273**, 1100–3. 1.2.2.2, 4.5

YOUSIF, N.A.B. & DENHAM, M.J. (2004). Action potential backpropagation in a model thalamocortical relay cell. *Neurocomputing*, **58-60**, 393–400. 1.2.1

ZHANG, Y. & SUGA, N. (2000). Modulation of responses and frequency tuning of thalamic and collicular neurons by cortical activation in mustached bats. *J Neurophysiol*, **84**, 325–33. 4.5

ZHANG, Y., SUGA, N. & YAN, J. (1997). Corticofugal modulation of frequency processing in bat auditory system. *Nature*, **387**, 900–3. 1.2.2.2

ZHU, J., UHLRICH, D. & LYTTON, W. (1999). Burst firing in identified rat geniculate interneurons. *Neuroscience*, **91**, 1445–60. 4.2.3, 4.5